

SURFACE WAVE PROPAGATION AND SOURCE STUDIES  
IN THE GULF OF CALIFORNIA REGION

Thesis by

Wayne Thatcher

In Partial Fulfillment of the Requirements

For the Degree of

Doctor of Philosophy

California Institute of Technology

Pasadena, California

1972

(Submitted June 15, 1971)

## ACKNOWLEDGMENTS

I have found the Seismological Laboratory of the California Institute of Technology an exciting and stimulating environment in which to work, and this thesis owes much to the help and encouragement provided by all of the staff and students of the laboratory. In particular I wish to acknowledge the generous interest and advice of Dr. Jim Brune. Much of Chapters I, II, and III reports on work done in collaboration with Dr. Brune, and several of his thoughts are crucial to the conclusions presented there. Help from Drs. Clarence Allen, Don Anderson, Charles Archambeau and Lee Silver is much appreciated. Among discussions with many fellow graduate students, those with Thomas C. Hanks have been particularly lively and stimulating.

Special thanks are due to the Comission Federale de Electricidad and the National University of Mexico (UNAM) for aid and cooperation in carrying out field work in Baja California. In this respect Dr. Cinna Lomnitz of UNAM is particularly thanked. Ralph Gilman played an important role in the deployment and maintenance of the seismic stations.

This manuscript was typed by Mrs. Alrae Tingley and the figures were carefully drafted by Lazlo Lenches.

This research was supported by the following National Science Foundation grants: GA 11333, GA 12868 and GA 21397.

## ABSTRACT

A number of aspects of seismic surface wave propagation and earthquake mechanism in the Gulf of California region are investigated in this thesis. In addition, several associated problems raised by this study are also explored in some detail.

Surface wave dispersion and P-wave travel time delays are measured to delineate the crust and upper mantle structure in the Imperial Valley-Gulf of California region. Crustal thicknesses beneath Baja California and Sonora are comparable and near 25 km, while within the Gulf crustal structure varies laterally from nearly oceanic on the western side to continental shelf thicknesses ( $\sim 20$  km) towards the north and east. Love wave group velocities for Baja California paths are unusually high and were not used to determine structure.  $P_n$  and teleseismic P-wave delays are used in a reconnaissance survey of crustal structure in the Imperial Valley and across the Peninsular Range batholith. The data are consistent with an increase in crustal thickness of 12 km from flank to crest in the Peninsular Ranges, and a decrease of 8 km across the Imperial Valley.

The high Love wave group velocities measured across Baja California are shown to be similar to velocities of the first higher mode. It is also demonstrated that higher Love modes can have group velocities very close to fundamental mode velocities for a range of wave periods and realistic earth models. The mode interference which is a consequence of this intertwining of group velocity curves has a significant effect on

measured phase velocities, and this problem is investigated in detail. An important conclusion of this study is that anomalously high Love wave phase velocities reported for the United States midcontinent and Japan are straightforwardly explained by mode interference without appealing to complex or anisotropic models, as had been done previously.

Seismic processes associated with actively spreading oceanic rises are examined in the study of a strong swarm of earthquakes located near an inferred spreading center in the Northern Gulf of California. Close-in travel time data constrain the origin times of swarm events and demonstrate that the epicenters are confined to the upper crust. Teleseismic P-delays suggest unusually low seismic velocities beneath the source. The previously suspected normal faulting nature of swarm earthquakes is also confirmed. Seismic coupling across 200 km between adjacent spreading centers in the Northern Gulf is indicated by a survey of recent seismicity.

It is noted in the study of the Gulf swarm that these sources have significantly higher surface wave amplitudes than events with similar assigned magnitudes in Northern Baja California. In the final chapter of this thesis a detailed analysis is made of the Baja earthquakes and it is concluded that as a group they have distinctly smaller source dimensions and larger stress drops than events within the Gulf of California. These differences are quite marked and are often very clearly seen even on records from band-limited seismographs. Several examples exist where propagation paths are very similar but the visual appearance of records differs considerably, suggesting that near-source or path

effects are not likely explanations of the observed differences.

For small magnitude North Baja earthquakes, both source dimensions and long period surface excitation average only about a factor or two larger than corresponding quantities previously measured for underground nuclear explosions of similar magnitude.

## TABLE OF CONTENTS

	Page
Introduction	1
Chapter I	
Crustal Structure in the Imperial Valley-Gulf of California Region	
Abstract	7
Introduction	8
Surface Wave Observations	9
(a) Baja California	12
(b) Gulf of California	17
(c) Sonora	23
P-Delay Observations	23
Chapter II	
Higher Mode Interference and Observed Anomalous Apparent Love Wave Phase Velocities	
Abstract	32
Introduction	33
Fundamental and Higher Mode Love Wave Dispersion	35
Higher Mode Excitation	37
The Effect of Attenuation	40
Simple Theoretical Considerations	41
Biases in the Routine Analysis of Phase Velocity Data	47
Discussion	49

## TABLE OF CONTENTS (continued)

Page

## Chapter III

Seismic Study of an Oceanic Ridge Earthquake Swarm  
in the Gulf of California

Abstract	53
Introduction	54
Swarm Activity and Gulf Seismicity	56
Location of March 1969 Swarm Events	64
Origin Times and P-Wave Residuals	74
Focal Mechanism	76
Seismic Moments and Apparent Stresses	78
A Comparison with Earthquakes in Northern Baja California	79
Conclusions	81

## Chapter IV

Regional Variations of Seismic Source Parameters in the  
Northern Baja California Area

Abstract	83
Introduction	84
Geologic and Seismic Setting of Northern Baja California	87
High Apparent Stress Earthquakes	90
SH Spectrum from Brune's Model	92
Analysis of Data	95

## TABLE OF CONTENTS (continued)

	Page
Source Parameters	107
Seismic Moments	110
Source Dimensions	112
Stress Drops	114
High Frequency Spectral Amplitude Decay	116
Radiated Energy and Apparent Stresses	117
Radiated Energy Estimates	118
Spectral Amplitudes at High Frequencies	126
Discussion and Speculations	131
Conclusions	133
References	136

## INTRODUCTION

This thesis is concerned with surface wave propagation in the Gulf of California, crustal structure there, and the investigation of earthquake source characteristics in the northern Gulf-Baja California area. It expands and amplifies on previous observations, and although the focus of the study is regional, the results have important general implications for surface wave propagation, earthquake source mechanism, and the seismic processes related with seafloor spreading.

Many of the seismic observations reported on here have particular relevance to the regional setting of the Gulf of California as an active site of seafloor spreading and a link between the East Pacific Rise and the San Andreas fault system. Various geological, geophysical, and oceanographic studies carried out as long ago as 1940 leave no doubt that the Gulf is the seismically active boundary between two separating lithospheric blocks, the Pacific and the Americas plates (Shepard 1950, Hamilton 1961, Rusnak and Fisher 1964, Wilson 1965, Sykes 1968, Larson et al. 1969). Plate theory and presently-existing marine magnetic anomaly patterns have allowed inferences to be made concerning the tectonic history of the region, and these reconstructions suggest that lithospheric consumption occurred off the west coast of Baja for most of the Cenozoic up to about 10 m. y. BP, and that spreading was initiated within the Gulf about 4.5 m. y. ago (Larson et al. 1969, McKenzie and Morgan 1969, Atwater 1970). Chapters I and III have the largest bearing upon regional relations and on the seismological aspects of seafloor spreading.

Chapter I investigates the crustal structure from the Imperial Valley, where the various strands of the San Andreas system begin, through the Gulf to its mouth, including the surrounding land areas of Baja California and Sonora. P-wave travel time delays in the Imperial Valley and surface wave dispersion in the Gulf region are used to infer the structure. Previous investigations include gravity and shallow seismic soundings in the Imperial Valley by Kovach et al. (1962) and Biehler et al. (1964) and a Gulf seismic refraction survey by Phillips (1964). The new studies made here have placed constraints on the crustal thickness in the Valley, suggested strong lateral variations in Moho depth across the Gulf, and obtained crustal structure in Baja California and Sonora.

Chapter III comprises a detailed seismic investigation of an unusually intense swarm of earthquakes which occurred in the northern Gulf during March 1969 close to one of the rhomb-shaped basins originally mapped by Shepard (1950) and now inferred to be the median trough of an actively spreading oceanic ridge. Sykes (1970) had noted the close relationship of oceanic ridges to earthquake swarms, vulcanism and normal faulting, but close-in observations and detailed study of swarms had been lacking. Some of the achievements of this study include precise location in time and space of oceanic ridge swarm earthquakes, confirmation of the normal faulting nature of swarm events, and detection of teleseismic P-wave travel time delays for these ridge sources.

In Chapter I it is shown that the group velocities of Love waves traversing the length of the Baja California peninsula are unusually high compared with those predicted on the basis of the observed Rayleigh wave dispersion for the same path. These results draw attention to similar anomalous observations reported for Love and Rayleigh wave phase velocities in Japan (Aki 1961, Aki and Kaminuma 1963) and the midcontinent of the United States (McEvelly 1964). Explanations have been previously advanced to explain these data in terms of differences in SH and SV wave velocities (McEvelly 1964, Kaminuma 1966c) and thin soft layers in the lower crust and upper mantle (Aki 1968, Hales and Bloch 1969). These proposed explanations have been generally felt to be somewhat inadequate because they are not supported by other independent data and are not easily tested. Chapter II investigates the effect of higher mode interference on measured Love wave phase velocities and concludes that mode interference must occur frequently in Love wave propagation and can successfully account for the discrepancies observed in Japan and the United States. Since this analysis has been carried out, James (1971) has convincingly demonstrated that mode interference explains anomalously high Love wave phase velocities which he measured in the Andes. In addition, although the high group velocities measured across Baja California are not unambiguously explained by higher mode propagation, the discussion of Chapter II shows that first higher Love modes can have group velocities similar to those observed in Baja.

In Chapter III it is pointed out that long period surface wave excitation for Gulf earthquakes is one to two orders of magnitude greater

than for northern Baja California shocks with the same short period amplitudes. The low surface wave excitation of the Baja earthquakes had been previously noted by Brune et al. (1963) and was interpreted by Wyss and Brune (1968) as being due to the existence of high shear stresses in the source region of these events. Chapter IV is a study of these sources, which are compared with earthquakes within the Gulf of California. It is found that there are very striking visual differences in seismograms written in southern California from events in the two regions. This difference in the high frequency amplitudes recorded on standard Wood-Anderson instruments appears too large to be a near-source or path effect and is interpreted here as reflecting directly significantly larger source dimensions and seismic moments for the Gulf earthquakes compared with similar magnitude events in northern Baja California. This conclusion is supported by preliminary examination of seismograms of southern California earthquakes, for which similar regional differences are indicated by the seismic records.

The indicated differences in seismic moment and source dimensions also imply differences in stress drops between Baja and Gulf earthquakes. The largest stress drops of Baja earthquakes are nearly two orders of magnitude larger than maximum stress drops from Gulf events. Along with differences in radiated energy estimates, the data set as a whole is consistent with order of magnitude greater shear stresses acting across faults in northern Baja California, though this interpretation is not unique.

A comparison of the northern Baja California earthquakes with small magnitude underground nuclear explosions reveals only about a factor of two greater long period excitation and source dimensions for the Baja shocks, pointing out a clear difficulty in earthquake-explosion discrimination at small magnitudes.

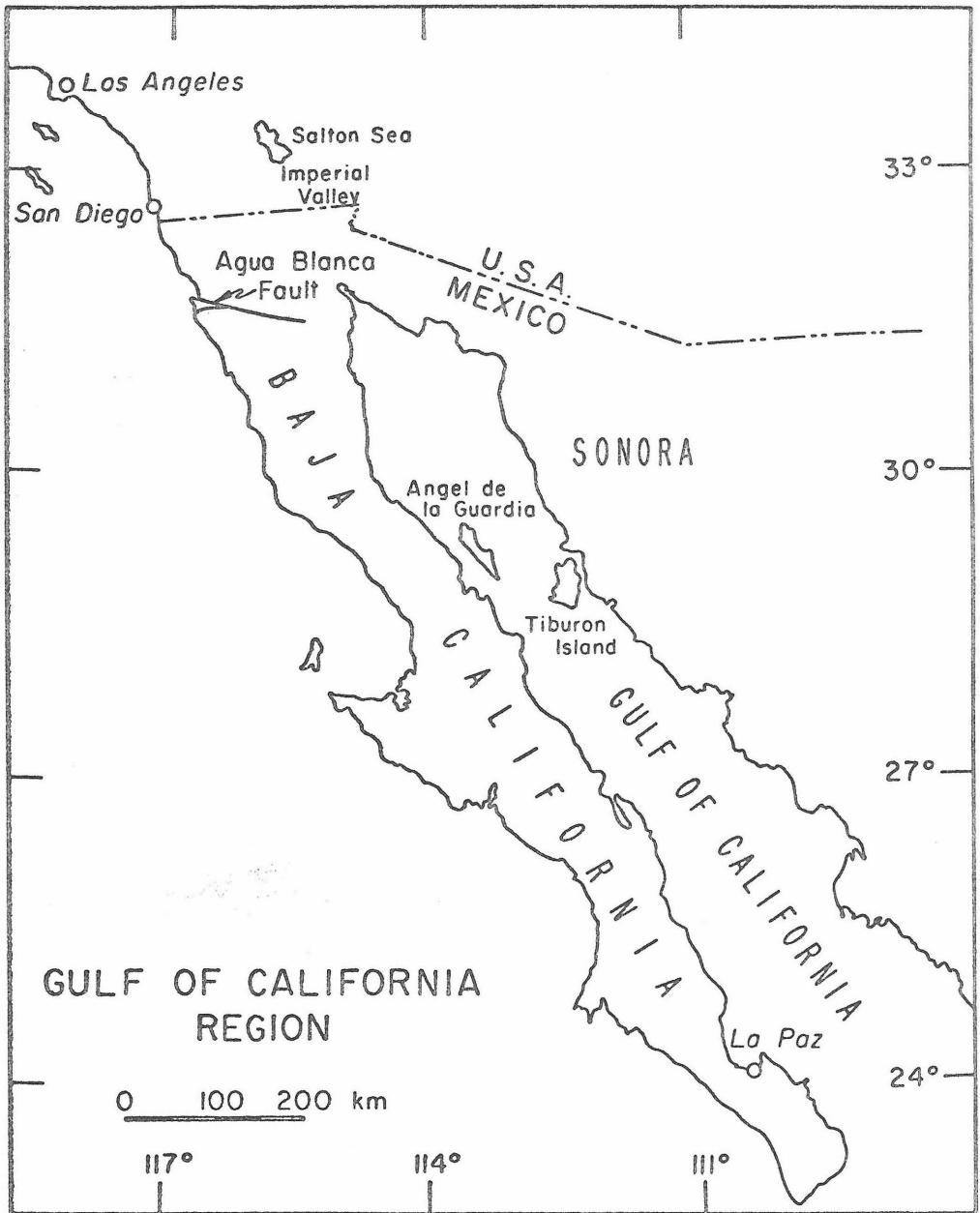


Figure 1. The Gulf of California Region

CHAPTER I  
CRUSTAL STRUCTURE IN THE IMPERIAL VALLEY-  
GULF OF CALIFORNIA REGION

ABSTRACT

Crust and upper mantle structure has been determined for several distinct portions of the Gulf of California region using seismic surface wave dispersion and body wave travel time delays. Fundamental mode Rayleigh wave data from 10 to 40 seconds period and first higher mode waves from 6 to 10 seconds period are used to delineate structure for five distinct sets of paths in and adjacent to the Gulf. Baja California and Sonora (mainland Mexico) have similar crustal thicknesses, about 26 and 24 km respectively. Fundamental mode Love wave group velocities for Baja paths are unusually high with respect to values expected on the basis of the observed Rayleigh wave dispersion, and were not used to determine structure. Short period higher mode Rayleigh waves provide a particularly good constraint on the average crustal thickness beneath Baja. Within the Gulf itself there is considerable variation in crustal thickness normal to its axis. Along the western edge average structure is near-oceanic with a crustal thickness of 9 km, but is near 20 km in the central and northeastern portions of the Gulf.

$P_n$  and teleseismic P-delays are used to infer structure in the Imperial Valley and across the Peninsular Ranges in Southern

California and Northern Baja California. Though such data alone are intrinsically ambiguous, they are consistent with a crustal thickening of 12 km from flank to crest of the Peninsular Ranges and a crustal thinning of about 8 km beneath the Imperial Valley. The crust may thicken to as much as 43 km beneath the Sierra Juarez, Northern Baja California.

## INTRODUCTION

The existence of an actively spreading oceanic ridge within the Gulf of California makes the determination of crust and upper mantle structure in this region of considerable current interest. Though in general the location of spreading centers and transform fault segments is known within the Gulf itself, the nature of the transition from this pattern in the Northern Gulf to the beginnings of the San Andreas system northeast of the Salton Trough is not yet well understood. The crustal structure from the mouth of the Gulf to its head has been delineated by the seismic refraction measurements of Phillips (1964), but there is little known of possible lateral variations in crustal thickness normal to the axis of the Gulf, and no data exist for the adjacent land areas of Baja California and Sonora. Further north in the Imperial Valley of Southern California, even the crustal thickness has not been seismically determined, though shallow crustal structure is known in a few regions and an extensive gravity survey has been carried out [Kovach et al. 1962, Biehler et al. 1964].

In this study seismic surface wave dispersion is measured

using wavetrains from earthquakes which traverse paths through and adjacent to the Gulf and are recorded on long period seismographs of the Caltech array in Southern California. Fundamental and first higher mode Rayleigh wave group velocity data for five distinct sets of paths (three within the Gulf, as well as Baja and Sonora) are each interpreted in terms of a crustal velocity model.

In addition to the surface wave data, relative arrival times of  $P_n$  and teleseismic P waves observed at stations in the Imperial Valley-Colorado Delta region are used to infer crust-upper mantle velocities and crustal thicknesses in this region.

#### SURFACE WAVE OBSERVATIONS

Surface waves generated by earthquakes in the Gulf traversing several specific regions have been analyzed from long period records of Caltech stations in Southern California and the WWSSN station at Tucson, Arizona. The location of stations and some average source-receiver paths are shown in figure 2. The epicenters and origin times for most of the events used have been relocated by Molnar and Sykes [1969] and the remainder are relocated here. Most epicentral distances are about  $10^\circ$  or less, and thus differences in location between those determined by the USCGS and the relocations used here (up to 30 km) produce significant differences in computed group velocities. Since the relocations had lower mean residuals than the CGS determinations, the relocations are preferred. In instances where comparison was possible there

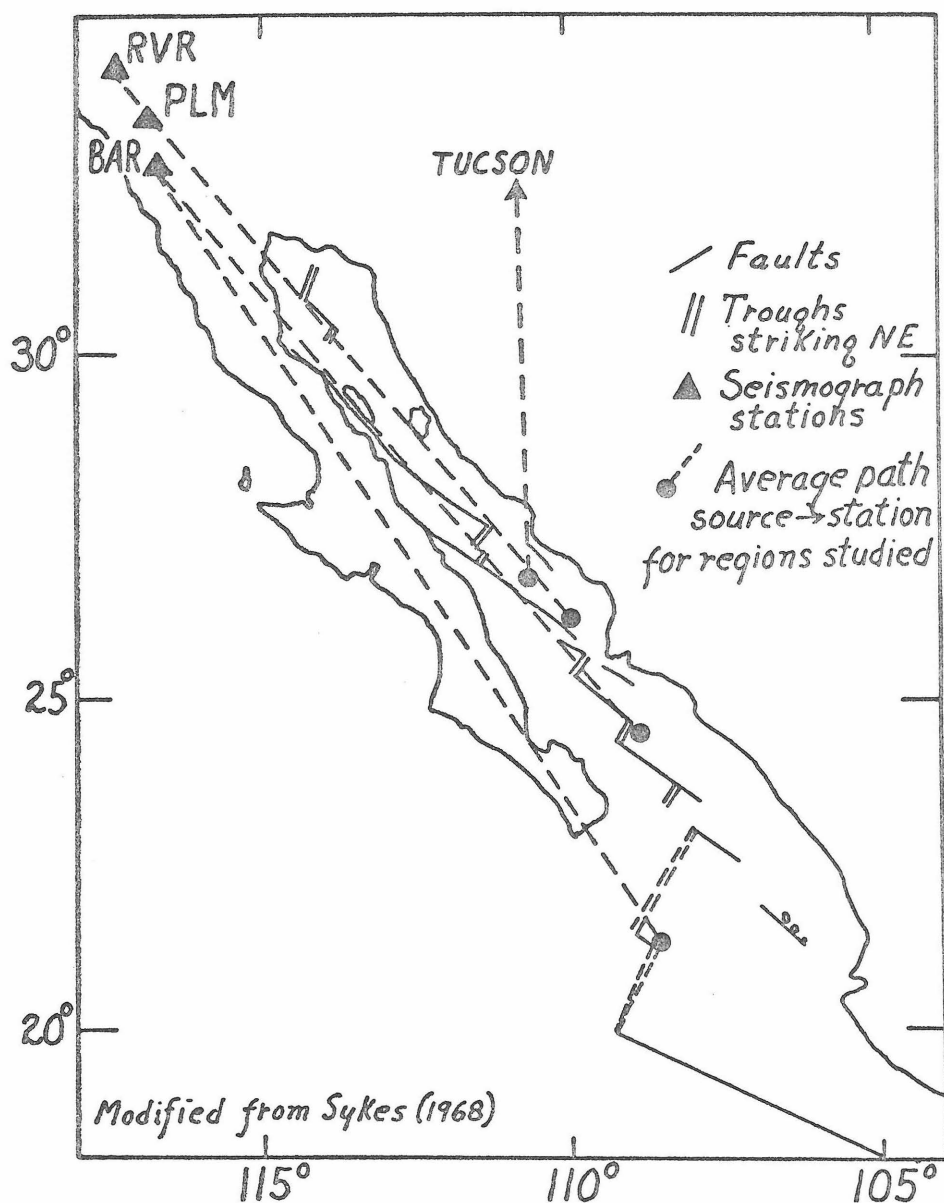


Figure 2. Gulf of California region with some average source-receiver paths used in surface wave study. The positions of northeast striking troughs and northwest trending transform faults are taken from Sykes (1968).

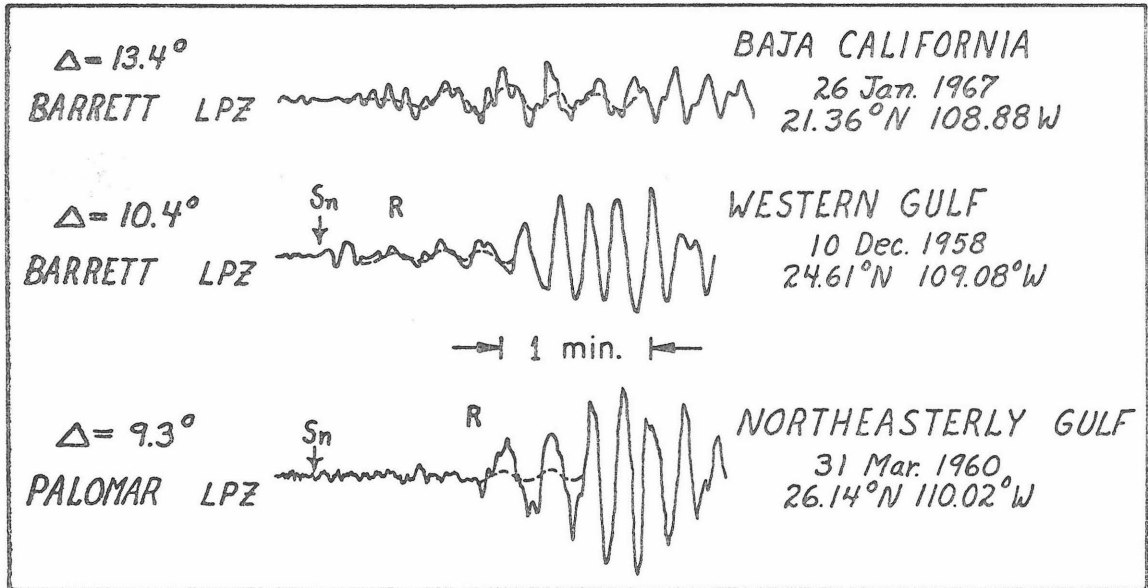


Figure 3. Typical long period Rayleigh wavetrains from sources in the Gulf travelling different paths to stations in southern California. Note in particular the well-developed short period higher modes for the Baja path and the  $S_n$  pulse shown clearly on the Gulf seismograms. Dotted lines are a visual filtering of the seismogram done in order to more clearly show the fundamental mode dispersion.

was often significant improvement in the agreement between group velocities for similar paths when relocated sources were used.

Figure 3 shows some typical Rayleigh wavetrains for sources in the Gulf traversing different regions to Southern California. For the Baja path note the well-developed short period higher modes of 6-10 second period superimposed on the longer period fundamental mode waves. The dotted line on the seismograms is a visual filtering of the short period waves, shown in order to display more clearly the fundamental mode dispersion. A distinctive feature of many Gulf path Rayleigh wave seismograms is the longer period (6-10 second)  $S_n$  pulse, particularly clearly shown in the second trace of figure 3. The velocity and characteristic period of this arrival make it extremely useful for obtaining constraints on upper mantle shear wave velocities. In this study  $S_n$  is regarded as a superposition of short period higher modes, acting essentially as a body wave critically refracted at an upper mantle velocity contrast.

We now consider in turn the observations made for each path, describe the data, and present crustal models which adequately fit it.

(a) Baja California

Three earthquakes, probably all on a small segment of transform fault south of the tip of Baja, provide sources with suitable paths along the entire length of the peninsula. A small correction has been made to the measured group velocities to subtract out the effect of about 10% oceanic path between the sources and the south tip of Baja. Phillips [1964] had a refraction line in this vicinity,

and his crustal structure has been used to subtract out the effect of the oceanic segment of the path. The data, sources, paths used, and the derived crustal model are all shown in figure 4. The fundamental mode Rayleigh wave data have been fit to a crustal model using the additional constraint on crustal thickness provided by the higher mode data shown in figure 5. The position of the first higher mode group velocity curve is very sensitive to crustal thickness: once the slope of the curve between 6 and 10 seconds is obtained from the crustal velocity contrasts, its exact position shifts significantly to the right or left with only a few kilometers increase or decrease in crustal thickness. Average crustal thickness for the Baja path is 26 km and is well constrained by the data shown in figure 5.

Next consider the Love wave group velocity data. Along with the observations, figure 4 shows the fundamental and first higher mode curves derived from the crustal model which fits the Rayleigh wave data. It is immediately apparent that the Love wave data are not in accord with the expected group velocities of the fundamental mode. They agree only near 20 seconds period, are nearly 0.3 km/sec high at 30 seconds and slightly higher at the longest periods measured. Past 30 seconds the data are close to the first higher mode curve. Two explanations for this discrepancy are possible, but unfortunately neither may be directly tested at this time. A horizontal long period station on the Baja peninsula would be of help in deciding between the two alternative explanations which follow. The most straightforward explanation is that both fundamental and first

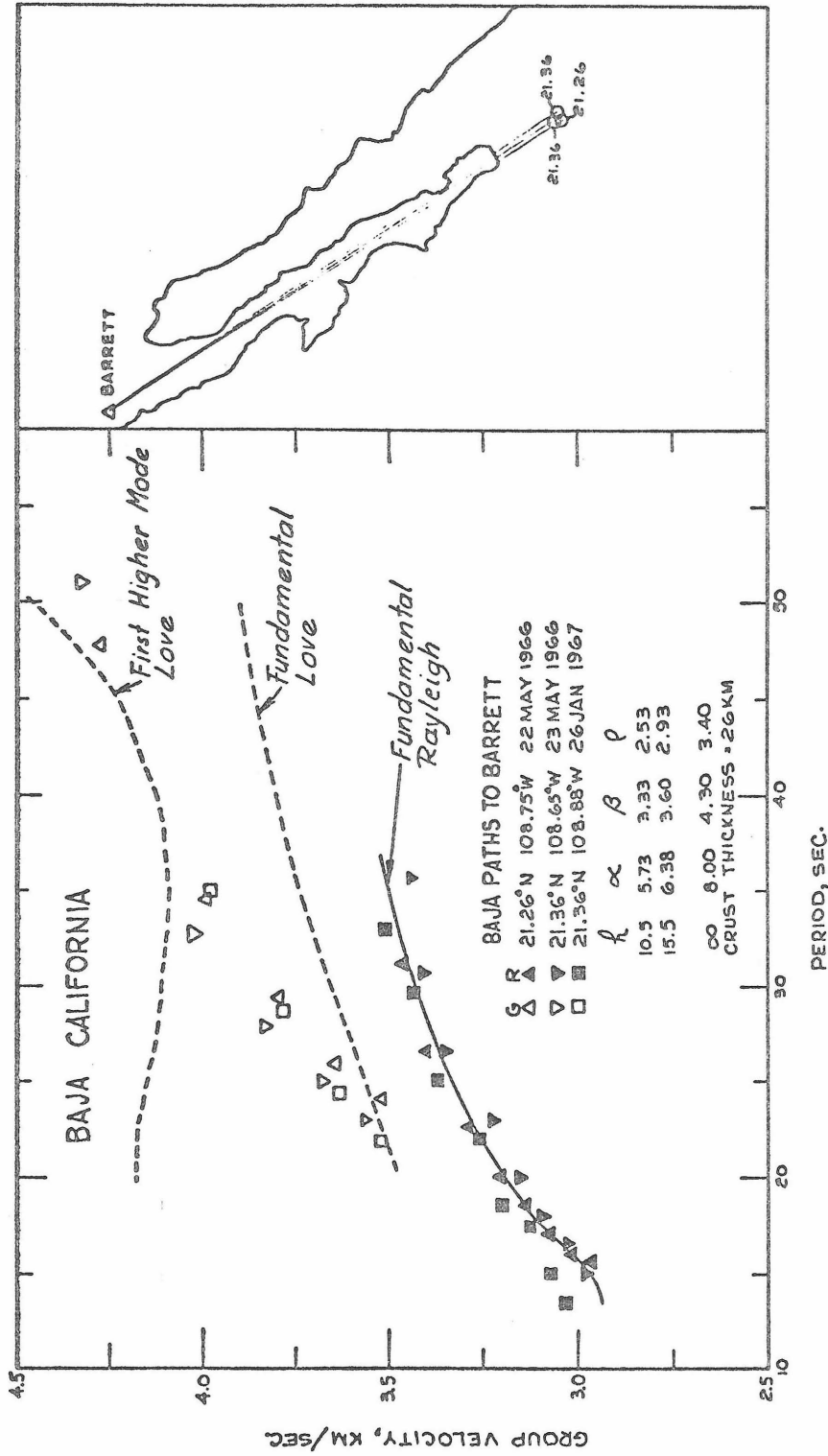


Figure 4. Earthquake sources, propagation paths, observed Love and Rayleigh wave dispersion, and model fit to the data (in this case only using Rayleigh wave observations) for Baja California. The Love wave dispersion curves are computed from the Rayleigh wave-derived structure. Note the departure of the Love data from the fundamental mode curve.

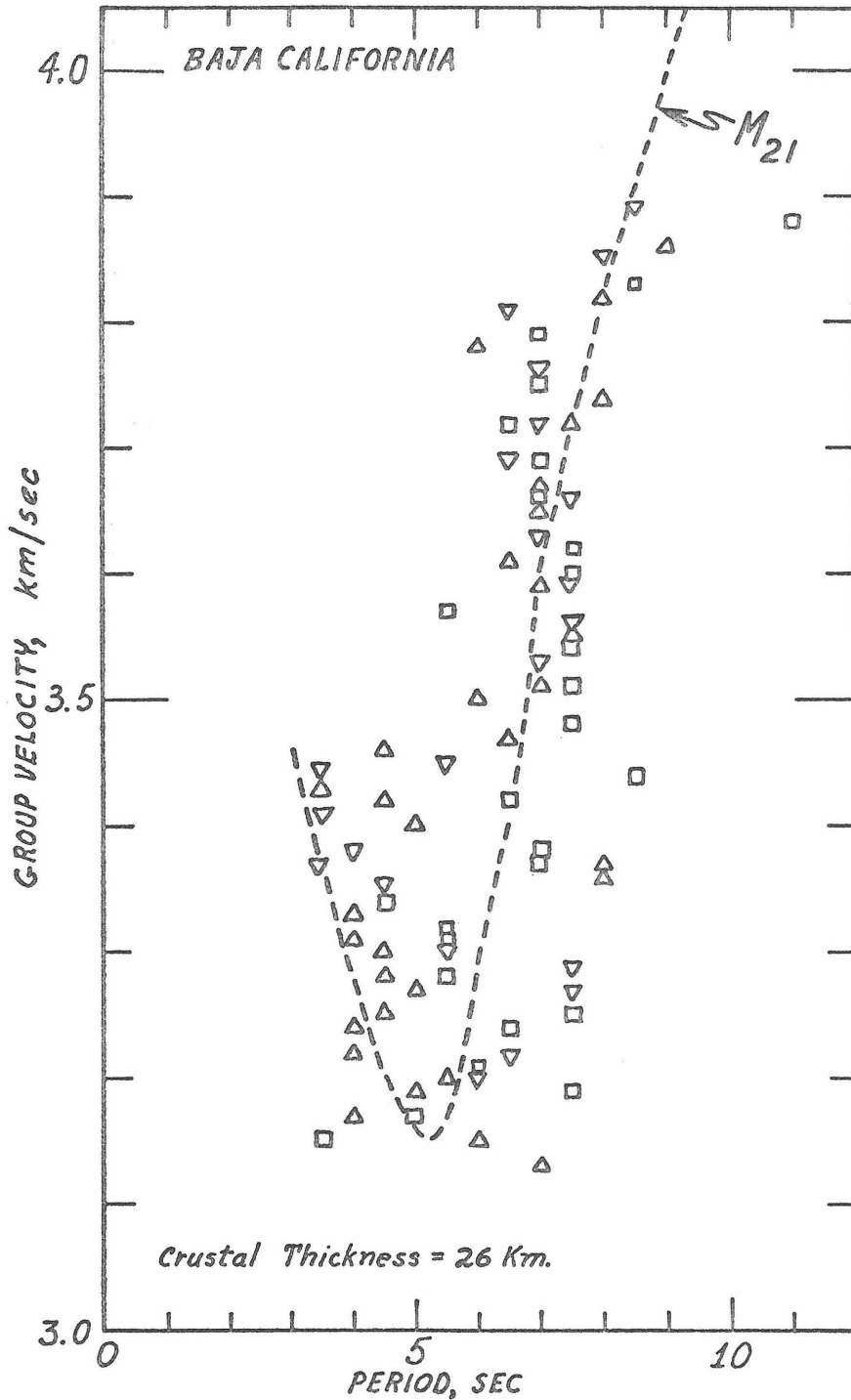


Figure 5. Baja California higher mode Rayleigh wave data and first higher mode curve for best Baja crustal model. Once crustal velocity gradients are fixed the position of the  $M_{21}$  curve is very sensitive to crustal thickness.

higher mode Love waves are being excited by the source and the resulting mixed mode wavetrain is not being interpreted correctly. It is shown in Chapter II that for a representative range of earth models the fundamental and first higher mode group velocity curves approach each other closely or overlap in a period range up to about 100 seconds, details varying from model to model. Though the closest approach of the curves in figure 4 is about 0.35 km/sec at  $T = 35$  seconds, the difference in arrival times at these epicentral distances is only 25 seconds and mode interference is still possible. In addition, the first higher mode group velocities may be depressed more by decreasing shear velocities in the low velocity channel without significantly changing the fundamental mode Love and Rayleigh wave dispersion for periods less than 40 seconds. However the explanation here in terms of higher Love mode excitation is not proven and the question is unresolved. It should be noted here that in several other regions of the world anomalously high Love wave phase velocities have been observed, and this may or may not be related to the high group velocity measurements reported in this study (i. e. measured phase velocities may be anomalously high if caused by higher mode interference, while corresponding group velocities are close to those expected for the fundamental mode). The effect of higher mode interference on measured phase velocities is dealt with fully in Chapter II and will not be considered further here.

Alternatively, we observe that Love waves are transversely polarized horizontal shear waves, and the width of Baja is at most

about 100 km, with sharp lateral gradients in crustal thickness on both boundaries. It is possible that SH waves with wavelengths greater than the width of the peninsula feel the adjacent oceanic and Gulf velocities as well as those beneath Baja, and this would adequately account for the higher velocities observed for Love wavelengths longer than about 80 km. Rayleigh waves, being longitudinally vertically polarized P-SV motion, would presumably be unaffected by this horizontal inhomogeneity. Unfortunately neither numerical nor analytical solutions exist for Love wave propagation with these boundary conditions, so again the suggestion cannot be verified.

(b) Gulf of California

The crustal models for various segments of the Gulf derived by Phillips [1964] from seismic refraction results demonstrate that there are great changes in crustal structure between the head of the Gulf and its mouth, as well as suggesting from one refraction line that there may be significant variations across the Gulf as well. With these indicated strong lateral velocity gradients it is to be expected that surface waves propagating up the Gulf may be guided or laterally refracted by the structures, and that the great circle path between source and receiver may not in all cases represent the true transmission path. Without a large aperture array it is not possible to accurately assess the importance of lateral refraction. However in several instances earthquakes whose great circle paths were almost identical had significantly different measured dispersion,

indicating the possible importance of non-least time paths, although source location error is another possible explanation of the discrepancy. With these possible drawbacks in mind, three groupings have been made of those Gulf surface wave data which (regardless of path) show similar dispersion. Though some paths from different groupings do overlap, each group does outline a general region within the Gulf. Each grouping of data shows the corresponding great circle paths between sources and stations and intercomparisons may be easily made by the reader. Note that the group velocities for the mainland portions of the path have been subtracted out from all the data using the fundamental mode Rayleigh wave data from the Baja paths.

Figure 6 shows the data and paths for a grouping designated as "Western Gulf." The three earthquakes sources used are in the southern Gulf, so the paths average the structure for almost its whole enclosed length. The Rayleigh wave group velocities between 15 and 25 seconds are the highest measured for Gulf paths. The fundamental ( $M_{11}$ ) and first higher mode ( $M_{21}$ ) dispersion curves for the crustal model which has been fit to the observations is shown in figure 6. Also shown for comparison is the fundamental mode dispersion curve derived from the "Central Gulf" data. Note the differences in the shapes of the curves as well as their differing group velocities. The structure is close to oceanic and the indicated crustal thickness is about 9 km. The  $S_n$  observations agree well with the  $M_{21}$  curve between 5 and 10 seconds. Near 20 seconds several group velocity points are high with respect to the model

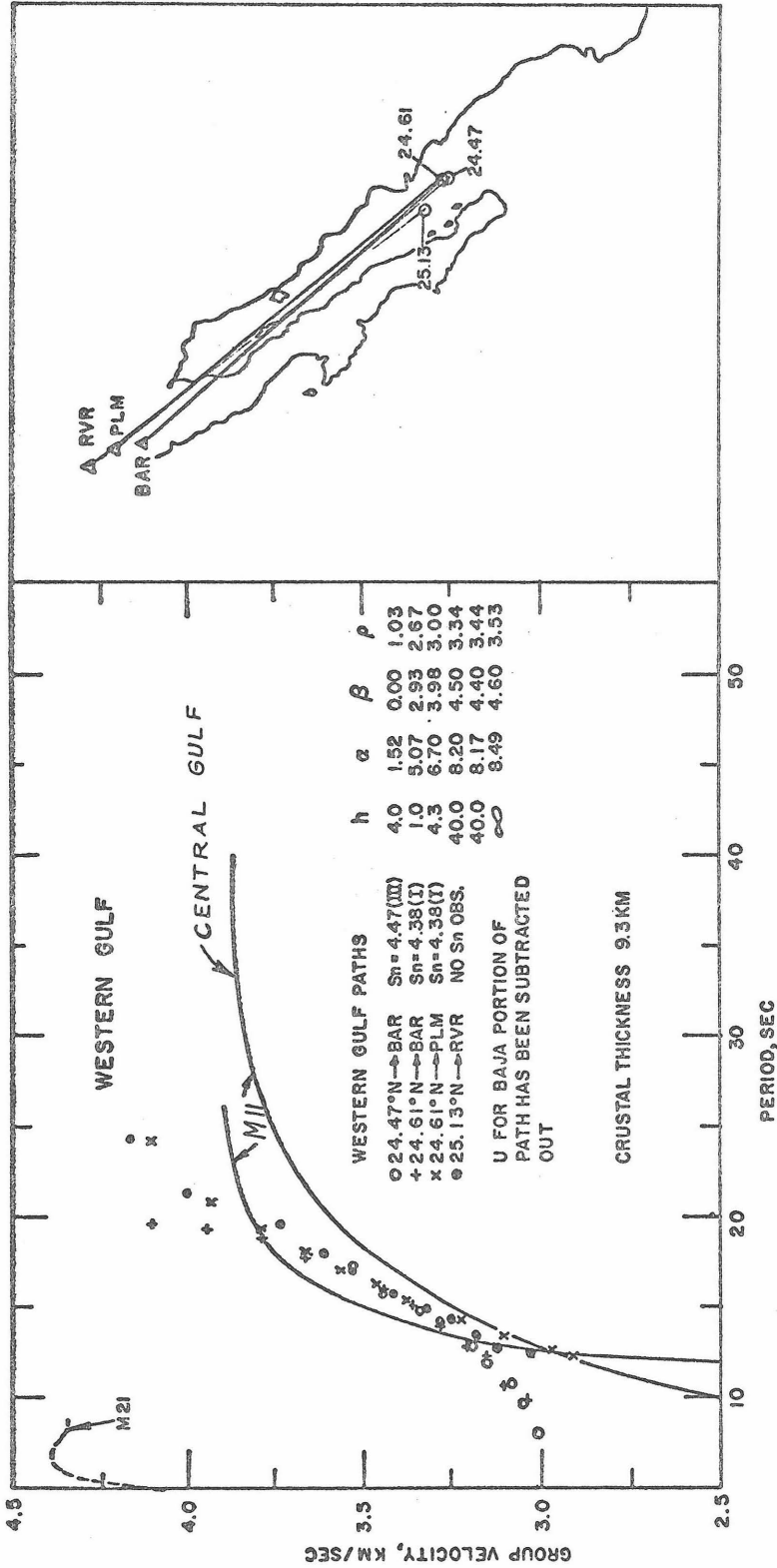


Figure 6. Earthquake sources, propagation paths, observed fundamental and first higher mode ( $S_n$ ) Rayleigh wave dispersion, and crustal model fit to the data for the western Gulf. Shown for comparison is the derived dispersion curve for the central Gulf.

curve. Such high group velocities had previously been observed for oceanic data in this period range by Sykes and Oliver (1964).

Additional independent evidence for near-oceanic structure close to the "Western Gulf" surface wave paths is provided by a refraction profile of Phillips [1964]. This profile, parallel to the axis of the Gulf, lies between Angel de la Guardia Island and the Baja mainland and indicates a Moho depth at 11 km. All of Phillips profiles from Guyamas south show approximately oceanic crustal structure.

A group of data from six earthquakes whose paths very roughly define a central region of the Gulf are shown in figure 7. These data comprise the least distinctive spatial grouping of Gulf great circle paths: a wide region of the Gulf is enclosed by the paths and several of them are close to those for the two other Gulf regions. The likelihood is greatest in this group of data that some or all of the paths may be non-least time ones or they may traverse more than one distinctly different crustal structure. Again these possibilities are difficult to unambiguously ascertain, and we have again fit all of the data with one average crustal structure. The crustal thickness is about 18 km and all the fundamental mode and  $S_n$  data adequately fit the derived dispersion curves.

Figure 8 is similar to the previous two and shows the results for paths in the Northeasterly Gulf region. The earthquake sources are more towards the mid-Gulf region, and hence this group of data may differ from the previous set only because the average crustal thickness is slightly greater over the paths shown in figure 8. At any rate, all the paths do define a narrow region, and a model which

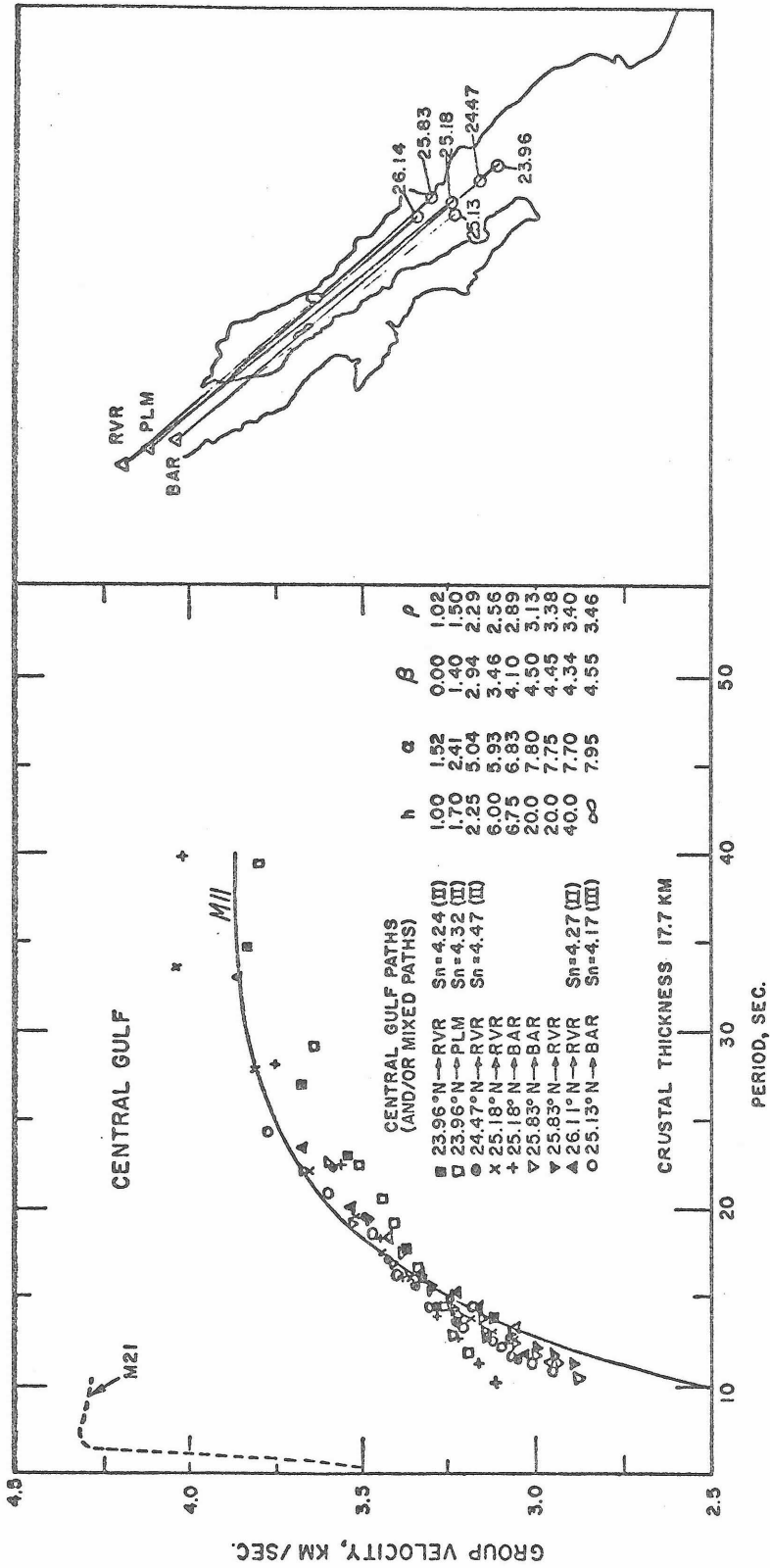


Figure 7. Earthquake sources, propagation paths, observed fundamental and first higher mode ( $S_n$ ) Rayleigh wave dispersion, and crustal model fit to the data for the central Gulf. This grouping of paths comprises the least distinct data set for the Gulf, and here the probability of lateral refraction and/or composite structures along the path is highest.

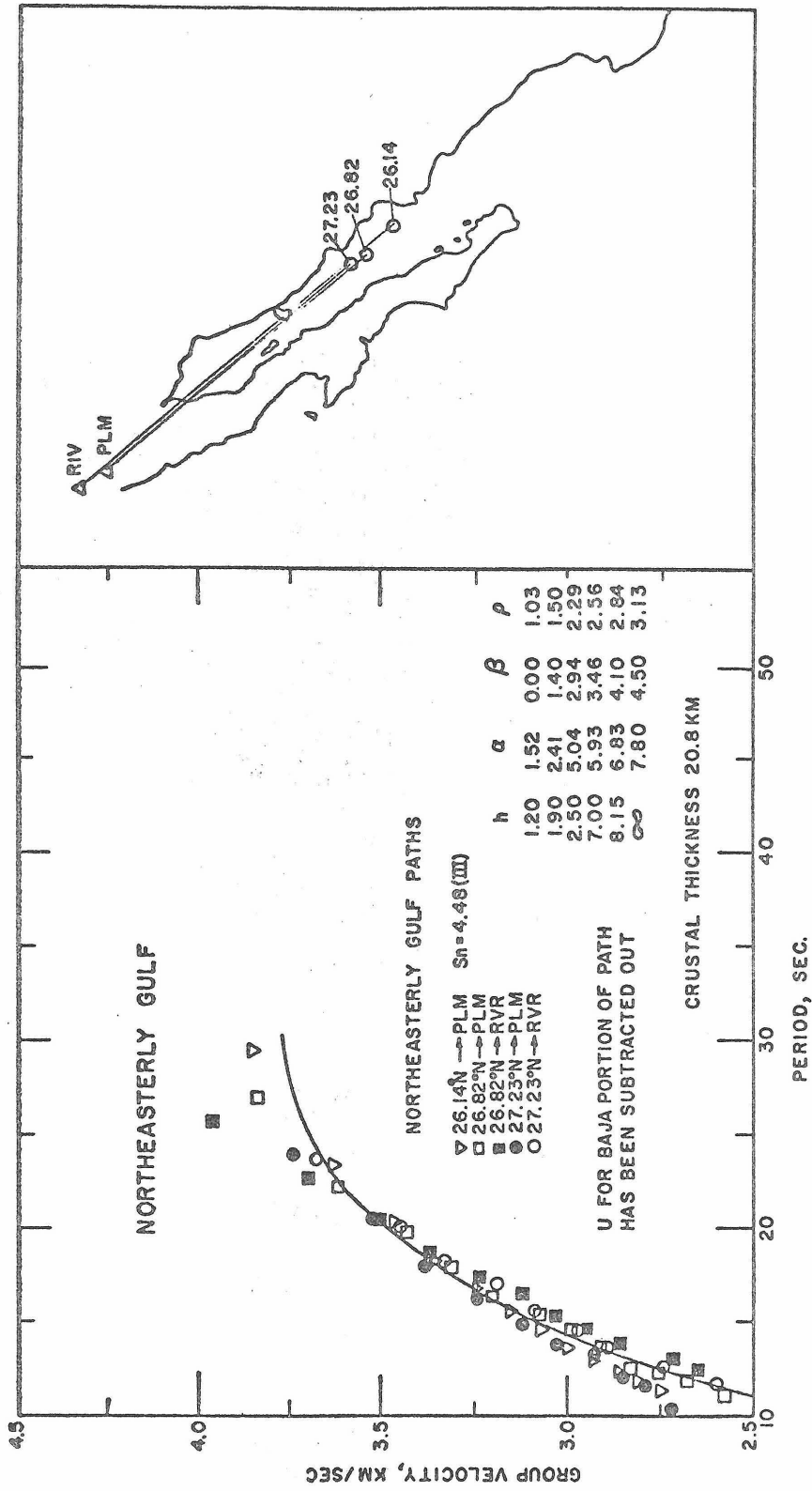


Figure 8. Earthquake sources, propagation paths, observed fundamental mode Rayleigh wave dispersion and crustal model fit to the data for the northeastern Gulf.

fits the data has a crustal thickness of about 21 km.

(c) Sonora

Fundamental mode Rayleigh wave dispersion for surface wave paths between the Gulf and Tucson Arizona has been measured and is illustrated in figure 9. Compared to the Baja observations, the Sonora path data are about 0.1 to 0.2 km/sec higher beyond 20 seconds and this increases as a function of period. The crustal thickness of the derived model is similar (24 vs. 26 km) but upper mantle velocity for Sonora is considerably higher, 4.45 km/sec.

#### P-DELAY OBSERVATIONS

En echelon patterns of fault traces, high heat flow and relative topographic depression all suggest that the Imperial Valley-Colorado Delta region may be a northward structural continuation of the Gulf of California. Relative arrival times of  $P_n$  and teleseismic P waves observed at stations in this area comprise the best presently-available seismic data on the crust-upper mantle velocities and crustal thicknesses in this region. Observations by several different investigators have been utilized here in order to make some tentative statements concerning crustal structure in this interesting region.

The travel times of seismic waves relative to a particular velocity depth structure can provide information on lateral changes in crust/upper mantle structure between adjacent regions. This comparison is particularly useful when the structure in one of the regions has been determined from other seismic observations. The regional

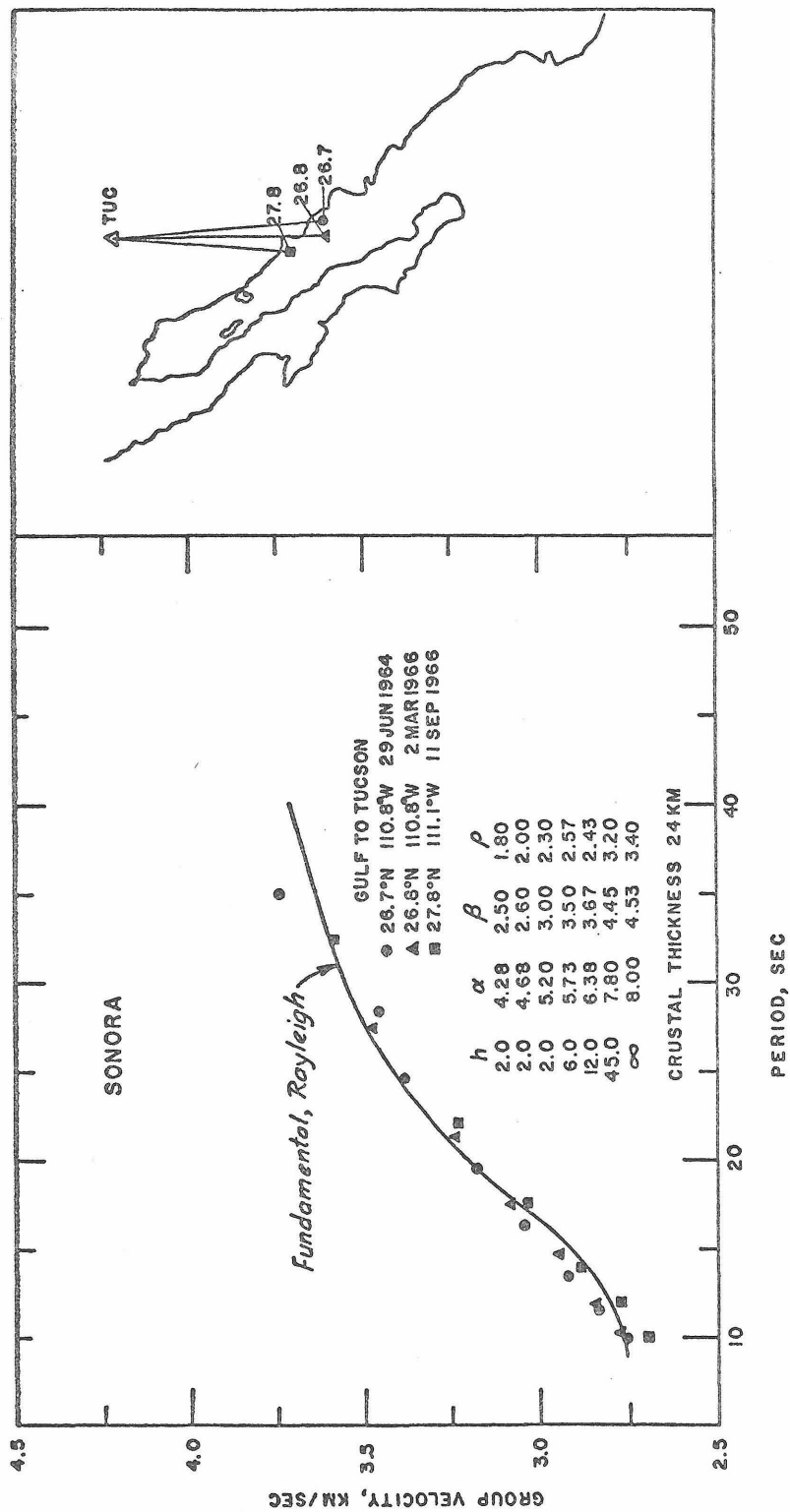


Figure 9. Sources, paths, observed Rayleigh dispersion, and model fit to the data for Sonora.

difference in velocity structure between the Imperial Valley and adjacent regions in Southern California is clearly demonstrated in figure 10, a  $P_n$  travel time plot which compares arrivals at permanent Caltech stations with those from a temporary array within the Imperial Valley. These data are taken from an unpublished preliminary study of the region carried out by D. N. Clay of Caltech. It is clear that  $P_n$  times to Imperial Valley stations are one to two seconds early with respect to a  $P_n$  line through Goldstone, Riverside and Palomar stations with an apparent velocity of 7.8 km/sec. This difference can be due to increase in  $P_n$  velocity along the path to the Imperial Valley, increase in crustal velocities in the Valley, decrease in crustal thickness, or all three factors. Let us consider each of these factors in turn. A reversed refraction line between NTS and Ludlow, California yields a  $P_n$  velocity of about 7.8 km/sec and a crustal thickness of about 28 km [Gibbs and Roller, 1966]. If all of the early  $P_n$  arrival time in the Valley were due to an increase in upper-mantle velocity along the path from Ludlow, the  $P_n$  velocity on this segment would be about 8.4 km/sec. Realistic changes in average crustal velocities in the Valley could not by themselves account for the early  $P_n$  times. Crustal thinning alone could explain them if Moho depth decreased by about 8 km beneath the Imperial Valley.

Unfortunately there is no direct evidence on  $P_n$  velocity within the Imperial Valley, and an increase from 7.8 km/sec is not definitely precluded. However, it should be especially noted that if the  $P_n$  velocity south of Ludlow through to the Gulf were consistently high,

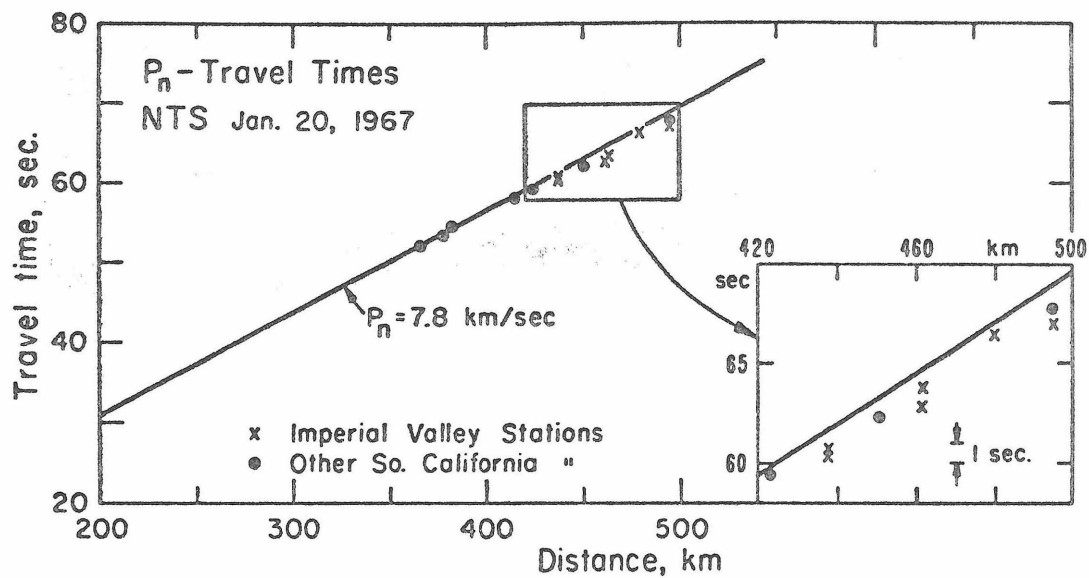


Figure 10.  $P_n$  travel time plot comparing arrival times at Caltech stations in southern California with those in the Imperial Valley using as sources underground explosions at Nevada Test Site (NTS). Note early arrivals in the Imperial Valley.

then the  $P_n$  anomalies would increase with epicentral distance, and this is not seen in the data examined here (see figure 12, to be discussed below). Also, a  $P_n$  velocity near 7.8 km/sec has been measured both north of the Valley and within the Northern Gulf. Phillips' [1964] refraction results show  $P_n$  velocities between 7.8 and 8.3 km/sec on 4 of his 16 Northern Gulf profiles, but none of these 4 are reversed, and he feels the lower value is much more probable for the Northern Gulf region.

In addition to the  $P_n$  delays, an unpublished study has been made by Brune of teleseismic P delays at stations from Barrett east to the California-Arizona border. He used earthquakes in the Western Pacific and was careful that their paths all had about the same azimuth from source to stations. The results are shown in figure 11, which is a plot of travel time residuals with respect to Palomar as the standard. Variations in P delays can again be caused by changes in average crustal velocity and crustal thickness, as well as vertical changes in sub-Moho velocity. Thus, for example, a teleseismic P arrival which is 0.5 seconds early with respect to Palomar (e.g. Barrett or Signal Mtn.) could indicate an increase in upper mantle velocity of 0.4 km/sec in a thickness of about 75 km, or a crustal thinning of nearly 12 km. With these numbers in mind the teleseismic P-delays can be compared with the  $P_n$  delays, which are plotted on the map in figure 12. The P-delays may be suggesting a thickening of the crust by as much as 12 km from Barrett towards the crest of the Peninsular Range batholith (Palomar, Jacumba stations). To be consistent with the  $P_n$  delays there must be a significant increase

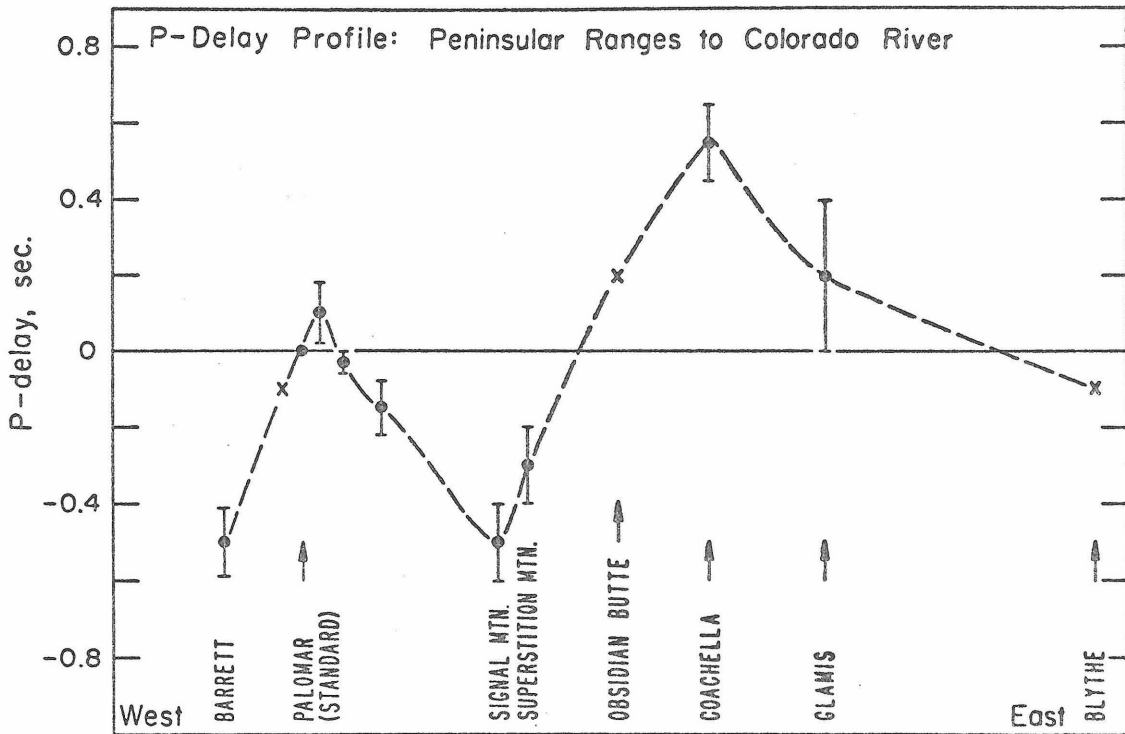


Figure 11. Teleseismic P-wave travel time residuals along a west to east profile north of the International border.

in upper mantle velocity beneath the crust of the Peninsular Ranges, and rather less to the west of it. East of the batholith the large P-delays (0.4 sec early) and  $P_n$  delays (1.5 sec early) at Superstition and Signal Mountains are consistent with 8-12 km of crustal thinning and a  $P_n$  velocity of 7.8 km/sec. However the upper mantle velocities could be high, perhaps 8.2-8.4 km/sec without any thinning required. Further east at Obsidian Butte the P delay is + 0.2 sec and  $P_n$  delay - 0.6 sec, suggesting either crustal thickening or lower crust and/or upper mantle velocities as compared with the stations to the west, Superstition and Signal mountains. Recent volcanic activity and locally high heat flow and potential geothermal steam support such speculation about lower seismic velocities in this area. Coachella is similar to Obsidian Butte, the P-delay decreases at Glamis, and by Blythe, on the California-Arizona border both  $P_n$  and P delays are near zero.

A quarry blast in Corona, California was recorded at Barrett and at two portable stations in the Sierra Juarez, a continuation of the Peninsular Ranges into Northern Baja California.  $P_g$  was the first arrival at Barrett ( $\Delta = 150.8$  km, and  $P_n$  was recorded at the two Baja stations (277.1 and 338.9 km distant). Assuming a crustal velocity of 6.2 km/sec and a  $P_n$  velocity of 8.0 km/sec gives an average crustal thickness near 43 km beneath the Baja stations. However at the further station, which is both nearer the crest of the Sierra Juarez and across the Agua Blanca fault, the  $P_n$  arrival suggests the crust is 10 km thicker than beneath the nearer station.

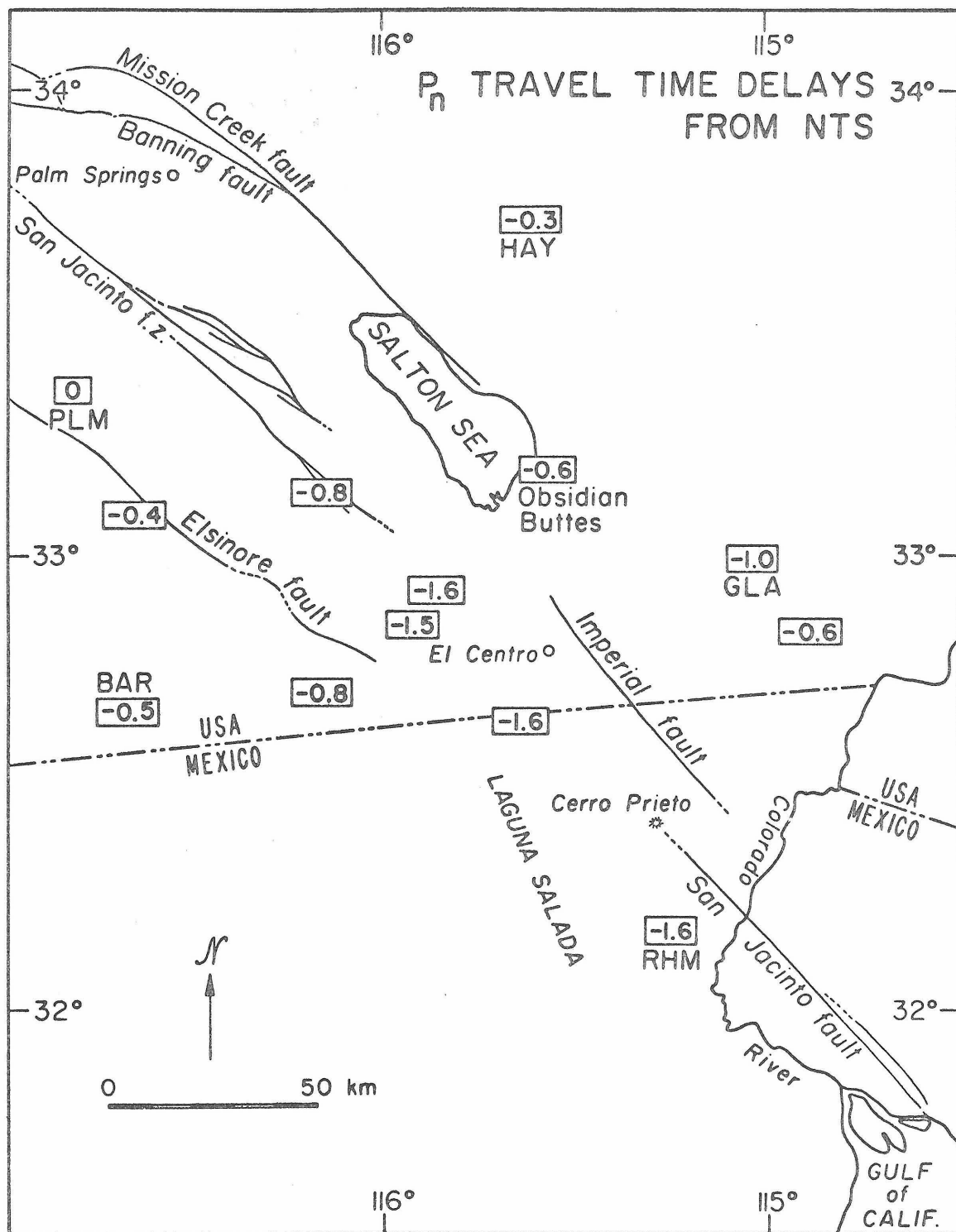


Figure 12.  $P_n$  travel time delays in the Imperial Valley-Colorado delta region.

## SUMMARY

Measurements of surface wave dispersion and P-delays have indicated significant differences in crustal structure between the Imperial Valley-Gulf of California province and the land areas both to the east and west of it (Peninsular Ranges-Baja California, and Sonora). The observation of unusually high Love wave group velocities across Baja has been noted, and the possibility of higher mode propagation was suggested. The general problem of higher mode propagation and the interference effects it produces are considered in detail in the next chapter.

## CHAPTER II

HIGHER MODE INTERFERENCE AND OBSERVED  
ANOMALOUS APPARENT LOVE WAVE PHASE VELOCITIES

## ABSTRACT

For a representative selection of spherical earth models compatible with seismic observations, there is a significant frequency range over which the fundamental and first higher Love mode group velocity curves approach each other closely or actually overlap. Higher Love modes can be excited comparably to the fundamental mode for both shallow and deep sources under a variety of circumstances, and thus higher mode interference is an important factor to be taken into account in the proper interpretation and analysis of Love waves.

Simple theoretical computations reveal the nature of the effect of mode contamination on measured phase velocities, and biases in the selection and analysis of surface wave data make it appear likely that fundamental mode Love waves experiencing higher mode interference will exhibit anomalously high apparent phase velocities, as observed in the United States mid-continent and in Japan. Thus it is suggested that it may not be necessary to resort to complex or anisotropic models to explain these observations.

Consideration of the effects of mode interference, as well as knowledge of source parameters (type, depth, orientation), are

important in determining dependable fundamental and higher Love mode phase velocity dispersion over a broad frequency band. Phase velocity filtering across a large array could effectively separate the modes. Love waves traversing continental regions from the source will suffer little or no contamination from higher modes for wave periods less than about 60 seconds, and thus are preferred to oceanic paths in obtaining reliable fundamental mode data in this restricted frequency range.

## INTRODUCTION

Unexpectedly high Love wave phase velocities have been observed in several different parts of the world: Aki and Kaminuma [1963] in Japan, and McEvelly [1964] in the mid-continent of the United States, found it impossible to explain both Love and Raleigh wave observations with a single simple plane isotropic layered earth model.

Two different explanations have been advanced to account for these anomalous observations. By assuming that the SH wave speed was 6 - 8% higher than that for SV, both McEvelly [1964], and Kaminuma [1966c] were able to explain their observations with a single anisotropic model. Takeuchi et al. [1968] showed that elliptical magma pockets in the upper mantle could alter the effective rigidities felt by SH and SV waves and account for the anisotropy the above models required. Aki [1968] proposed a laminated model which included thin soft layers in the lower crust

and upper mantle beneath Japan, and he demonstrated that such a model could fit all of the surface wave data. Hales and Bloch [1969] suggested the same is true for the central and western United States and perhaps world-wide.

The only other comprehensive study of regional surface wave dispersion, which includes both Love and Rayleigh wave data, is the paper of Brune and Dorman [1963] on the Canadian shield, and they found no difficulty in fitting all observations with one simple model.

We propose that the anomalous Love wave observations are the result of higher mode interference. In support of this hypothesis we shall show fundamental and higher mode group and phase velocity curves computed for three well-accepted spherical earth models which fit observed surface wave data. The importance of higher modes in Love wave propagation is demonstrated by citing evidence from the literature on the excitation of the higher modes relative to the fundamental. In order to quantitatively demonstrate the effect of mode superposition on measured Love wave phase velocity, a simple theoretical result is obtained and the apparent phase velocities are evaluated numerically for a range of relevant parameters. The significance of these results is discussed in terms of the actual selection and analysis of surface wave data, and it appears that the inconsistent Love wave-phase velocity observations may be explained by higher mode interference. In concluding, there is a brief discussion of methods which may be used to obtain reliable contamination-free fundamental mode Love wave phase velocity data, as well as possibly to isolate the higher modes for study of

the deeper mantle.

## FUNDAMENTAL AND HIGHER MODE LOVE WAVE DISPERSION

Phase and group velocity dispersion for the fundamental and first two higher modes have been computed for three standard spherical earth models using the accurate "earth-stretching approximation" of Anderson and Toksoz [1963]. Figure 13 shows the oceanic model CIT11A of Kovach and Anderson [1964]. Note especially the broad region of overlap of the fundamental and first higher mode group velocity curves and the distinct separation of the corresponding phase velocities. Results for a shield model almost identical to the Canadian shield model of Brune and Dorman [1963] (CANS D with an increasing gradient below 400 km taken from Anderson and Harkrider's [1968] shield model) are shown in Figure 14. Note that the fundamental and first higher mode group

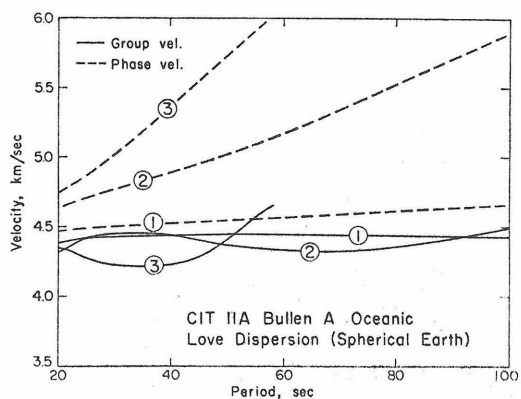


Fig. 13 Love wave phase and group velocity dispersion for the first three modes of the spherical oceanic earth model CIT11A.

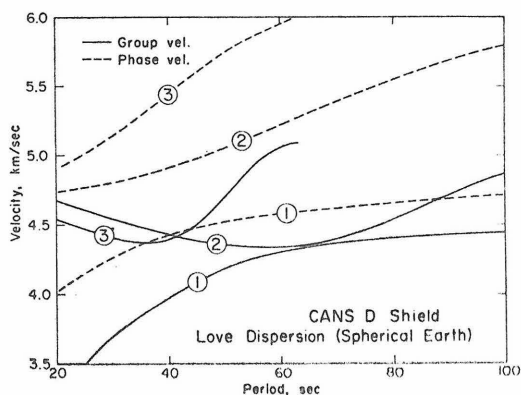


Fig. 14 Love wave phase and group velocity dispersion for the first three modes of a spherical shield earth model slightly modified from CANS D.

velocity curves approach to within 0.01 km/second of each other near a period of 65 seconds, close to where Brune and Dorman's Love wave data terminate (they stopped their analysis where the Sa phase was expected to arrive on the seismogram). Finally, in Figure 15 is the dispersion for Anderson and Harkrider's [1968] tectonic model.

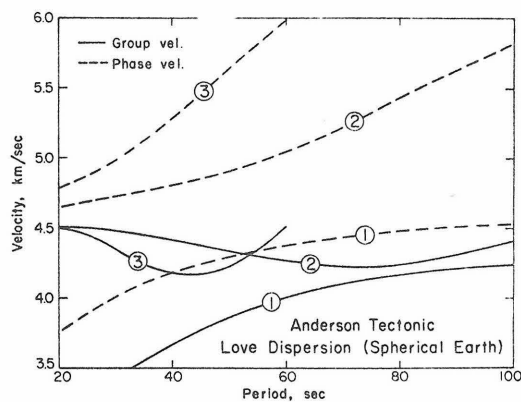


Fig. 15 Love wave phase and group velocity dispersion for the first three modes of the spherical tectonic earth model of *Anderson and Harkrider* [1968].

Thatcher and Brune [1969]

It should be noted that the presence or absence of overlap or near-overlap of the fundamental and higher mode group velocity curves as well as the details of the overlap can be accurately studied only for computations carried out for spherical earth models. The overlap depends significantly on the structure below 400 km depth. Other spherical earth calculations have been previously reported by Anderson and Toksoz [1963], Jobert [1964, 1966], Kovach and Anderson [1964], and several of these models show features similar

to those described above.

The group velocities of the two modes need not exactly coincide at a given frequency in order to produce mode mixing: it is only necessary that both modes be in the same group velocity window used in the phase velocity analysis, or, in the case of the graphical method, that the time separation of the mode arrivals be of the order of a wave period or less.

### HIGHER MODE EXCITATION

The degree to which higher modes are excited relative to the fundamental depends on both the source parameters of the earthquake (type, depth, orientation) and on the earth model through which the waves are being propagated.

Ben Menahem and Harkrider [1964] have studied the far-field displacement produced by dipolar sources in plane layered media, and several conclusions from their study are relevant here. The surface radiation pattern was shown to be a function of the depth and orientation of the force configuration, and differed for different wave periods. Furthermore, it was illustrated that the fundamental and first higher mode Love wave radiation patterns for the same source and wave period may differ considerably.

Harkrider and Anderson [1966] computed the partitioning of surface wave energy between different Love modes for buried point sources and several plane layered earth models. The spectral excitation of each mode for a surface source is computed by them for

an oceanic and a shield model (refer to their Figures 4 and 5, p. 2976). Their results for an oceanic model and buried horizontal point force are reproduced here in Figure 16. Note that for periods less than about 100 seconds the energy densities of the first 2 modes are comparable even for surface sources (for Rayleigh waves this is not the case, the fundamental having about an order of magnitude more spectral energy for a surface force). The importance of the first higher mode relative to the fundamental does not increase as rapidly with depth for the Love modes as it does for the Rayleigh. Hence higher Love modes should in general be observed more often for shallower source foci than higher Rayleigh modes. It should be noted that the observation of first higher mode Rayleigh waves by Kovach and Anderson [1964] are in qualitative agreement with the energy partitioning among the various Rayleigh modes computed by Harkrider and Anderson [1966].

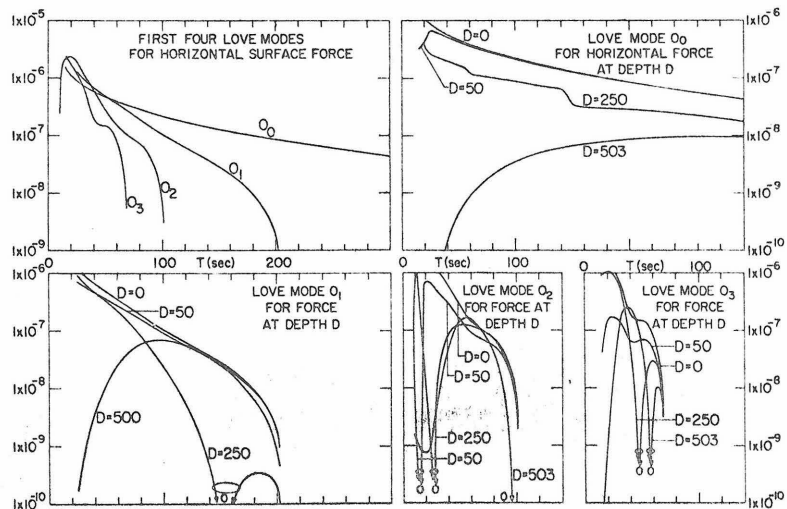


Fig. 16 Love wave spectrum energy densities per unit oceanic propagation path in units of  $10^{15}$  ergs/km for buried horizontal forces of strength  $(L) = 2 \times 10^{15}$  dynes sec (from Harkrider and Anderson [1966], p. 2978, figure 9).

The same authors have also computed the spectral energy density partitioning among modes for surface waves propagating through a shield-type velocity structure. For a surface source they showed that the fundamental Love mode has about a factor of two greater amplitude than the higher modes in the period range less than 100 seconds. We might surmise that the degree to which the low velocity channel is developed exerts a strong influence upon the relative excitation of the higher Love modes. Of course the actual ground displacements due to the different modes depend on the displacement versus depth curves for the individual modes at specified wave periods, as well as on the partitioning of spectral energy density. If we refer to such curves in Anderson and Toksoz [1963] for example, we see that surface displacements are comparable to the maximum displacements for several of the higher modes throughout a wide period range.

Jobert [1962, 1964, 1966] has computed Love wave spectral amplitudes in spherical earth models due to buried torque sources by summing toroidal oscillations up to order number  $n$  approximately 2000. For a "Gutenberg type" continental model she found that the spectral amplitudes of the higher modes were in general about one-fifth as strong as the amplitude of the fundamental. Her models were not derived from surface wave observations however, and none produced the overlapping of fundamental and higher mode group velocity curves which we have illustrated for CANSD, CIT11A, and Anderson's tectonic model. As we have noted previously, higher mode excitation and mode overlap appear to be sensitive to

how pronounced the low velocity channel is and to the structure below 400 km depth. However at present we cannot with complete certainty say whether the lower amplitude of the higher Love modes computed by Jobert is a result of sphericity or of the details of the mantle structures studied by her. At any rate, even if these amplitudes are taken as a minimum, interference of fundamental and first Love modes will still significantly alter the observed phase velocities, as is shown below.

It should be pointed out that examination of the excitation curves of Jobert and those shown in Figure 16, as well as from particle displacement versus depth curves and radiation patterns, reveals that the ratio of fundamental to first mode ground motion is relatively constant as a function of frequency for shallow sources, but may fluctuate considerably for deeper ones.

#### THE EFFECT OF ATTENUATION

The amplitude decay versus period observed for surface waves and free oscillations is consistent with an upper mantle relatively more attenuating than regions above or below it, and this highly attenuating zone may well be confined to regions of phase change and/or partial melt [Anderson and Archambeau, 1964; Anderson et al., 1965]. Then, taking the low velocity zone to be a region of low  $Q$  (high attenuation), it follows that surface waves with particle motions largely confined to this channel will be attenuated to a greater degree than those which are not. Study of dis-

placement versus depth plots for the higher mode waves in realistic earth models [ viz. Anderson and Toksoz, 1963; Kovach and Anderson, 1964] would lead us to expect the shorter period higher mode waves to be more attenuated than fundamental mode waves of corresponding periods, but that for periods of about 40 seconds and greater, differential attenuation of higher modes should not be important. This may explain, along with the shape of the group velocity curves, why contamination by higher modes does not appear at periods less than about 20 to 30 seconds.

#### SIMPLE THEORETICAL CONSIDERATION

In order to quantitatively understand the physical consequences of the mode interference we have shown will occur between fundamental and higher mode Love waves, consider the superposition of two sinusoidal waves. Let these waves have the same frequency but differing wave numbers, and let them arrive at an observation point  $x$  at approximately the same time  $t$  (and hence, have about the same group velocity). Ignoring terms corresponding to the initial phase at the source, we then have

$$\begin{aligned}
 & A(k) \exp(-ik_1x + i\omega t) + \lambda A(k) \exp(-ik_2x + i\omega t) \quad , \quad k = \omega/c \\
 & = A(k) \{ 1 + \lambda^2 + 2\lambda \cos[(k_1 - k_2)x] \}^{\frac{1}{2}} \exp(-i\psi + i\omega t) \quad (1)
 \end{aligned}$$

where

$$\psi = \psi(x) = \tan^{-1} \frac{\sin k_1x + \lambda \sin k_2x}{\cos k_1x + \lambda \cos k_2x}$$

and  $\lambda$  is an amplitude scaling factor (in general  $\lambda = \lambda(k)$ ). We observe that the composite waveform is modulated in amplitude by the square root term in (1), and the beat wavelength is given by

$$\lambda_b = \frac{T}{\frac{1}{c_1} - \frac{1}{c_2}} \quad (2)$$

Table 1 shows the beat wavelength as a function of wave period for fundamental and first higher mode interference in the three earth models CIT11A, CANSO, and Anderson tectonic. Observe that in all cases the beat wavelength is greater than 850 km, and that at 50 second period and beyond is greater than about 1700 km and varies only mildly as a function of frequency.

We note that the position of minima will be modified if the initial phase at the source varies as a function of frequency and is

TABLE 1. Beat Wavelength as a Function of Wave Period for Fundamental and First Higher Mode Interference in Three Representative Earth Models

$T$ , sec	$\lambda_b$ , km		
	CIT11A	CANSO	Anderson Tectonic
30	2385.0	1136.0	855.2
40	2461.3	1812.6	1276.6
50	2429.9	2153.4	1682.5
60	2362.7	2241.3	1907.2
70	2287.7	2263.8	1965.2
80	2216.8	2324.8	2030.9
90	2228.5	2372.9	2040.4
100	2240.1	2554.1	2064.3

different for the two modes. However, in analogy with the result of Knopoff and Schwab [1968] for the apparent initial phase of Rayleigh waves, we expect the effect to be small and vary little with frequency at teleseismic distances.

Examining the special cases  $\lambda = 0, 1$  in equation (1) we have

$$\begin{aligned}\psi(\lambda=0) &= -k_1 x \pm 2n\pi \\ \psi(\lambda=1) &= -\frac{1}{2}(k_1 + k_2)x \pm 2n\pi\end{aligned}\tag{3}$$

If the true wave number is  $k_1$  when only the fundamental mode is excited, then we must conclude that when both modes are excited comparably, the apparent wave number is  $\frac{1}{2}(k_1 + k_2)$ , and hence the apparent phase velocity is

$$\frac{1}{c} = \frac{1}{2} \left( \frac{1}{c_1} + \frac{1}{c_2} \right)\tag{4}$$

except across a node in the beat pattern (see discussion below).

For  $\lambda$  not near 0 or 1 we consider the apparent phase velocity measured between two stations on the same great circle as the earthquake. Using, for example, the formula in Brune and Dorman [1963] (p. 170, equation 1), we obtain that

$$c = \frac{x_b - x_a}{T \left[ \frac{\delta\psi}{2\pi} + N \right]}\tag{5}$$

where  $\delta\psi = \psi(x_b) - \psi(x_a)$  which must be evaluated numerically for specific values of  $x_a, x_b, k_1, k_2$ , and  $\lambda$ .  $N$  is an undetermined integer. We should note that  $\psi$  is indeterminate within  $\pm 2n\pi$ :

in Fourier analyzing a digitized seismogram to determine the phase

spectra, values of  $n$  are chosen for each frequency such that the phase is a continuous function of frequency. In equation 5 the value of  $N$  is chosen which results in the most "reasonable" phase velocity curve. In practice, this ambiguity is almost never a problem for station separations less than about 600 km or so (for smaller separations all but the appropriate curve are highly unreasonable).

We observe that since the interfering waves are beating, there is in general a phase shift across each amplitude minimum, the sharpness and character of which depends on the relative excitation  $\lambda$ . When the excitation of the two modes is comparable, the phase shift is approximately  $\pi$ , all of it occurs very close to the minimum, and the jump in phase is infinitely sharp for  $\lambda = 1$ . For  $\lambda < 1$  the phase shift is positive, decreases from  $\pi$  as  $\lambda$  decreases, and may be spread over a few hundred kilometers about the minimum. For  $\lambda > 1$  there is a negative phase shift whose sharpness decreases and whose magnitude increases for increasing  $\lambda$  such that  $c \rightarrow c_2$  as  $\lambda \rightarrow \infty$ . If the beat wavelength is large compared to the station separation (see figure 17), most measurements made of phase velocity will not be across an interference minimum, and hence

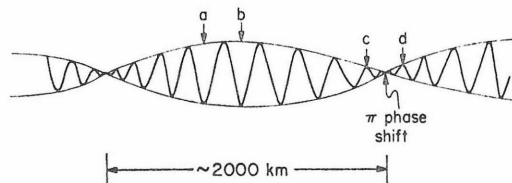


Fig. 17 Illustration of the effect of equal-mode interference on the measurement of phase velocity. Phase velocity measured between  $a$  and  $b$  will appear to be between the two phase velocities. Observations between stations  $c$  and  $d$  will give quite erratic results and low amplitudes and will usually be discarded.

the apparent phase velocity will appear to be between that of the fundamental and the higher mode. The probability of crossing a minimum is approximately proportional to the ratio of station separation to beat wavelength. Whenever two stations do happen to straddle an amplitude minimum there will be a strong tendency to disregard the data, both because the amplitudes are low and because the phase spectra will often appear incoherent. Such measurement biases are discussed further in the next section.

Figures 18 through 20 show curves of apparent phase velocity computed from equation 5 for three spherical earth models and a range of appropriate values of station separation, epicentral distance, and relative excitation. In each curve we assume for simplicity that  $\lambda$ , the relative excitation, is not a function of frequency (the restric-

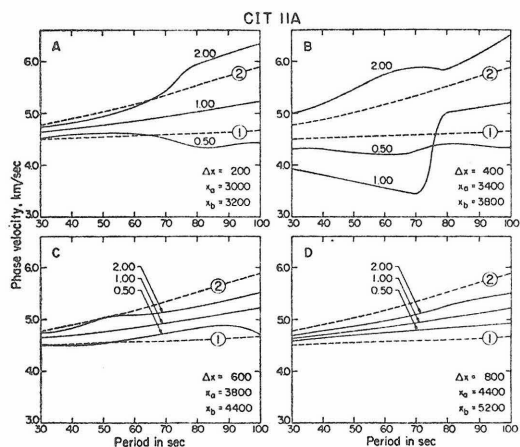


Fig. 18 Apparent phase velocity computed for interference between fundamental and first higher mode Love waves, CIT11A earth model, for representative values of relative excitation parameter  $\lambda$ , station separation  $\Delta x$ , and epicentral distances  $x_a, x_b$ . Numbers on each curve refer to values of  $\lambda$ . Dotted curves are fundamental ( $\lambda = 0$ ) and first higher mode ( $\lambda = \infty$ ) phase velocity curves.

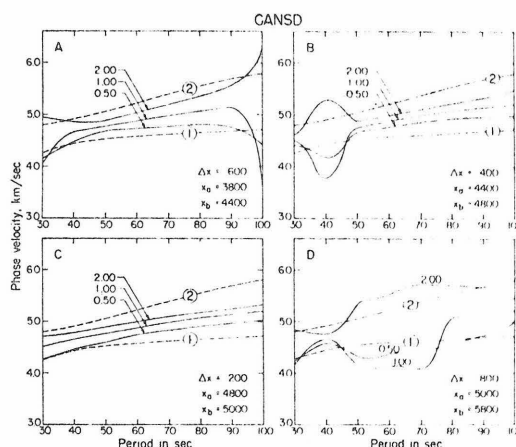


Fig. 19 Apparent phase velocity computed for interference between fundamental and first higher mode Love waves, CANSO earth model, for representative values of relative excitation parameter  $\lambda$ , station separation  $\Delta x$ , and epicentral distances  $x_a, x_b$ . Numbers on each curve refer to values of  $\lambda$ . Dotted curves are fundamental ( $\lambda = 0$ ) and first higher mode ( $\lambda = \infty$ ) phase velocity curves.

tion is one of convenience, not necessity). We have attempted to be as representative as possible in the cases shown in the figures: the range of possibilities and their approximate frequency of occurrence are represented as accurately as possible in the number of cases illustrated. By avoiding all amplitude minima in our choice of plotted results we could have eliminated all of the irregularly fluctuating curves. Since the beat phenomenon is periodic, the same pattern of phase velocity curves will eventually occur, and the approximate "wavelength" over which the predominant variations will repeat themselves is of the order of the average beat wavelength, or in the vicinity of 2000 km. This is about the range in epicentral distances computed for each earth model shown in the figures. The fundamental ( $\lambda = 0$ ) and first higher mode ( $\lambda = \infty$ ) phase velocity curves are

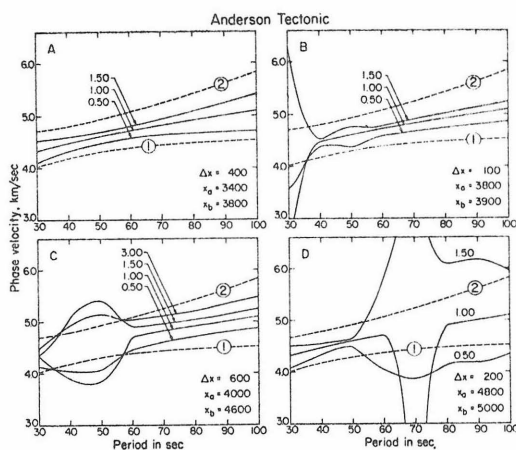


Fig. 20 Apparent phase velocity computed for interference between fundamental and first higher mode Love waves, Anderson's tectonic earth model, for representative values of relative excitation parameter  $\lambda$ , station separation  $\Delta x$ , and epicentral distances  $x_a, x_b$ . Numbers on each curve refer to values of  $\lambda$ . Dotted curves are fundamental ( $\lambda = 0$ ) and first higher mode ( $\lambda = \infty$ ) phase velocity curves.

shown for reference on each of the graphs. We note that for larger station separations than are shown in the figures the phase velocity fluctuations can be chosen, for  $\lambda < 1$ , to be less extreme by an appropriate choice of  $N$ , though departures from the fundamental mode curve are still significant.

#### BIASES IN THE ROUTINE ANALYSIS OF PHASE VELOCITY DATA

We have shown that in Love wave propagation higher mode interference is expected to play an important role in contaminating what are supposed to be fundamental mode phase velocity observations. It might be supposed that in some cases the rapid fluctuations in apparent phase velocity which occur across a beat minimum would be observed in the results of Love wave dispersion studies. However, the manner in which surface wave data are selected and analyzed makes it highly unlikely that such fluctuating data would be seen in the final results of any phase velocity study.

First of all, highly subjective criteria are employed by seismologists in the routine selection of "good" surface wave data. Amplitudes must be large, and the presence of beats in the visible wave train or discontinuities in the phase spectra are justifiable grounds for discarding any particular event. Without further justification these "poor data" are summarily ascribed to processes such as multipath propagation, lateral refraction, inhomogeneities causing distorted wave fronts, multiple events, interference, and other miscellaneous causes. It is necessary to go no further than

the studies in the mid-continent U.S. and Japan to encounter justifications such as these. These difficulties can and do occur: we wish merely to point out that data which are "poor" as a consequence of mode mixing will be eliminated from analysis by the same criteria as are employed to exclude what is poor for other reasons. Conversely, mixed mode wavetrains which produce smooth apparent phase velocity curves will not be eliminated by any of the requirements enumerated above, will hence be regarded as "good" data, and will exhibit anomalously high apparent phase velocities.

Even data which satisfy all preliminary requirements may be eliminated in the course of analysis. Whatever method the investigators of the mid-U.S. and Japan employed to determine phase velocity, they state that the graphical peak-and-trough method [Brune et al., 1960] was at least employed as a check on the consistency of results. It seems that in most instances one could not successfully correlate phases across an amplitude minimum of the beating waves because of the phase shift involved in the crossing of such a point (refer again to Figure 17).

Further, every phase velocity method in current use involves either implicit or explicit smoothing of the phase spectra. The peak-and-trough method is an implicit smoothing. The least squares method, employed by Aki and Kaminuma [1963] in Japan does the same. Investigators such as Pilant and Knopoff [1964] and Knopoff et al. [1966] directly apply polynomial smoothing of the phase spectra. All of these methods would tend in many cases to decrease fluctuations in apparent phase velocity which might exist in the real data.

In addition (as, for example, in McEvilly's study) data for a particular event are often collected over a restricted frequency range, and hence any possible phase velocity fluctuations not eliminated by smoothing would often be excluded because data beyond a certain period began to scatter or behave anomalously in some respect.

We conclude then that commonly-accepted procedures employed in the routine selection and analysis of surface wave data militate against observations of rapid fluctuations in Love wave phase velocity curves which we have shown can in principle sometimes occur as a result of higher mode interference.

Perhaps we hardly need add that few investigators would have enough confidence in their results to present in published form any extreme phase velocity fluctuations which they might discover. The many explanations alluded to above which are commonly given to account for such anomalies would be enough justification for completely disregarding these data.

## DISCUSSION

The majority of the anomalous Love wave data for Japan are from a shallow earthquake in the Aleutians recorded at selected stations in Japan [ Aki and Kaminuma, 1963]. Kaminuma [ 1966a], with short period data (the longest period Love waves were 34 seconds) from 11 earthquakes recorded at three stations in Central Japan, verified some of the earlier results. In all of the Japan studies, station

separations were small (about 600 km and less) and there were large segments of ocean path between source and receivers.

In McEvelly's [ 1964 ] study of the U.S. mid-continent, 9 of the 13 earthquake paths to the array of six closely spaced stations used by him traversed significant ocean paths (station separations about 400-500 km). Dr. McEvelly has kindly shown us the more detailed Love wave results for the U.S. midcontinent contained in his Ph.D. thesis (St. Louis U., 1964), and these data strongly support the contentions made here. For three of the four sources used which traverse entirely continental paths, all the phase velocities determined are for wave periods less than 40 seconds and most velocities are significantly less than the mean of all the data. The fourth source (in Alaska) exhibits anomalously higher phase velocities for periods from 40 to 60 seconds, but with considerable scatter, and the higher values may be explained as due to contamination by the first higher mode. A source in China traversing roughly three-quarters continental path has data only from 40 to 70 seconds period with phase velocities  $4.70 \rightarrow 4.85$  km/sec, characteristic of the higher mode phase  $S_a$ . The remaining eight sources, all traversing large proportions of ocean path, show the unusually high phase velocities which comprise the bulk of the data. Five of these are from oceanic sources and would be expected to have greater higher mode excitation than continental shocks.

Anomalous dispersion could also be expected in the long period results from the three continental sources. The graphs for the tectonic earth model shown in Figure 20 are probably most relevant

to these two regions, and it appears that if higher Love mode excitation is indeed significant, then the anomalous Love wave phase velocity observations are adequately explained.

From a knowledge of the source characteristics and the propagation path, it is possible, in principle, to predict when higher mode contamination is expected to be significant and when it might be absent. Therefore, it is to be expected that a careful (or accidental) choice of data can isolate the fundamental Love mode and eliminate inconsistent phase velocity observations. In addition, phase velocity filtering over a large array could separate the modes effectively and allow better studies to be made of the deeper mantle. The length of the array would have to be of the order of the beat wavelength or greater, and for best results be in a region with no significant lateral variations. A Love wave profile in Western North America from Arizona to the Arctic Ocean [Wickens and Pec, 1968], shows some features attributable to mode interference, but also illustrates the difficulty in unambiguously analyzing Love wave phase velocity data over a long linear array within which lateral variations are expected to be important.

For wave periods less than about 60 seconds one would expect no significant higher mode interference for waves traversing long continental paths between source and station. The great difficulty which has been encountered in attempting to measure regional Love wave phase velocities across oceans makes sense when one observes that higher mode interference is expected to be most marked for

oceanic dispersion studies. Using sources which travel long continental paths before crossing an oceanic region of interest should allow the modes to be sufficiently separated for reliable phase velocity measurements to be made for wave periods up to about 60 seconds.

CHAPTER III  
SEISMIC STUDY OF AN OCEANIC RIDGE EARTHQUAKE  
SWARM IN THE GULF OF CALIFORNIA

ABSTRACT

Detailed seismic investigation of an unusually intense earthquake swarm which occurred in the northern Gulf of California during March 1969 has provided new information about seismic processes which occur on actively spreading oceanic ridges and has placed some constraints on the elastic wave velocities beneath them. Activity during this swarm was similar to that of a foreshock-mainshock-aftershock sequence, but with a "mainshock" composed of over 70 events with magnitudes between 4 and  $5\frac{1}{2}$  occurring in a six hour period about a day after swarm activity was initiated. "Aftershocks," including many events greater than magnitude 5, continued for over two weeks. Near-source travel time data indicate all sources located are within 5-10 km of each other and that hypocenters are confined to the upper crust. Teleseismic P-delays for rays travelling beneath this ridge may be interpreted in terms of an upper mantle with compressional velocities five to ten per cent less than normal mantle to a depth of 200 km. Average apparent stresses for all swarm events studied are very similar, show no consistent pattern as a function of time, and are close to values obtained from other ridges. The focal mechanism solution shows a large component of normal faulting. An apparent non-orthogonality of nodal planes common to this mecha-

nism solution and to normal faulting events on other ridges disappears when the indicated low upper mantle velocities beneath the source are taken into account.

A survey of recent seismicity (post 1962) in the northern Gulf suggests seismic coupling across about 200 km between adjacent inferred spreading ridge segments.

Surface waves from these Gulf Swarm earthquakes have amplitudes from one to two orders of magnitude greater than Northern Baja California events with similar short period body wave excitation.

## INTRODUCTION

Seismic investigations have provided considerable stimulus and support to the hypotheses of seafloor spreading and rigid plate tectonics. The focal mechanisms of earthquakes on mid-ocean ridges determined by Sykes [1967, 1968], Tobin and Sykes [1968], Banghar and Sykes [1969] have been a striking confirmation of Wilson's [1965] transform faulting hypothesis and have given strong stimulus to the development of the concepts of plate tectonics by Morgan [1968], McKenzie and Parker [1967] and Le Pichon [1968].

Other seismic investigation has outlined several important characteristics of mid-ocean ridges. Surface and body wave travel time studies of the Mid-Atlantic ridge near Iceland by Trygvasson [1962, 1964] suggest a zone of anomalously low seismic velocity extends from the Mohorovicic discontinuity to a depth of the order of 200 km. Talwani et al. [1965] found that gravity and seismic

refraction data from profiles over the Mid-Atlantic ridge were consistent with a low density region whose upper surface is at the crust-mantle interface beneath the ridge crest but deepens away from the axial zone. Recently Wyss [1970b] has applied the method of comparing the excitation of short period body waves and long period surface waves to infer that relatively low average stresses are acting in the source region of ridge earthquakes. Sykes [1970], in a study of the available seismic data pertinent to spreading ridges has recently pointed out the close relationship between ridges, earthquake swarms, normal faulting and vulcanism.

The Gulf of California is one of the few places on the globe where seafloor spreading and lithospheric generation is occurring in a region accessible to close-in land-based seismic observation. The Gulf of California has been spreading at a half-rate of 3 cm/year for the past  $4\frac{1}{2}$  million years, as demonstrated by Larson and others [1968] in their examination of the magnetic lineations at the mouth of the Gulf. That it is actually spreading at present is clearly demonstrated by the seismicity and focal mechanism investigations of Sykes [1968]. The crustal structure varies from oceanic at the mouth of the Gulf to continental shelf type (crustal thickness 20-25 km) near the north end, but with considerable lateral variation indicated normal to its axis [Phillips 1964; Thatcher, Ch. 1, this thesis].

This paper is a detailed study of an unusually intense earthquake swarm which occurred in the northern Gulf near  $31^{\circ}10' N$ ,  $114^{\circ}26' W$  during March 1969, and includes analysis of seismic data recorded less than 60 km from the epicenters of this oceanic ridge

swarm. In addition the seismicity of the Gulf since 1962 is surveyed and its relationship to swarm activity is examined.

### SWARM ACTIVITY AND GULF SEISMICITY

The northern third of the Gulf of California is shown in the bathymetric map of figure 21, modified from Fisher et al. [1964]. The closed basins striking roughly northeast are presumed spreading centers, representing a median depression at the ridge axis, and the

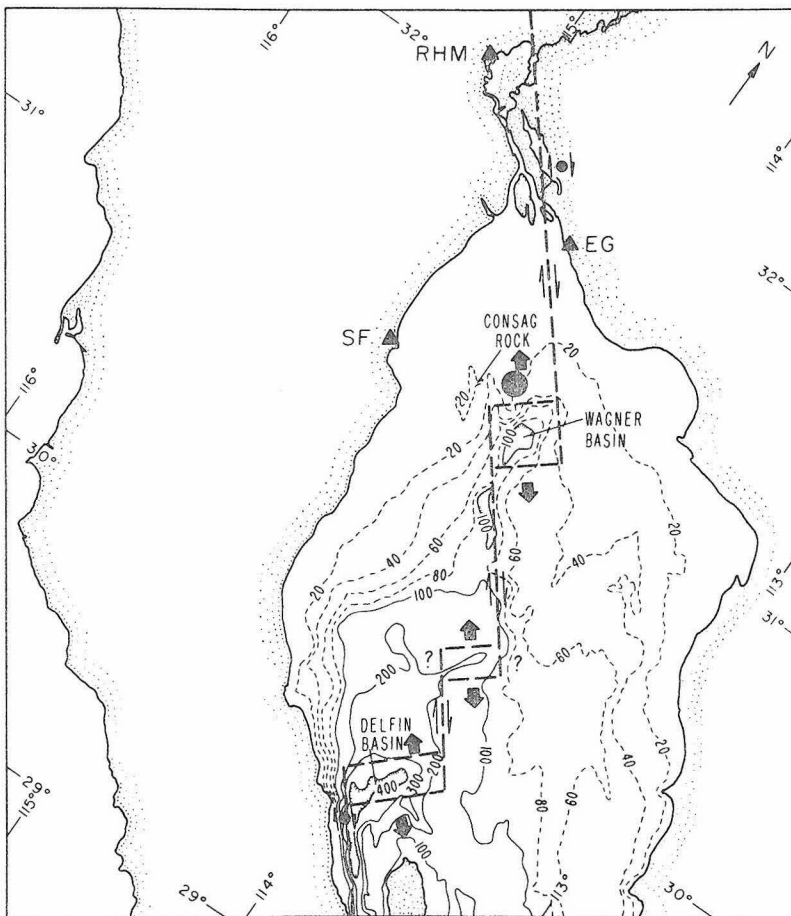


FIG. 21 Bathymetric map of the northern Gulf of California, modified from Fisher *et al.* (1964). Closed basins striking roughly north-east are presumed spreading centres and elongate north-west trending bathymetric lines are inferred transform fault segments. Local seismograph stations and best swarm location are shown, along with two focal mechanisms by Sykes (1968).

elongate northwest striking bathymetric lines which connect them mark the traces of transform faults. Two focal mechanisms obtained by Sykes [1968] and shown on the map are consistent with this interpretation of the bathymetry and the known geology. The three seismograph stations used in the location of swarm events are Rio Hardy (RHM), a permanent station about 130 km to the north of the epicenters, and San Felipe (SF-) and El Golfo (EG-), two portable seismographs each located about 50 km from the swarm. The locations determined are within about five kilometers of the dot shown on the map and lie between Wagner Basin, a closed bathymetric depression on the seafloor, and Consag Rock, an andesitic knob protruding above the surface of the Gulf about 20 km to the west of the basin.

Swarm activity began at 08 16 GMT on 20 March with an event of local magnitude 5.2 (all magnitudes quoted for the March 1969 swarm are local magnitudes as determined at Pasadena unless otherwise noted). At 08 17 and 08 23 shocks of magnitude 5.7 and 5.2 respectively occurred, and during the next 18 hours about a dozen events greater than magnitude 4 were detected. On 21 March at 02 34 very intense activity was initiated, and in the following 6 hour period 75 quakes with  $M_L \geq 4$  occurred, 20 of these being greater than magnitude 5. Activity fell to half these values in the following 6 hours, but activity continued for over a week, with over 200 events greater than magnitude 4 and 40 above magnitude 5 recorded at Pasadena by 28 March.

The seismic activity of earthquake swarms and aftershock sequences may be conveniently displayed as a function of time by a

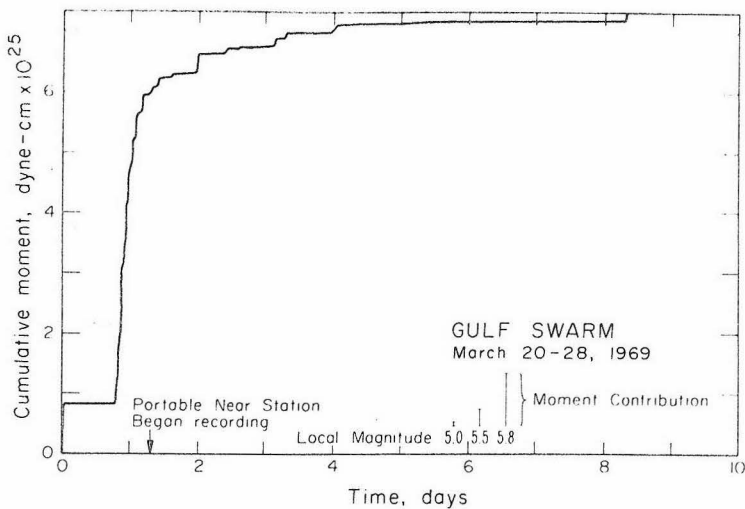


FIG. 22 Cumulative seismic moment plotted as a function of time for main Gulf swarm—Local earthquake magnitude has been translated into moment using the magnitude-moment relation of Wyss & Brune (1968). Note that seismic moment is proportional to displacement across a dislocation (fault surface) times fault area.

Thatcher and Brune [1971]

plot of cumulative seismic moment versus time. In the dislocation theory of seismic sources [Burridge and Knopoff 1964; Aki 1966], seismic moment is directly proportional to the fault area times the average slip across the fault surface. It is a more precise seismic source parameter than either magnitude or energy, and may be determined with factors of 2 to 3 accuracy from measurements of the amplitudes of long period surface waves [Aki 1966]. It has been extensively used by Brune [1968], Wyss and Brune [1968], and Wyss [1970a] in seismic source studies in the western United States. For the purposes of this plot, the approximate empirical relation between local magnitude and seismic moment of Wyss and Brune [1968] for the western U.S. is used to relate magnitude to moment for all Gulf

events with  $M_L \geq 4.0$ . The accuracy of this equation for the northern Gulf region is verified by the values determined for the moments of swarm events using the amplitude spectra of long period Rayleigh waves, discussed below. To be noted in figure 22 is that the peak 6 hour period of activity a day or so after the initiation of the swarm accounts for over three-quarters of the cumulative moment of the entire sequence--rather like a foreshock-mainshock-aftershock pattern, but with the "main shock" made up of an extraordinary series of magnitude 4 and 5 earthquakes occurring during one 6 hour period. The cumulative moment during this period corresponds about to a single magnitude 6.2 event.

The frequency-magnitude relationship has been used by many authors to characterize regional seismicity, and is a measure of the mean earthquake magnitude. The slope, or b-value, of such a plot for the March 1969 Gulf swarm is about 0.90 using Pasadena local magnitudes (208 samples). Using the smaller USCGS sample for the swarm (78 events) and, their body wave magnitudes, the b-value is about 1.35. The difference in the two b-values may be reflecting the differences in the two magnitude scales as well as the differences in the number of samples. Evernden [1970] observed that b-values from  $m_b$  data were consistently larger than  $M_L$  b-values for world-wide earthquakes but only for those over magnitude  $5\frac{1}{2}$  or so. The b-value of 0.90 is close to values found for the San Andreas system in southern California by Allen et al. [1965] using Pasadena  $M_L$  data.

The seismicity of the Gulf of California from 1 January 1962

to date has been surveyed using USCGS epicenter listings. It should be noted that detection of Gulf events is strongly affected by seismograph station distribution, and hence relatively more events of magnitude less than  $m_b = 5.0$  will be reported in the northern Gulf as compared to the southern Gulf (where there are few established stations close to the active region). Even in the northern Gulf it is clear from study of the March 1969 swarm that many events with  $m_b \leq 4.5$  or so are missed in CGS listings. Still, with these limitations and with only an eight year sampling of northern Gulf seismicity, an interesting pattern of activity is evident. Table 2 is a listing of all sequences of more than 5 events occurring during a time interval of a month or less since 1962 in the northern Gulf. Both the Wagner basin and the Delfin basin area, about 150 km to the south

Table 2

*Summary of Northern Gulf Seismic Activity since 1962 January 1 from USCGS epicentre listings*

Time interval	Approximate location	Number of events listed	Body wave magnitudes ( $M_b$ )
1 18-23 Nov 1963	30°N 113.5°W Delfin Basin	14	4.1-5.7*
2 3-4 Feb 1964	31.3°N 114.3°W Wagner Basin	9	4.0-4.8
3 27 Aug-18 Sept 1967	31.2°N 114.2°W Wagner Basin	7	4.0-4.4
4 5-6 Dec 1967	30.5°N 114.2°W Northern Delfin Basin Region	9	3.8-5.0
5 2-18 Feb 1969	30°N 113.5°W Delfin Basin	11	4.4-4.8
6 20 Mar-6 Apr 1969	31.3°N 114.2°W Wagner Basin	78	3.9-5.5 (14 events with $m_b \geq 5$ )

\*First events of this sequence is the  $m_b = 5.7$  shock for which Sykes (1968) determined a strike slip mechanism.

(see figure 1) are regions of recurring activity, and furthermore the seismicity in the two areas appears to be coupled: the earthquake sequences are paired, and when activity is initiated in one basin it is followed in one to three months by activity in the other. No significant activity occurred in the area between the two basins in the time interval between the two sequences. Five of the six sequences are swarm-like, each with many events of roughly similar magnitude rather than one clearly dominant event preceded and/or followed by much smaller shocks. The exception, sequence 1, had a main shock of  $m_b = 5.7$  with a strike-slip focal mechanism [Sykes 1968] followed by aftershocks up to magnitude  $m_b = 5.3$ . The choice of sequences of 5 events or more was arbitrary but convenient--it would be hazardous to draw any conclusions with fewer events than this because of the biased omission of smaller magnitude shocks (three "sequences" of 4 events each were detected, and 2 of these could have been interpreted as preceded or followed by 2-3 events in the other basin).

The location of sequence 1 very close to the bathymetric depression of the Delfin basin indicates a small segment of transform fault in the vicinity and demonstrates that even when stresses and thermal conditions approach closely those of an actively spreading ridge, the earthquake mechanism and the aftershock sequence are still characteristic of a "normal" mainshock-aftershock series along a transform fault. This argues against attributing ridge swarms to inhomogeneities in physical properties [Mogi 1963] unless these inhomogeneities are very localized. The close association of ridge swarms with magmatic activity and the creation of new lithosphere

may provide the localized stress concentrations necessary to cause swarms [ Mogi 1963; Sykes 1970] , but the details of swarm mechanism are far from being resolved.

The Imperial Valley, in southernmost California approximately 200 km north of the Gulf, experiences considerable seismic activity including swarms [ Richter 1958] , and a search of USCGS and Pasadena local bulletins was made for sequences such as those found in the Gulf. The findings are summarized in Table 3. It should be kept in mind that the largest of these events recorded by the USCGS had a body wave magnitude of only 4.6, and that many shocks recorded in the Imperial Valley by the Caltech network would not have been reported had they occurred in the Gulf, where only USCGS listings are used in this comparison of seismicity. The events in Table 3 locate close to Obsidian Buttes, Quaternary volcanic rocks which protrude through the thick sediments of the valley near the south end of

Table 3

*Summary of Imperial Valley Seismicity from 1962 January 1 Pasadena Local Bulletin and USCGS listings*

Time interval	Approximate location	Number of events listed	Magnitudes ( $M_L$ )
1 27 Oct-2 Nov 1963	33° 15'—115° 40'	19 (9 by CGS)	3.0—4.4
2 16-17 June 1965	33° 05'—115° 40'	18 (12 by CGS)	3.0—4.4
3 17-22 Dec 1968	33° 02'—115° 50'	10 (Mainshock only by CGS)	2.5—4.7 ( $M_L = 4.7$ and aftershocks)
4 31 July-6 Aug 1969	32° 55'—115° 33'	13 (None reported by CGS)	1.8—3.3

the Salton Sea. A comparison of Tables 2 and 3 demonstrates that between the Valley and the Gulf differences exist in both the frequency of shocks and in their maximum magnitudes, at least for the time interval examined here.

Also, besides swarm events, large strike-slip earthquakes, along presumed transform faults, e.g. the 1940 El Centro earthquake ( $M_L = 7.1$ ) and the 1966 shock in the Colorado delta ( $M_L = 6.3$ ), characterize the seismicity of the Imperial Valley-Colorado delta region. It is possible to correlate two of the valley sequences with the northern Gulf pairs, but the two others are not simply correlated. If any seismic coupling does exist between the northern Gulf and the Imperial Valley, it is not demonstrated by the data examined here.

To the south of Delfin basin, Gulf seismicity (USCGS) reveals no correlative patterns with northern Gulf activity. A sequence in the mid-Gulf region (approx.  $27^\circ\text{N}$ ,  $110^\circ\text{W}$ ) from 29 June to 6 July 1964 consisted of 13 earthquakes including an  $m_b = 6.0$  event on 5 July preceded and followed by several shocks of up to magnitude 5.4. The earthquakes were located 60 km from the nearest inferred spreading center, the focal mechanism determined by Sykes [1968] was strike-slip, and the sequence had a foreshock-mainshock-aftershock character. A recent sequence further south (17-19 August 1969 at approx.  $25^\circ\text{S}$ ,  $109^\circ\text{W}$ ) began with two large events ( $m_b = 5.7$  and 6.1) within two minutes of each other and had 18 smaller aftershocks. Its location and character suggest transform faulting. These two sequences and the ones listed in Table 2 were the only ones detected in the Gulf of California since 1962. Though intermediate

cases are not definitely precluded, available evidence from Gulf earthquakes suggest that it is possible to make a distinction between oceanic ridge and transform fault sequences on the basis of location, maximum magnitude, time-magnitude behavior, and focal mechanism.

### LOCATION OF MARCH 1969 SWARM EVENTS

Two portable seismographs located about 50 km from the epicenters of these events were set up about a day and a half after the swarm began. Figure 23 shows their location and in figure 22 the time of their installation with respect to swarm activity is noted.

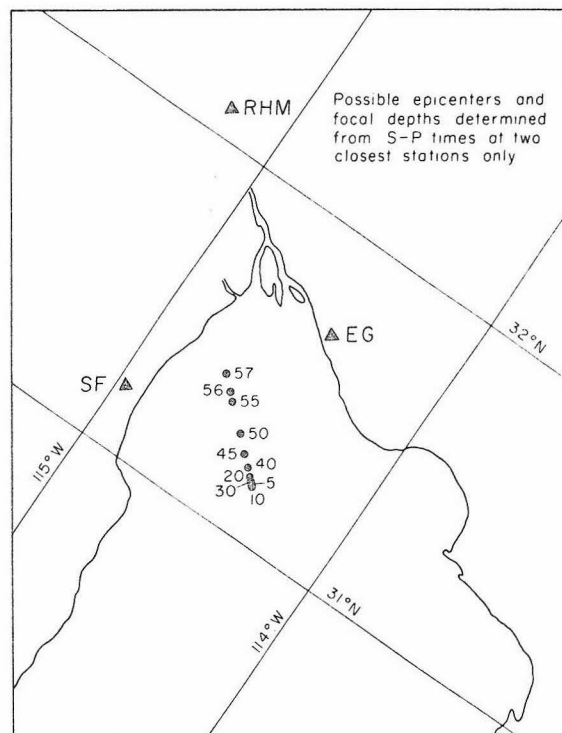
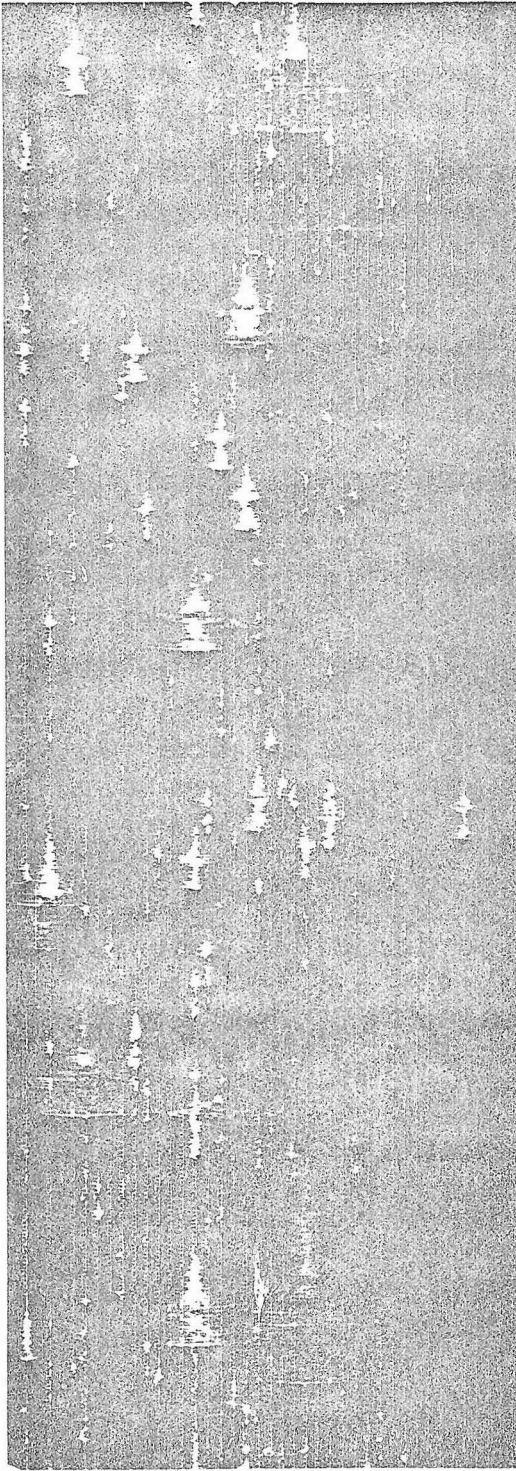


FIG. 23 Possible epicentres (with hypocentral depths which correspond to them) obtained using *S-P* times at two nearest stations only.

The region of the swarm is illustrated in figure 23, along with the locus of possible epicenters and their corresponding hypocentral depths determined using only S-P times at the two closest stations. The crustal structure used is from a seismic refraction survey in the region by Phillips [1964], and Poisson's ratio was taken to be 0.25 in order to determine P-travel times from S-P intervals. Figure 24 which is a sample seismic record from portable station SF-, shows many events with S-P times within a few tenths of 7.0 seconds. Other records from the portable stations show similar consistency. From readings of these two stations alone, focal depth is not well determined, and any depth less than about 55 km will satisfy the data. However there are several other important observations which help constrain the depth.

The focal depth is most strongly constrained by readings at RHM, approximately 130 km to the northwest of the swarm, as well as by readings at more distant (200-300 km) Caltech stations in southern California. Figure 25 is a short-period record of a typical swarm event recorded at RHM. The critically refracted  $P_n$  arrival is followed about 5 seconds later by a strong second arrival, interpreted here as the crustal phase  $P_g$ . Using Phillips' [1964] crustal structure (crustal thickness 25 km,  $P_n$  velocity 7.8 km/sec) travel time curves were constructed for a range of possible focal depths down to 50 km. No fit to the data was possible for a source in the upper mantle. The best fit to the near-source body wave observations was provided by placing the sources in the upper crust at a



→ 1 min. ←

SF-Portable Station  $\Delta = 53$  km

FIG. 24 Sample seismic record from portable station SF-, located about 50 km from the events shown (note S-P times of about 7 s). Absolute timing accuracy is about  $\pm 0.1$  s.

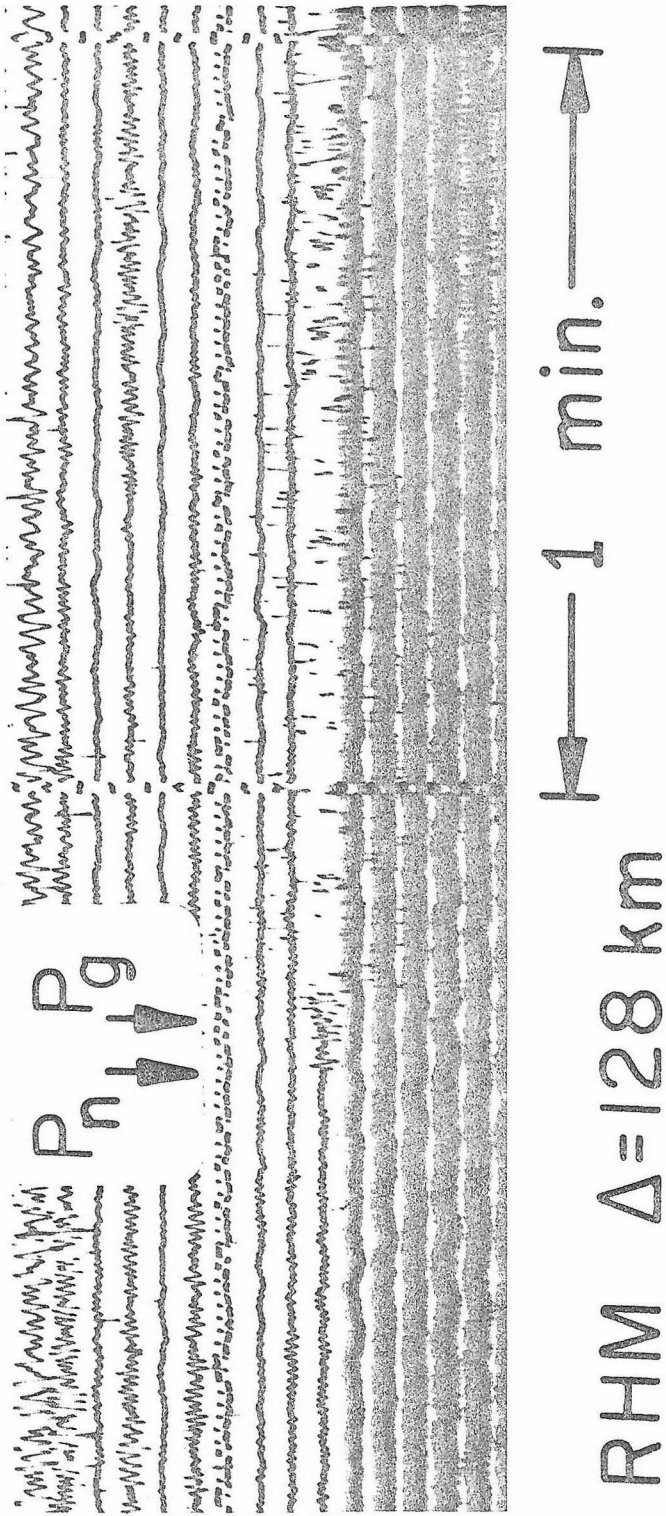


FIG. 25 Typical swarm event recorded at RHM, permanent station, 130 km to the north of epicentres. Seismograph is short-period Benioff. Note the first arrival  $P_n$ , and the strong second arrival about 5 s later, interpreted here as the crustal phase  $P_g$ . These data provide the strongest body-wave constraint on the focal depth of swarm events.

depth of 7 km--the  $P_g - P_n$  times at RHM and in southern California could only be satisfied if the hypocenters were located above the 6.70 km/sec layer in Phillips' crustal model, and 7 km satisfied the data best. The travel time curves and the data to which they were fit are shown in figure 26 along with the velocity model used in constructing the plot. Note that over 60 pieces of data support the interpretation made here. In addition, readings of  $P_g - P_n$  at Caltech stations in the Imperial Valley region (Glamis,  $\Delta = 225$  km; Hayfield,

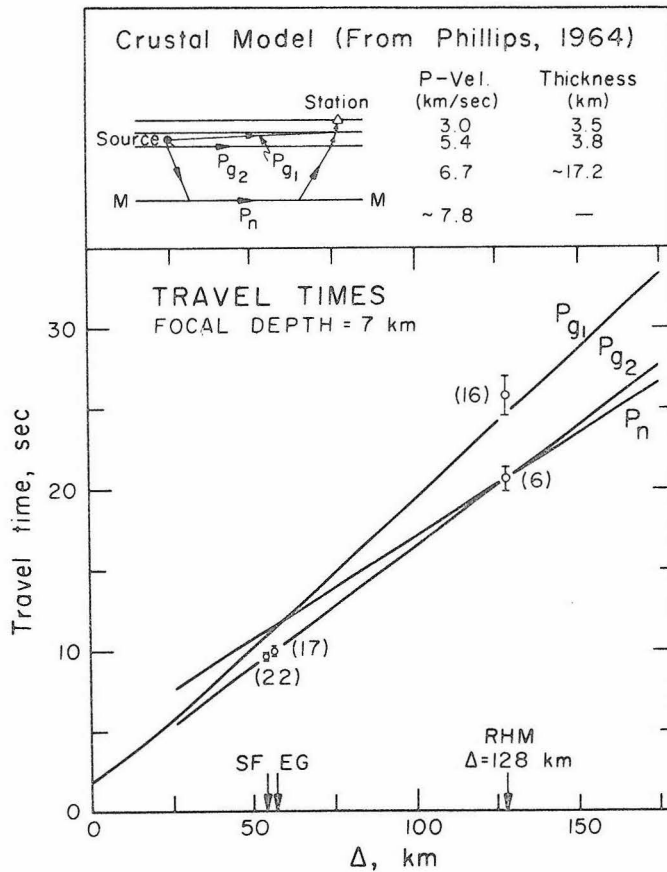


FIG. 26 Travel-time curve which provides a good fit to all the near station data. Crustal model is from Phillips (1964). The data are shown with their error bars (2 standard deviations) and the number in parentheses refers to number of pieces of independent data which each point represents.

$\Delta = 290$  km) fit this interpretation well. Moderate changes in crustal structure would change the results only slightly and we feel that a hypocenter in the upper crust for these swarm events is well established. A seismic study is presently being carried out in the Imperial Valley to clarify the relationship between the San Andreas system and the ridge-transform fault pattern of the Gulf of California, which may extend into mainland North America as far as the Imperial Valley-Salton Sea area. Figure 27 is a map of the same area as figure 23 showing the better determined epicenters of the USCGS (their locations

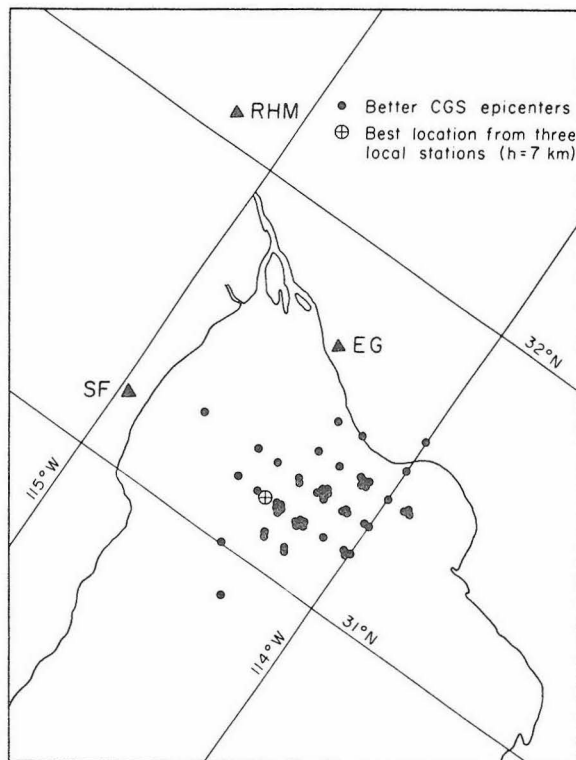


FIG. 27 Region of swarm of March 1969, showing better located USCGS epicenters (shown without asterisk in their listings and determined by them to the nearest tenth of a degree). Also shown are the local seismograph stations used in locating swarm events with better precision, as well as the best location found for many events using these near-source travel times.

are given to the nearest tenth of a degree), as well as the best location determined in this study using many travel time observations from the three local stations. The broad distribution in USCGS epicenters is not believed to be real--the consistently similar S-P times recorded at local stations indicate all events studied here occur within approximately 5 km of each other. Our preferred location lies within 10-15 km of the center of the cluster of USCGS epicenters. If the true focal depths were greater than 45 km, the USCGS epicenters would have to be consistently in error by more than 30 km, greater even than mislocation errors in island arc regions. From what is known of the relative importance of lateral inhomogeneities in mid-ocean ridges and in island arcs, such a large mislocation appears unlikely--a relatively hot, low-velocity upper mantle beneath a spreading ridge would tend to produce travel time delays which have little preferred azimuth distribution at teleseismic distances, and in such events a trade-off between origin time and focal depth will occur, so that locations may be too deep, but there should be little epicentral bias.

Another line of evidence which can place limits on the focal depths of earthquakes is the shape of the seismic surface wave spectrum. The dependence of focal depth upon spectral amplitude is most marked for surface waves of Rayleigh type, and is a consequence of the variation in excitation as a function of depth. For each wave period of the fundamental mode, the horizontal excitation has a node (zero crossing) at a depth of about one-quarter wavelength, while the curve of vertical excitation versus depth has a low gradient

at the quarter wavelength depth. Beyond a half wavelength both horizontal and vertical excitation decrease rapidly with increase in depth. Thus the cumulative effect of focal depth alone on Rayleigh wave spectra is to produce:

- (1) a minimum at a wave period ( $T_m$ ) which corresponds to the focal depth ( $Z_o$ ), i.e.  $T_m \approx 4Z_o/C(T_m)$ , where  $C(T_m)$  is the phase velocity at period  $T_m$ , and
- (2) a fall-off in the spectrum for periods less than about  $2Z_o/C(T_m)$ .

For focal depths less than 60 km or so these diagnostic changes in spectral shape occur for periods between 30 and 10 seconds, and are less pronounced for normal faulting than for strike-slip mechanisms. Differences in focal mechanism can alter the depth effects by up to a factor of 2 or so [ Tsai 1969] and for some mechanism parameters the spectral minimum may be absent at certain azimuths from the source [D. G. Harkrider, personal communication]. In addition, the spectrum in this period range is subject to several other complications, including the effect of source dimension, uncertainty of Q-correction, and contamination by short period higher modes with group velocities similar to those of the fundamental mode. For the Gulf swarm earthquakes, location of many events within a region of less than 10 km or so indicates finiteness should not seriously effect the spectra. Similarly, contamination by higher Rayleigh modes in the critical period range should not occur for continental Rayleigh waves, though oceanic Rayleigh dispersion studies by Sykes and Oliver [1964] and Kovach and Anderson [1964] suggest that such

contamination would occur for oceanic paths. The fundamental mode group velocity curve for oceanic Rayleigh waves is not well defined for periods less than 20 seconds, and higher modes are frequently excited in the period range 10 to 30 seconds with group velocities which make them difficult to separate from fundamental mode wave-trains. The uncertainty in Q-correction at short periods complicates the interpretation as well, but may be minimized by checking spectral shape at short distances, where corrections are smallest. Tsai [1969] shows several convincing cases for determining focal depth of continental strike-slip sources using continental Rayleigh wave spectra, but his results are more equivocal for oceanic paths and sources, and we believe this is a result of the difficulties mentioned above.

The Rayleigh wave spectra from a number of Gulf events recorded at several locations and azimuths in the United States have been measured. The event shown in figure 28 is typical of many others, and its shape suggests the source is shallow. The spectrum is corrected for instrument response but not for Q, since even within its uncertainties attenuation will not significantly alter the shape of the spectrum shown here, since the epicentral distance is only about  $8^{\circ}$ . Geometrical spreading and dispersion corrections (independent of period) have not been made for the data in the plot illustrated.

Spectral amplitudes for periods less than about 10 seconds are less certain than for longer periods because of uncertainties in Q, but this uncertainty has been minimized because of the short path from the Gulf to ALQ (New Mexico). The significance of the short

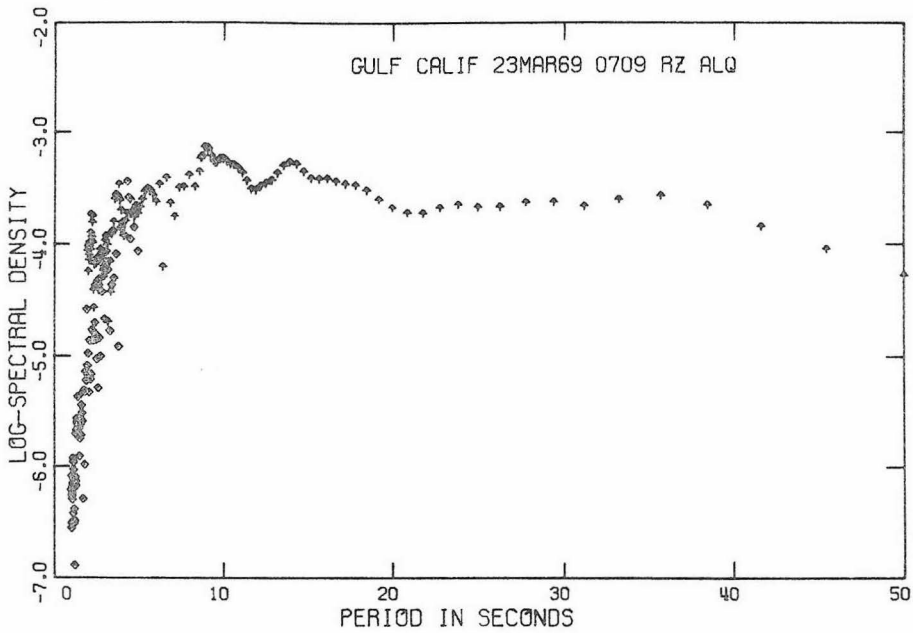


FIG. 28 Rayleigh wave spectrum from a typical swarm event (1969 March 23 07 09,  $M_L = 4.6$ ) recorded at WWSSN station ALQ (Albuquerque, New Mexico,  $\Delta = 7.63^\circ$ ). Long and short period records have been patched together to include all of the fundamental mode spectrum between 1- and 50-s period. Short period higher modes in the period range 5-10 s have been excluded from seismograms analysed on the basis of their expected group velocities. Spectrum corrected for instrument response but not for geometrical spreading or attenuation.

Thatcher and Brune [1971]

period amplitudes is that their relatively high excitation (even without attenuation corrections, which would increase their values) indicate a source in the shallow crustal layers. A deep crustal or upper mantle source would not significantly excite these short periods.

## ORIGIN TIMES AND P-WAVE RESIDUALS

For a number of larger 1969 swarm events recorded at the portable stations, it was possible to compare the origin times determined from near-source readings with those determined by the USCGS using teleseismic P-times. Table 4 shows the results of this comparison for nine events listed by the CGS for 21 March 1969, and the average difference in origin time is about three seconds.

Table 4

*Comparison of USCGS Origin Times with those determined from S-P times at portable stations 1969 March 21*

$M_b$	USCGS	This paper	Observed - CGS
4.6	15 07 13.6	15 02 11.0	-2.6
5.1	15 57 42.0	15 57 43.4	+1.4 <sup>1</sup>
4.7	16 29 40.4	16 29 34.2	-6.2
4.7	17 55 47.2	17 55 42.7	-4.5
5.2	18 00 20.6	18 00 17.2	-3.4
4.3	20 11 51.0*	20 11 49.4	-1.6*
4.2	20 36 50.3*	20 36 46.4	-3.9*
4.2	21 05 38.1*	21 05 33.9	-4.2*
4.6	23 03 25.2*	23 03 22.2	-3.0*
			Average = -3.1 s
			(for better determined events)

<sup>1</sup>USCGS focal depth is 2 km for this event

\* Less well-determined epicentres

Thatcher and Brune [1971]

This difference could be the result of P-delays beneath the source and/or incorrect assignment of focal depth by the USCGS. In the absence of near-source travel time readings the trade-off between origin time and focal depth makes it difficult to accurately determine origin time and hence detect low seismic velocities beneath the

source. However, all but one of the events listed by the CGS were constrained to 33 km depth, and the one shock with an assigned focal depth of 2 km had an origin time which was early by about one second compared to the locally determined one. Thus the discrepancies in both focal depth and origin time are resolved, given that the sources are located in the upper crust, as found above. With origin times determined from local stations, it is possible to more accurately examine teleseismic travel time data for evidence of low seismic velocity beneath this spreading ridge segment. Arrival times for P-waves from Gulf swarm events reported in USCGS EDR bulletins were used with the near-source origin times to obtain travel times which were compared with those of several of the more recently determined P-tables [Carder et al. 1966; Herrin et al. 1968; Johnson 1969]. Only five stations at epicentral distances beyond 30° consistently reported times for better located events listed in Table 3, but residuals from these stations, shown in Table 5, demonstrate that P-delays of about two seconds occur in this distance range.

Table 5

*P-wave travel-time residuals for swarm events of 1969 March 21*

Station	$\Delta$ (degrees)	Observed- <i>P</i> table   Station correction (seconds)
COL	39.54	+2.4 → 3.2
MBC	45.19	+2.0 → 2.8
SJG	45.40	+1.5 → 2.3
ALE	54.53	+0.5 → 1.2
NUR	82.68	+2.3 → 3.1
Average =		+1.7 → 2.5 ( $\pm 0.6$ ) s

Residuals are referred to *P*-times of Carder *et al.*, Herrin *et al.*, and Johnson (assumed depth 7 km)  
Station corrections from Cleary & Hales (1966)

The range in residual at any individual station reflects the slightly differing travel time tables of the different investigators. P-wave station corrections tabulated by Cleary and Hales [1966] add between 0.4 and 0.7 sec to the P-delays for the stations listed in Table 5. If the travel time delay is confined to the upper 200 km of the mantle, then P-wave velocities beneath this ridge are 5 to 10 per cent less than those for a normal mantle.

### FOCAL MECHANISM

The poor azimuth distribution of WWSSN stations with respect to the Gulf of California, as well as the relatively low body wave magnitude of even the largest swarm shocks ( $m_b = 5.5$  was the largest) made it difficult to accurately determine P-wave focal mechanisms for this swarm. In addition, many of the largest events occurred during the peak period of activity and P-wave first motions were obscured by preceding events. However, the first large event of the swarm (21 March 1969 08 17 41.9,  $m_b = 5.4$ ,  $M_L = 5.7$ ) was registered clearly at enough stations to approximately define nodal planes, and figure 29 is a projection of its P-first motions on the lower hemisphere of the focal sphere. S-wave polarization data supplement the P observations. Though the nodal planes are not precisely defined, they are determined within confined limits, and note that two orthogonal nodal planes cannot be fitted to the observations with this projection. Furthermore, a survey of published ocean ridge normal faulting mechanisms (by the Lamont group) with

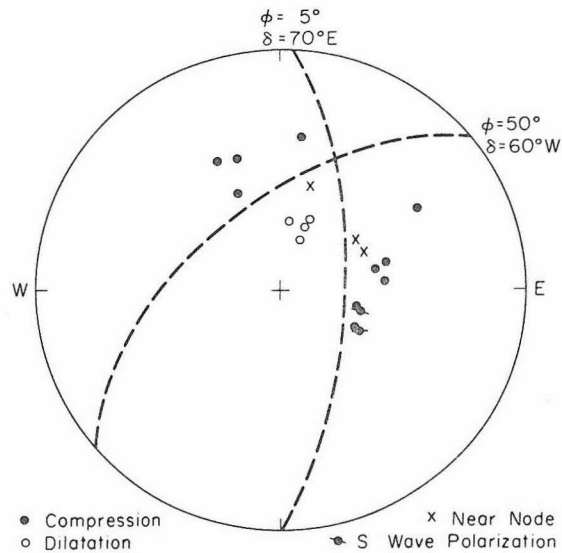


FIG. 29 Focal mechanism for Gulf swarm event on 1969 March 20 08 17 41.9. Projection of the lower hemisphere of focal a sphere constructed from Jeffreys-Bullen velocity structure.

Thatcher and Brune [1971]

nodal planes confined by the data reveals that this is generally the case, and the derived nodal planes cross at 60 to 70 degrees rather than at right angles. The nodal planes for strike-slip mechanisms in oceans are almost invariably orthogonal. The discrepancy may be simply explained by the fact that the projection most commonly employed and the one used here utilizes extended distance tables constructed from the Jeffreys-Bullen velocity structure, which differs considerably from that which is presumed to occur directly beneath ridges. With the P-velocity decrease that is suggested by the travel time residuals discussed in the previous section, simple

refraction at the Mohorovicic discontinuity and/or the top of the low velocity layer can account for the shifting of each nodal plane by 10 to 15 degrees. Note that this refraction will not effect strike-slip mechanisms because of their symmetry.

### SEISMIC MOMENTS AND APPARENT STRESSES

The seismic moments and average apparent stresses were determined for 15 of the March 1969 swarm events. Moments were obtained using measurements of the amplitude spectral densities of long period Rayleigh waves recorded on WWSSN seismograms at several stations in the central and eastern United States (ALQ, FLO, GEO, OXF, WES) suitably corrected for instrument response, and the effects of propagation and radiation pattern (Ben Menahem and Harkrider 1964). Seismic energy ( $E_s$ ) was defined from the Gutenberg and Richter energy-magnitude relationship, and the average apparent stress ( $\overline{\eta\sigma}$ ) determined from the formula [ Aki 1966]

$$\overline{\eta\sigma} = \frac{\mu E_s}{M_0} ,$$

where  $M_0$  is the seismic moment,  $\mu$  is the shear modulus ( $3 \times 10^{11}$  cgs) and  $\eta$  the seismic efficiency factor. Table 6 contains the results. Events are arranged chronologically, but no clear pattern emerges between the apparent stresses of earlier and later events. Small events in the months before and after the swarm show no significant differences in surface wave excitation, and thus there is no indication

Table 6

*Seismic moment and apparent stresses for March 1969 swarm events*

Date	Time	Moment, $M_0$ $10^{24}$ dyne-cm	$M_L$	$E_s$ $10^{20}$ dyne-cm	Apparent stress ( $\eta\bar{\sigma}$ ) bars
21 March	1010	15.25	5.5	1.12	2.2
	1224	0.70	5.3	0.56	24.0
	1557	1.00	5.1	0.29	8.7
	1629	2.04	5.0	0.20	3.0
	1800	1.15	5.2	0.41	10.7
	2303	0.75	4.9	0.14	5.6
22 March	0725	3.56	5.5	1.12	9.2
	1823	3.72	5.2	0.41	16.4
	2256	0.75	4.8	0.10	13.7
23 March	0709	0.22	4.6	0.05	6.7
	1132	0.22	5.2	0.41	20.4
	1539	0.60	5.2	0.41	16.4
24 March	0902	0.88	5.3	0.56	15.6
28 March	1519	1.20	5.3	0.56	14.0
3 April	1055	1.00	4.9	0.14	4.2

Thatcher and Brune [1971]

of any systematic differences in stresses acting in the source region before and after the swarm. For the 15 events studied, the average of the apparent stresses is  $11 \pm 5$  bars, in good accord with the average for ridges and transform faults in the Atlantic and northeast Pacific determined by Wyss [1970b], his average for 27 events being  $17 \pm 12$  bars.

#### A COMPARISON WITH EARTHQUAKES IN NORTHERN BAJA CALIFORNIA

Northern Baja California, about 100 to 200 km west of the Gulf swarm earthquakes, is a region of high seismic activity in a tectonic environment very different from that of the Gulf of California. Northern Baja California is underlain by granitic batholithic rocks of

regional extent as compared to the oceanic or transitional nature of the crust beneath the Gulf. The relatively low excitation of surface waves from earthquakes in this region was first noted by Brune et al. [1963] and was interpreted by Wyss and Brune [1968] as possibly due to relatively high tectonic stresses acting in the source region of these shocks. Just how profound the difference can be is illustrated in figure 30, which compares Rayleigh waves from a Gulf swarm shock and a north Baja event of comparable magnitude recorded with identical instrument magnification at Oxford, Mississippi. The average apparent stress for this event and for others in north Baja is about 200 bars, and small source dimensions are also indicated. A detailed study of the source parameters of these earthquakes is postponed to Chapter IV.

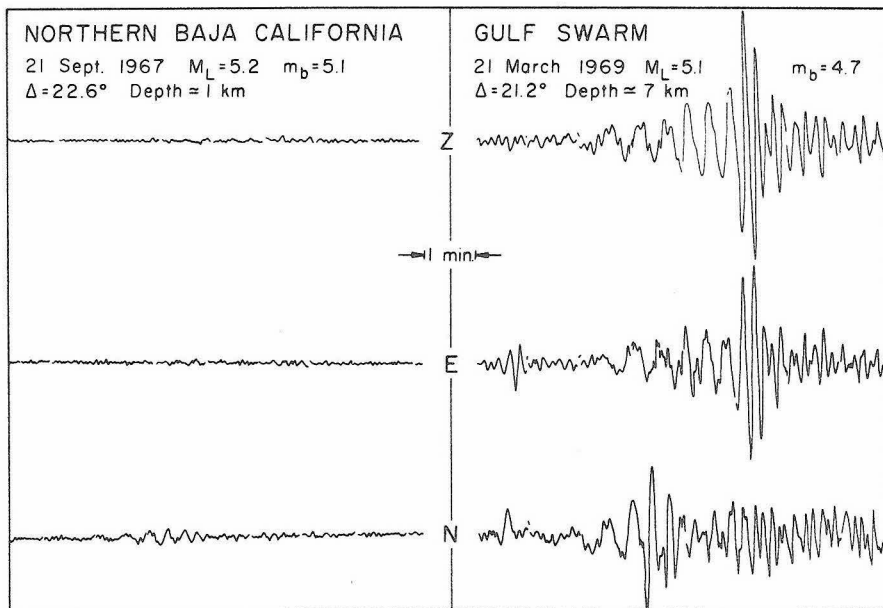


FIG. 30 Comparison of long period Rayleigh wavetrains recorded at OXF (Oxford, Mississippi) for a Gulf swarm shock and an event in northern Baja California of about the same local magnitude.

Though not yet investigated in detail, the importance of presumed high stress earthquakes in the problem of discriminating earthquakes from underground nuclear explosions is well known. For a given magnitude, both show relatively low excitation of long period surface waves. Studies of the  $M_s - m_b$  discrimination criterion do not consider significant numbers of high stress earthquakes. Basham [1969] was able to discriminate the north Baja shock shown in figure 30 from explosions at the Nevada Test Site using an  $M_s - m_b$  plot. However, a large population of high stress earthquakes could seriously affect such a discrimination tool: the difference between high stress earthquakes and possible nuclear explosions from the same region might be quite subtle, and existing discrimination methods may not in general be capable of resolving them.

## CONCLUSIONS

Seismic study of a remarkable earthquake swarm in the Northern Gulf of California has provided some details on seismic activity and structure beneath a spreading oceanic rise. Swarm sequences here are characterized by shallow hypocentral depths, predominantly normal faulting, and a distinctive activity as a function of time (viz. Figure 22). Teleseismic P-delays from these swarm sources suggest anomalously low upper mantle velocities beneath this spreading ridge, and compressional velocities 5 to 10 per cent less than normal mantle to a depth of 200 km are consistent with the observations.

It is also of some interest to compare the seismic character-

istics of spreading ridge earthquakes with those in adjacent parts of the Northern Gulf region. Within the Gulf itself, recent seismicity listings suggest seismic coupling across about 200 km between two adjacent inferred spreading ridge segments in the Northern Gulf. Data examined here demonstrate no such coupling between the Northern Gulf spreading centers and centers of Quaternary volcanism in the Imperial Valley region. Finally, it was observed that earthquakes in Northern Baja California typically have surface wave amplitudes one to two orders of magnitude less than Gulf earthquakes with similar short period excitation.

CHAPTER IV  
REGIONAL VARIATIONS OF SEISMIC SOURCE PARAMETERS  
IN THE NORTHERN BAJA CALIFORNIA AREA

ABSTRACT

The basic observation of this study is that seismograms written in southern California from earthquakes within the northern Gulf of California are clearly different from those of most Northern Baja California events. The principal visual difference is in the large high frequency amplitudes of the Baja sources compared with the great long period excitation seen on Gulf seismograms. This is interpreted here as a source effect, reflecting the relatively small source dimensions and low seismic moments of the Baja earthquakes. In principle, the differences in the seismograms could result from a near-source or propagation path effect, but the great similarity in paths traversed and the large magnitude of the observed difference argues against this explanation. In this respect, some exceptional North Baja sources with large moments and source dimensions demonstrate that very different seismograms are produced by sources with virtually identical propagation paths. In addition, preliminary examination of seismograms from events within southern California suggests the same kinds of regional variations there.

The Northern Baja earthquakes characteristically have source dimensions at least a factor of four smaller and seismic moments an order of magnitude less than events of similar local magnitude within

the Gulf of California. A consequence of these differences in moment and dimensions is that the Baja events have generally larger stress drops, ranging up to 100 bars compared with an average near 2 bars for the Gulf data. Stress drops decrease with decreasing moment with the Baja earthquakes, but are roughly constant for the Gulf sources.

For  $M_L < 5$ , Northern Baja California earthquakes have source dimensions and seismic moments which are only about a factor two greater than those for underground nuclear explosions of comparable magnitude.

## INTRODUCTION

The low excitation of surface waves relative to body wave magnitude is a striking seismic feature of many earthquakes in Northern Baja California (Brune, et al., 1963, Wyss and Brune, 1968), and suggests some unusual source characteristics for the events in this region. This paper investigates these earthquakes by measuring their shear wave spectrum and interpreting the observations in terms of seismic moment, rupture dimensions, and stress drop of each individual event. It is found that the North Baja sources have both significantly lower seismic moments and smaller source dimensions than earthquakes of similar magnitude near the west coast of Baja and within the Gulf of California. These differences are frequently very obvious and are clearly seen on Wood Anderson seismograms such as those reproduced in figure 31. The three earthquakes shown all have the same magnitude ( $M_L = 5.7$ ) and were recorded at comparable

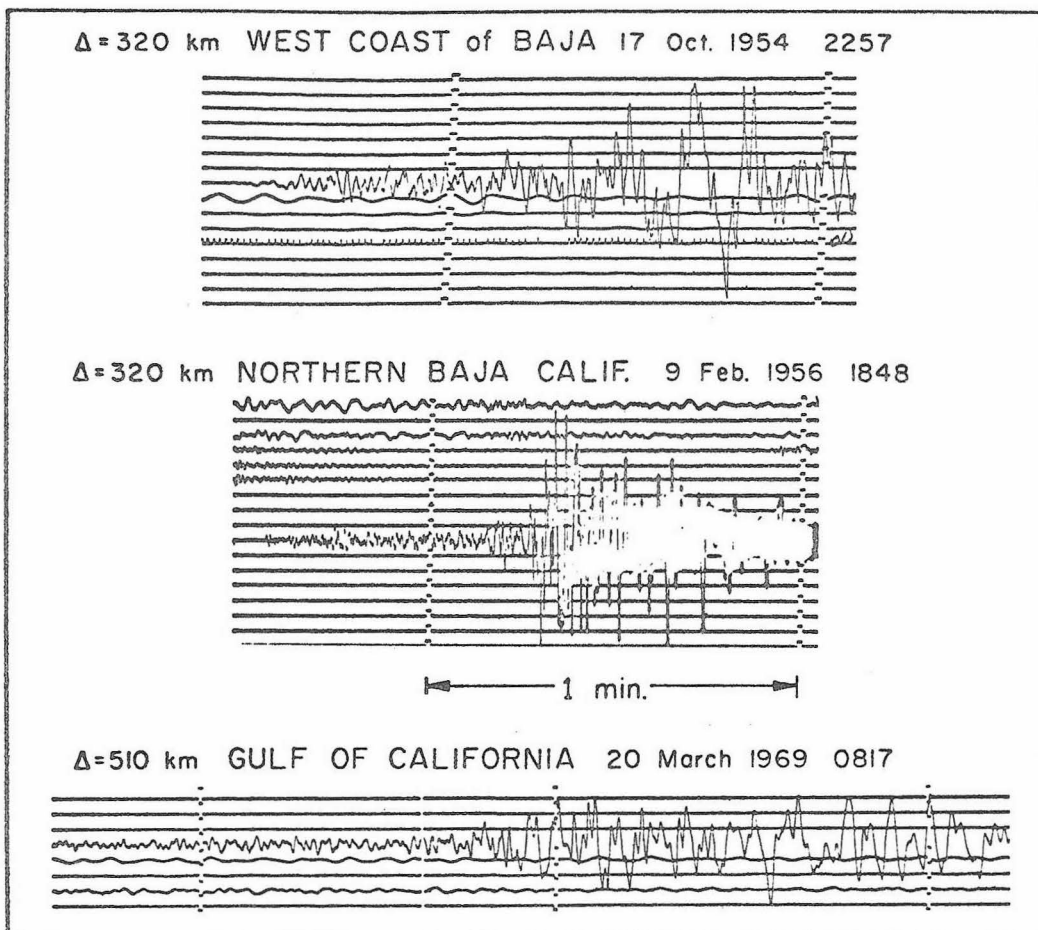


Figure 31. Wood-Anderson seismograms (at Pasadena) of three earthquakes with  $M_L = 5.7$  recorded at comparable epicentral distances. Note especially the clear difference in the high frequency content of waves from the typical Northern Baja California source (middle), which has considerably smaller seismic moment and source dimensions than the other two events illustrated. See text for discussion and Table 8 for spectrally-determined source parameters of these earthquakes. Their SH spectra are shown in figure 35.

epicentral distances along almost identical azimuths between source and station. The first and third events have comparable long period excitation and their source dimensions are both near 25 km. Note that the long period motion on these two seismograms still persists on the next line of the record, over 15 minutes later. The second seismogram is that from a typical North Baja event and clearly demonstrates the unusual high frequency excitation of these sources. Its long period excitation (determined from other seismograms) is roughly an order of magnitude smaller and the source dimensions about a factor of six less than corresponding quantities for the other two events shown in figure 31.

Before continuing into the detailed discussion of data analysis and results, this study will first consider some relevant background material. This will include the regional setting of Northern Baja California, previous interpretation of high apparent stress earthquakes, and a brief resume of the theory used to interpret the observed SH spectra. After results are presented, there is included a discussion of Gutenberg and Richter's method of estimating seismically radiated energy, which is compared with the spectrum integration method. Finally, the high frequency spectral amplitudes predicted by several recently proposed source models are considered in the light of the observations made in this study.

## GEOLOGIC AND SEISMIC SETTING OF NORTHERN BAJA CALIFORNIA

Northern Baja California is composed of two distinct structural trends (see figure 32). One comprises the extensive crystalline rocks of the Lower California batholith striking north-northwest roughly parallel or sub-parallel to the trend of the San Andreas and related transform faults within the Gulf of California, and including the topographically impressive reverse faults which mark the eastern termination of the batholithic rocks (Laguna Salada, San Pedro Martir). The other trend transects the crystalline and related rocks, cutting transversely across the peninsula south-southwesterly and made up of at least two major right-handed strike slip faults, the Agua Blanca and San Miguel fault zones. The San Miguel zone has however a more northerly strike and some indications of a vertical component of motion. Allen et al. (1960) observed many features indicating recent displacements across the Agua Blanca and suggest total offset of as much as 14 miles in the Cenozoic. Their study as well as the paper by Allison (1964) provide useful summaries of the geology of the region.

Directly to the east of this region is the northern Gulf of California with its transform faults and spreading centers which mark the active boundary of the Pacific and Americas plates. It is currently very seismically active and earthquakes here have relatively high surface wave excitation.

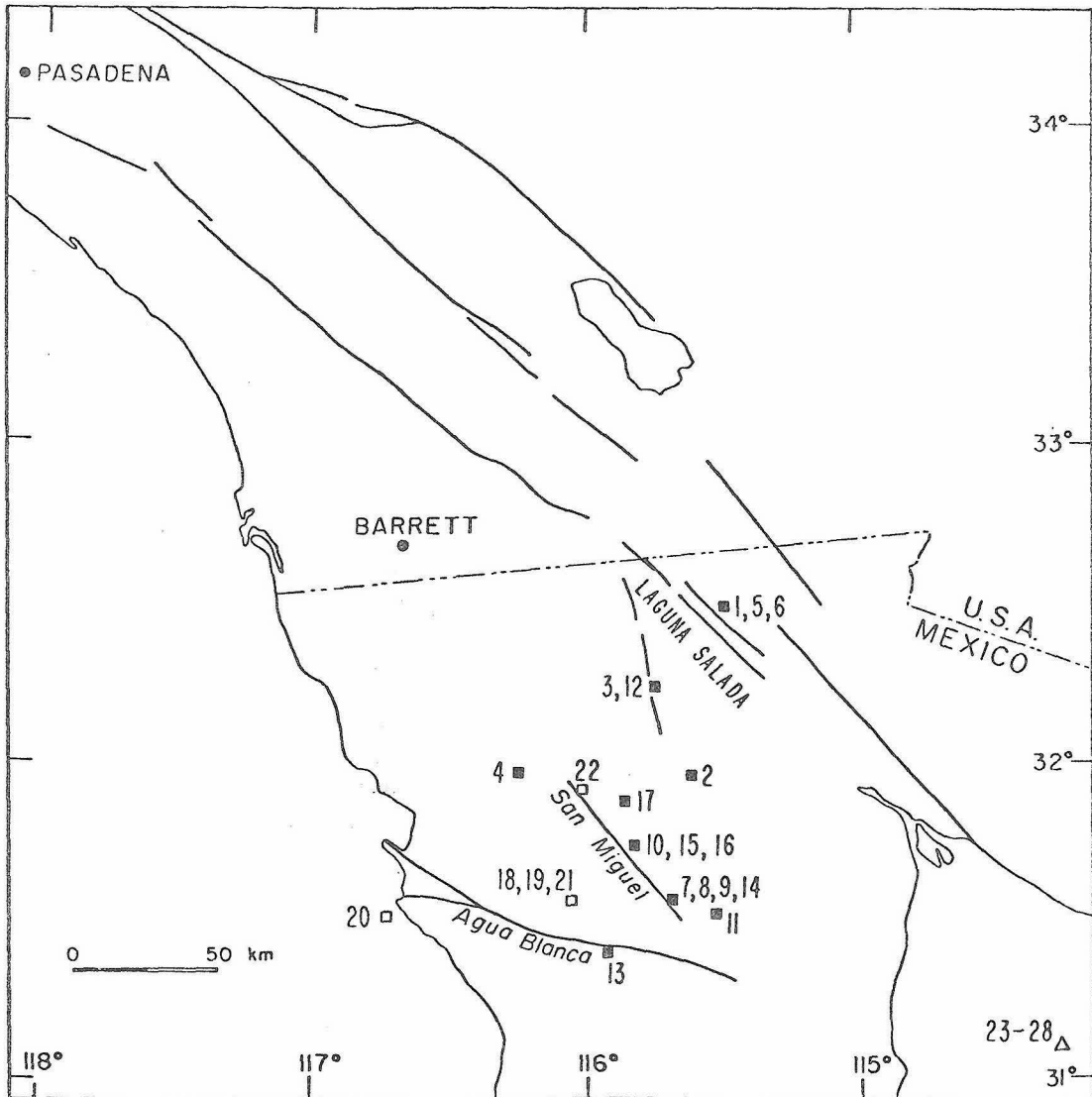


Figure 32. The Northern Baja California region, showing known active faults and earthquakes and local seismograph stations used in this study. Symbols are keyed to figures 38-41, and the numbers to Table 7.

The strain release map of Allen et al. (1965) for the time interval from 1934-1963 demonstrates that Northern Baja is one of the most active areas in the Southern California region. Much of this strain release took place during two sequences of shocks, one in 1954, the other in 1956, and these events and their aftershocks comprise much of the data examined in this study. The sequences of October-November 1954 consisted of successive  $M_L = 5.7, 6.0$  and  $6.3$  events and their aftershocks, and USCGS locations suggested to Richter (1958) their possible location on the Agua Blanca fault. Later relocation of the three largest shocks by Molnar and Sykes (1969) has placed the  $M_L = 6.3$  event (#22 in figure 32) considerably to the north, though (S-P) times at Caltech stations indicate it can be no more than about 20 km from the  $M_L = 6.0$  earthquake (#21). These and other events examined here are shown in figure 32. The second major sequence was the San Miguel earthquake ( $M_L = 6.8$ ) of 9 February 1956 and its extensive aftershock sequence. The mainshock was accompanied by at least 19 km of surface faulting with the motion being predominantly horizontal and right lateral on a near-vertical fault plane, and with an average slip of 85 cm (Shor and Roberts, 1958, Brune and Allen, 1967). Reconnaissance surveys have also shown very high microearthquake activity in the Laguna Salada area, and a generally high level of seismicity persists along the many active faults in Northern Baja California.

## HIGH APPARENT STRESS EARTHQUAKES

The relatively low excitation of surface waves by many North Baja sources was interpreted by Wyss and Brune (1968) to be due to high tectonic stresses acting in the source region of these events. This interpretation was based upon two seismic measurements, surface wave amplitude near 20 seconds period, and the maximum amplitude of short period SH waves (usually between about 2 and 5 cps) registered on a standard Wood-Anderson torsion seismograph. The surface wave amplitude is proportional to seismic moment ( $M_0$ ), and the Wood-Anderson amplitudes determine local magnitude ( $M_L$ ), which Gutenberg and Richter (1956) have empirically related to seismically radiated energy ( $E_s$ ). Using dislocation theory, Aki (1966) and Brune (1968) were able to relate these two quantities to the average of the stresses before and after rupture using the following results:

$$E = \bar{\sigma} A \bar{u} \quad (6)$$

$$E_s = \eta E \quad (7)$$

$$M_0 = \mu \bar{u} A \quad (8)$$

Therefore

$$\eta \bar{\sigma} \equiv \eta \left( \frac{\sigma_1 + \sigma_2}{2} \right) = \mu \frac{E_s}{M_0} \quad (9)$$

where

$E$  = total strain energy released by faulting

$\bar{\sigma}$  = average stress

$\sigma_1, \sigma_2$  = shear stresses across fault before and after rupture

$\eta$  = seismic efficiency factor, the ratio of seismically radiated energy to total strain energy released

$\bar{u}$  = average slip across fault surface

A = fault area

$\mu$  = shear modulus

The quantity  $\eta\bar{\sigma}$  is called the average apparent stress or simply "apparent stress" (Wyss, 1970a). It is not the true average stress because of the multiplicative term  $\eta$ , the seismic efficiency factor, which is in general not known. Unfortunately, as shall be discussed below, the seismically radiated energy is a similarly elusive quantity which is determined by the pre-stress and which is difficult to measure from seismic waves. It is the quantity apparent stress which Wyss and Brune found to be unusually high for the Baja earthquakes.

It should be noted that "high apparent stress" earthquakes have been reported in several other localities. Wyss and Brune interpret them as occurring in San Geronio Pass on the "big bend" of the San Andreas Fault, and in the California-Nevada border region east of the Sierra Nevada. Wyss (1970c) interprets many intermediate focal depth sources in the lithosphere beneath South America as high apparent stress events and attributes this to increased strength within the downgoing plate in this depth range. In his study of the aftershocks of the 1968 Borrego Mountain earthquake, San Jacinto Fault zone, southern California, Wyss (1970a) observed that apparent stresses increased as a function of focal depth and were higher for

sources located away from the main fault break. In contrast, aftershocks of the 1966 Parkfield earthquake on the San Andreas Fault in Central California had apparent stresses which did not significantly vary with focal depth and were lower than at Borrego. Again he interpreted the high apparent stresses as indicative of relatively great strength in the source region. Finally, Hanks (1971a), in a study of the Kuril Trench, interprets many shallow focus events occurring there as having high apparent stresses. Using bathymetric data and focal mechanisms as well, he infers that the apparent stresses are consistent with a compressive stress of several kilobars acting normal to the trench axis.

#### SH SPECTRUM FROM BRUNE'S MODEL

As has been emphasized earlier, the interpretation of apparent stress is made considering only two seismic parameters, moment and magnitude. These are determined using two different portions of the seismic spectrum, the long period part of a surface wave train and the short period segment of the body wave spectrum. The shear stress dislocation model recently proposed by Brune (1970) employs three independent parameters (moment, source dimension, and fractional stress drop) which determine the shape of the far field SH body wave displacement spectrum. The observations made in this study are interpreted in terms of Brune's theory and so his source model is briefly considered here. In addition, the model has implications for estimates of seismically radiated energy which will be investigated later.

Brune models an earthquake source as a tangential stress pulse applied instantaneously to the interior of a dislocation surface. He considers the effective shear stress ( $\sigma$ ) available to accelerate the two sides of the fault as the difference between the initial stress  $\sigma_1$ , and dynamic "frictional stress"  $\sigma_f$  which is of the opposite sense and always acts to resist the fault slip. i.e.,

$$\sigma = \sigma_1 - \sigma_f \quad (10)$$

If the fault slippage proceeds until the shear stress acting across the fault has decreased to  $\sigma_f$  ("complete effective stress drop") and the effects of finite rupture propagation velocity are suitably averaged over azimuth, the far-field displacement spectrum shown by the upper curve in figure 33 results. At low frequencies the spectrum is flat and is proportional to seismic moment. At a "corner frequency" ( $f_0$ ) which is inversely proportional to the source dimension the spectral amplitudes begin to decrease, and at high frequencies the spectrum falls off as  $\omega^{-2}$ . In this case only, the stress drop is equal to the effective shear stress, and only two independent parameters (source dimensions and moment) are needed to define the spectrum. If, on the other hand, the stress drop is only a fraction of the effective shear stress, then the spectrum is modified as shown in the lower curve of figure 33. Defining the fractional stress drop ( $\epsilon$ ) by

$$\epsilon = \frac{\sigma_1 - \sigma_2}{\sigma} \quad , \quad \sigma_2 \geq \sigma_f$$

it is seen that the long period flat level of the spectrum is reduced to

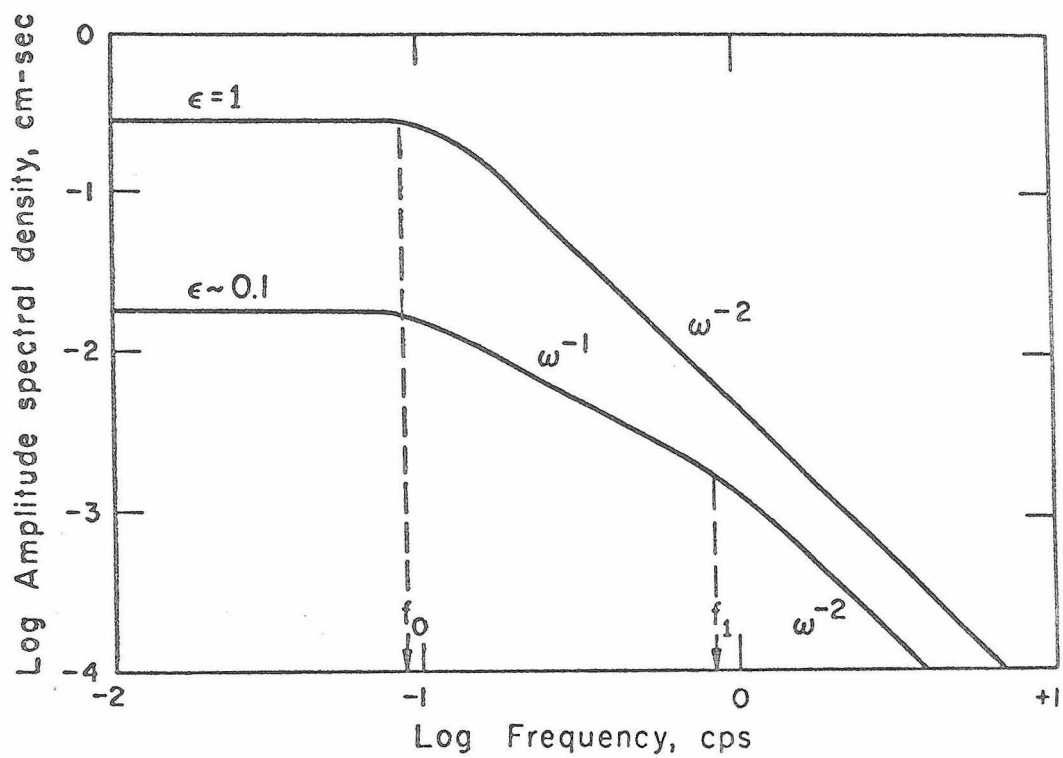


Figure 33. Theoretical RMS averaged SH far-field displacement spectra for the source model of Brune (1970).

$\epsilon$  times what its value would be for complete effective stress drop. Furthermore, the spectral amplitudes at frequencies higher than the corner frequency  $f_0$  begin falling off as  $\omega^{-1}$ , and only fall off as  $\omega^{-2}$  past some higher frequency ( $f_1$ ) given approximately by  $f_1 \approx f_0/\epsilon$ . This  $\omega^{-1}$  fall-off considerably increases the seismic energy radiated at high frequencies.

### ANALYSIS OF DATA

The SH displacement spectra of 21 Northern Baja California earthquakes with magnitudes in the range from  $3\frac{1}{2}$  to 6 have been measured using data obtained from Caltech stations in Southern California. These data have been supplemented by long period seismograms from Palisades, New York, kindly provided by the Lamont-Doherty Geological Observatory. In addition, the spectra from six earthquakes within the Gulf of California are compared to those of the Baja sources. Sources and stations used are summarized in Table 7.

Seismograms used from the Caltech stations at Pasadena ( $\Delta \approx 300$  km) and at Barrett ( $\Delta \approx 100$  km) were written on standard ( $t_0 = 0.8$  sec) and long period ( $t_0 = 6$  sec) torsion seismographs and long period Benioff instruments ( $t_0 = 1$  sec,  $t_g = 90$  sec) whose response curves are shown in figure 34. Used together, the 0.8 sec and 6.0 sec torsion instruments provide a useful bandwidth of from 0.05 to 5.0 cps, the high frequency amplitudes being limited by anelastic attenuation at distances greater than about 100 km. The

TABLE 7  
Listing of Earthquakes Studied

## NORTHERN BAJA

Event No.	Date	Time	Lat	Long	Stations Used	$M_L$
1	06 May 1961	02 11	32.5°	115.5°	BAR	3.7
2	20 May 1961	11 09	31°58'	115°37'	BAR	3.8
3	22 March 1961	15 11	32°15'	115° 5'	BAR, PAS	4.0
4	31 May 1961	07 23	31°58'	116°18'	BAR, PAS	4.0
5	06 May 1961	02 08	32.5°	115.5°	BAR	4.1
6	06 May 1961	02 41	32.5°	115.5°	BAR	4.2
7	13 Feb 1956	07 44	31°35'	115°40'	PAS	4.4
8	11 Feb 1956	16 59	31°35'	115°40'	PAS	4.6
9	10 Feb 1956	04 18	31°35'	115°40'	PAS, PAL	5.0
10	10 Feb 1956	15 10	31°45'	115°55'	PAS	5.0
11	14 Feb 1956	14 18	31°30'	115°30'	PAS, PAL	5.0
12	01 Dec 1958	03 50	32°15'	115°45'	PAS, PAL	5.0
13	21 Sept 1967	00 01	31°25'	115°57'	PAS, PAL	5.1
14	11 Feb 1956	06 24	31°35'	115°40'	PAS, PAL	5.4
15	10 Feb 1956	18 12	31°45'	115°55'	PAS, PAL	5.5
16	09 Feb 1956	18 48	31°45'	115°55'	PAS, PAL	5.7
17	09 Feb 1956*	14 32	31°54'	115°51'	Geodetic Data Only	6.8

## OCTOBER-NOVEMBER 1954

18	24 Oct 1954	14 06	31.4°	116.0°	PAS	4.7
19	24 Oct 1954	11 21	31.4°	116.0°	PAS	5.4
20	17 Oct 1954*	22 57	31°31'	116°43'	PAS, PAL	5.7
21	24 Oct 1954*	09 44	31°35'	116°03'	PAS	6.0
22	12 Nov 1954*	12 26	31°56'	116°01'	PAS, PAL	6.3

TABLE 7 (Continued)

## GULF OF CALIFORNIA

Event No.	Date	Time	Lat	Long	Stations Used	M <sub>L</sub>
23	24 March 1969	02 19	31°10'	114°26'	PAS	4.3
24	22 March 1969	04 29	31°10'	114°26'	PAS	4.4
25	21 March 1969	22 28	31°10'	114°26'	PAS	4.7
26	21 March 1969	07 57	31°10'	114°26'	PAS	4.9
27	21 March 1969	17 55	31°10'	114°26'	PAS, WES	5.1
28	20 March 1969	08 17	31°10'	114°26'	OXF, NUR	5.7

\* Location from Molnar and Sykes (1969)

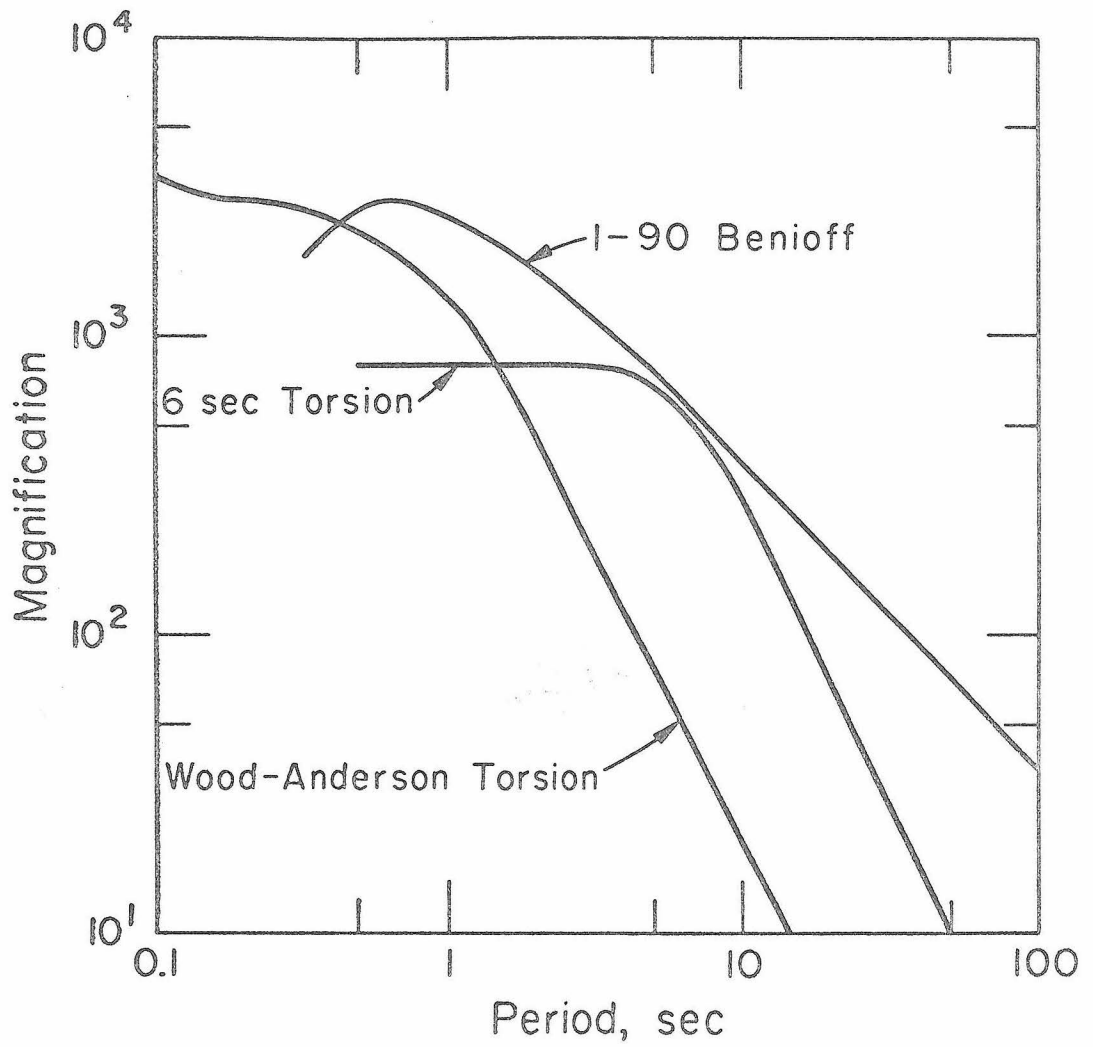


Figure 34. Response curves of instruments from Caltech stations used in this study.

long period response of the Benioff is rather better, and useful amplitudes out to 0.02 cps have been obtained. The Palisades records were from long period seismographs ( $t_o = 15$  sec,  $t_g = 75$  sec; recently calibrated by John Savino of Lamont) which supplied spectral information from 0.02 to 0.2 cps.

The location of sources and local stations used in this study are shown in figure 32.

Considering first the locally recorded events, the spectral amplitudes have been corrected for anelastic attenuation using  $Q = 300$ , similar to Press's (1964)  $Q$  of 500 determined from the attenuation of the Lg phase in California. Local variations in  $Q$  may differ by a factor of two from this value without significantly affecting anything except the observed rate of spectral amplitude decay at high frequencies.

The teleseismic body wave data have been corrected for attenuation using curves in Julian and Anderson (1968). The change in shape of the spectrum due to attenuation is small. The absolute level of the spectrum has not been determined, since at teleseismic distances it is strongly dependent on radiation pattern, which is unknown for the sources studied here. Hence for events 20, 22 and 28, only the AR moment has been determined.

The sample lengths used in the spectral analysis varied considerably, but were always of sufficient duration to define the longest period waves used in estimating the "long period level" of the spectrum. Experimentation with differing sample lengths showed factor of two fluctuations in long period level, and longer sample lengths which

included more high frequencies caused reduction of the amplitude fall-off past the corner frequency. In general, samples from short period seismograms were of shorter duration than those from long period records.

The data examined here have been interpreted in terms of seismic moment and source dimensions using Brune's theory. The recent results of Hanks and Wyss (1971) in adequately estimating these parameters using teleseismic body wave spectra of earthquakes with geodetically measured fault length and slippage confirm the usefulness and accuracy of the theory.

None of the earthquakes studied in this paper using spectra have observed surface breaks or offsets and in general their radiation patterns are not known.

The observed spectra have been fit to a flat long period level and a high frequency amplitude fall-off (see, for example, figures 35-37). An average radiation pattern correction of 0.6 has been used to correct amplitudes, as well as a factor of two correction to account for SH reflection at the free surface.

For the locally recorded events the geometrical spreading correction is for simple  $1/R$  amplitude decay with distance. This corresponds to the expected behavior of the "direct wave" from the source. Several distinctly different phases are commonly recorded in the S-wave train of local earthquakes, and in general each one has a different amplitude decay (Gutenberg, 1944). The sample lengths

used often include several of these different phases, each travelling different paths and possessing differing attenuation characteristics, and hence using the  $1/R$  correction for geometrical spreading is somewhat imprecise. However, in checking the seismic moments obtained from the SH spectra with those determined using surface wave amplitudes, it has been found that the agreement is good. This of course does not verify that the shape of the spectrum has been preserved in propagation between source and station. The surface wave moments were computed by the AR method (Brune et al., 1963, Wyss and Brune, 1968), by summing the areas of the envelopes of the surface waves from the source recorded on the 3 components of Press-Ewing seismographs. Unfortunately, these instruments were not installed in Pasadena until late 1956, and the useful 6 sec torsion seismographs were discontinued in late 1959, so that comparisons for events before 1957 is not possible using Pasadena records. For events recorded at Barrett, the moments obtained from SH spectra are compared with some determined by Wyss and Brune for the same events by the AR method. Only events with  $AR \geq 10 \text{ mm}^2$  at Pasadena were considered reliable enough to make comparisons with spectrally determined moments. Whenever possible, seismic moments obtained from spectra were checked against those obtained from the Palisades 15-75 records using the AR method. This procedure should be approximately valid because the shape of the response curve of this instrument is very similar to that of the Press-Ewings, particularly at periods near 20 seconds where the largest area contributions to AR occur.

The overall agreement between the AR moments and those deter-

mined from SH spectra is considered satisfactory (see columns 3 and 4 of Table 8). Two values disagree by a factor of 4, but in all other cases factor of 2 to 3 agreement is the rule. There appears to be no consistent bias.

All of the data collected and analyzed in this study are shown in Table 8. However, consider first some observed spectra, which illustrate the quality of the basic data and show how it has been interpreted here. Figure 35 shows the observed spectra for the three earthquakes whose Wood-Anderson seismograms were seen in figure 31. The source dimensions and moments of the West Baja and Gulf of California events could not be determined with Pasadena seismograms alone because the high long period excitation drove the 1-90 Benioff instruments at this station offscale. As a result, records from Palisades for the West Baja event ( $\Delta \cong 36^\circ$ ), and the WWSSN station at Atlanta for the Gulf shock ( $\Delta \cong 25^\circ$ ) have been patched together with the local Wood-Anderson data. The long period level and corner frequency of each of the spectra are considered well-determined by the observations. Observe that because the amplitude scale is logarithmic the average amplitude lines appear somewhat high. Again note the striking contrasts between the Northern Baja event and the other two shown.

Figure 36 is similar to figure 35 and compares two events with local magnitudes 5.2 and 5.1, one in Northern Baja and the other in the Gulf of California. These particular earthquakes are shown to make a further comparison of two contrasting events discussed in Chapter III. There a comparison was made of the surface wave

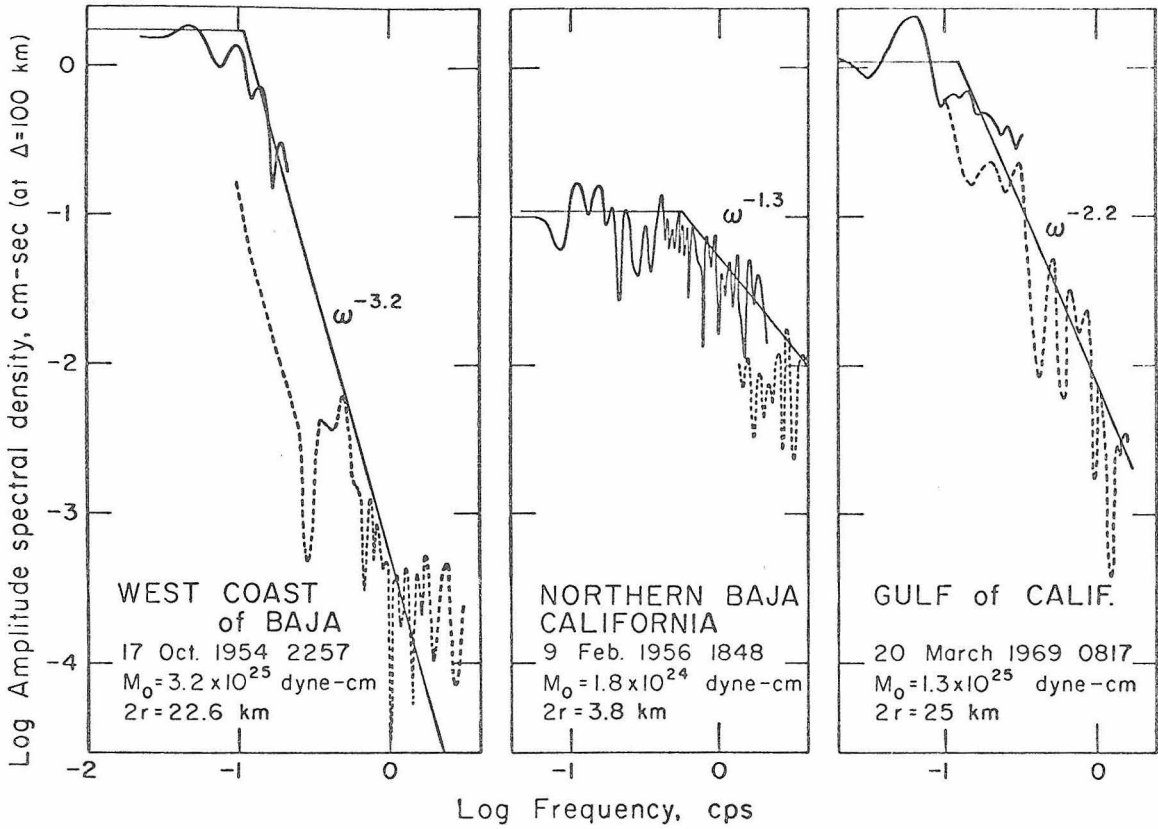


Figure 35. SH displacement spectra for the three earthquakes whose seismograms are illustrated in figure 31. The spectral amplitudes have been reduced to a standard epicentral distance of 100 km. All earthquakes have an assigned magnitude of 5.7.

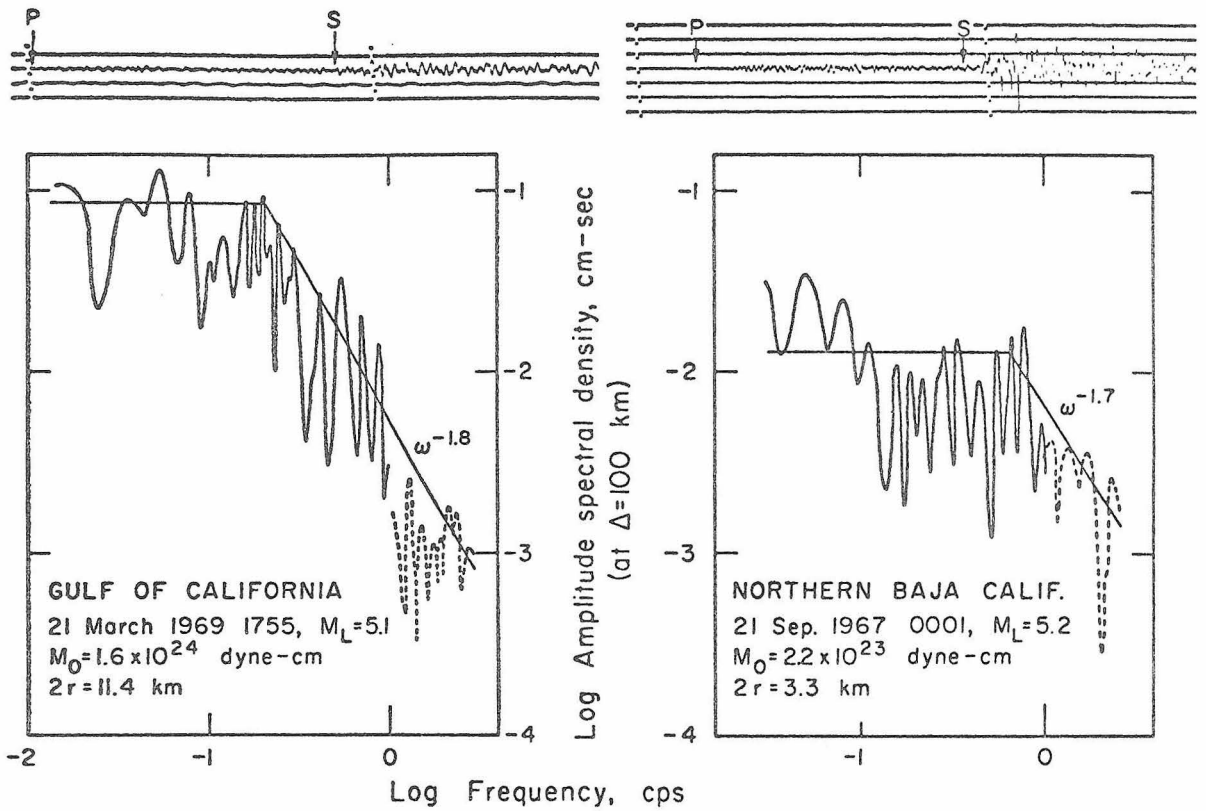


Figure 36. SH displacement spectra and corresponding Wood-Anderson seismograms for a Northern Baja and a Gulf of California source of comparable local magnitude. Scaling and symbols as in figure 5. These two earthquakes are closely comparable to those discussed in Chapter III and shown in figure 30.

excitation by a swarm event and one from North Baja of the same magnitude. Figure 30 reproduced the long period seismograms of those two events, and the remarkably low long wave excitation of the Northern Baja source was very clear. Figure 36 here shows the SH spectra for the same Baja event and a Gulf swarm event almost identical to the one illustrated in figure 30. An exact comparison was not possible because the swarm event was not recorded clearly enough on the 1-90 Benioffs at Pasadena. The spectra shown are again strikingly different, demonstrating clearly the relatively small moment and source dimensions of the Baja earthquakes. For the North Baja source in figure 36 there is less spectral amplitude information at frequencies higher than the corner frequency, and hence the source dimensions are somewhat less reliably determined than in the cases of the other spectra shown. However the great difference in source size between the Gulf and Baja sources is a strong conclusion.

Also shown in figure 36 are the corresponding Wood-Anderson seismograms recorded at Pasadena, and again the differences in the frequency content of the two records are clear.

Six earthquakes used in this study were recorded at Barrett, with epicentral distances varying from 80 to 140 km, so that frequencies as high as 6-10 cps could in principle be recorded. Unfortunately, the Wood-Anderson seismographs at Barrett do not, for a variety of reasons (related to the instrument set-up there), accurately record these high frequencies. As a result only 1-90 Benioffs were reliable enough to use and only out to about 4 cps.

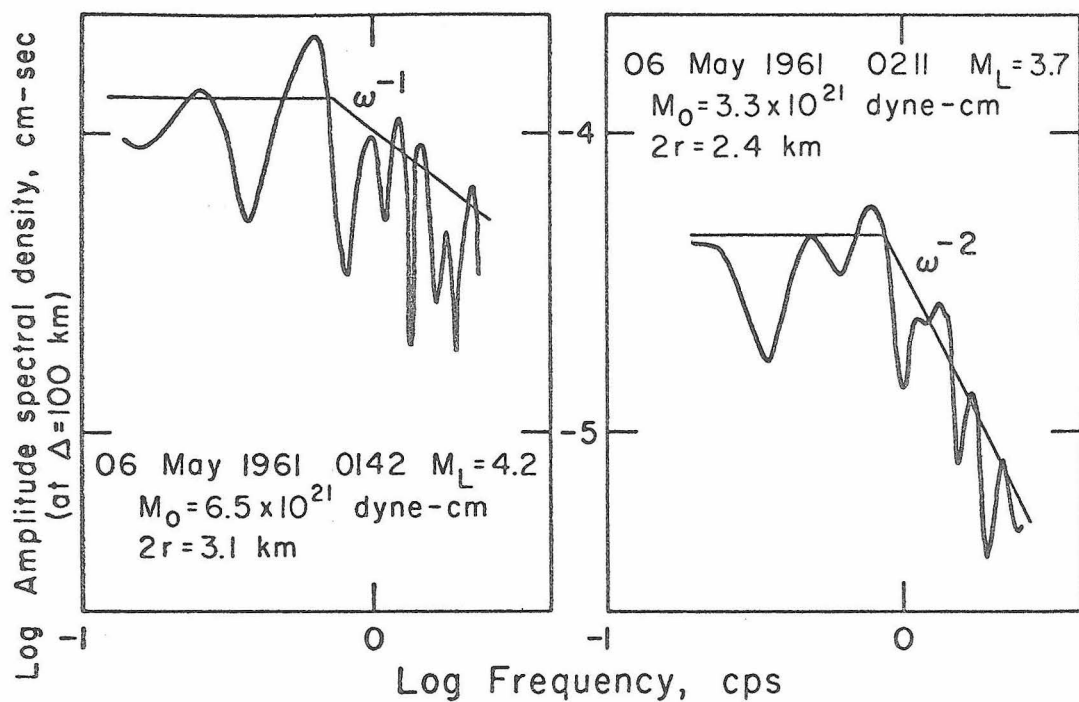


Figure 37. SH displacement spectra for two earthquakes recorded on 1-90 long period Benioff seismographs at Barrett, about 140 km from the epicenters. The spectrum on the left has a rather poorly defined corner frequency and high frequency fall-off compared with other data examined in this study.

Hence, although definite decreases in spectral amplitude occur between about 1 and 4 cps for these sources, their source dimensions are not so well determined as those for the other data shown in figures 35 and 36. Figure 37 illustrates the quality of these data, showing one spectrum with a very definite fall-off in amplitude at high frequency, and another whose high-frequency decay is not so marked. These two earthquakes were recorded at Barrett about 140 km from their epicenters.

Figures 35 to 37 are a representative sampling of all data examined here and convey some idea of the range and quality of the observations and the reliability of their interpretation.

### SOURCE PARAMETERS

By fitting the observed spectra to those derived from Brune's model, the parameters seismic moment and source dimensions have been estimated. These two quantities determine the average fault slippage, and hence the average stress drop on the rupture surface.

The amplitude fall-off at high frequencies is a spectral parameter which is observed here, but it is not considered a reliable source parameter with these data and is not used to infer fractional stress drop.

Radiated energies are estimated using Gutenberg and Richter's energy-magnitude relation, and compared with a lower bound spectral estimate made assuming complete effective stress drop. From the Gutenberg-Richter estimate and the measured seismic moment,

TABLE 8

Source Parameters of Earthquakes Studied

Event No.	$M_L$	$M_0$ (dyne-cm $\times 10^{21}$ )	$M_0$ (AR) (dyne-cm $\times 10^{21}$ )	$2r$ (km)	$\Delta\sigma$ (bars)	High Freq. Fall-off	$E_{GR}$ (dyne-cm $\times 10^{17}$ )	$\bar{\eta}\sigma$ (bars)	$\frac{E_{GR}}{E_{MIN}}$
NORTHERN BAJA									
1	3.7	3.3	-	2.4	0.3	-2.0	0.43	4	35
2	3.8	6.0	-	2.3	1.7	-0.6	0.63	4	15
3	4.0	2.8	2.9	2.3	0.9	-0.7	1.3	16	110
4	4.0	5.7	0.8	2.8	0.9	-1.0	1.3	8	50
5	4.1	8.2	-	2.3	2.5	-1.4	2.0	9	20
6	4.2	6.5	2.3	3.1	1.1	-1.0	3.2	16	160
7	4.4	6.1	-	3.1	0.7	-2.0	6.3	31	340
8	4.6	35.	-	2.6	6.1	-1.9	14.	11	15
9	5.0	41.	174(PAL)	4.6	1.3	-1.0	63.	46	250
10	5.0	55.	-	2.3	13.	-0.9	63.	38	20
11	5.0	187.	323(PAL)	6.7	2.1	-2.0	63.	10	40
12	5.0	142.	54	2.5	32.	-1.6	63.	13	4
13	5.2	224.	150	3.3	21.	-1.7	130.	20	4
14	5.4	264.	310(PAL)	2.1	98.	-1.9	290.	47	2
15	5.5	1260.	1000(PAL)	4.9	40.	-1.9	420.	14	2
16	5.7	1780.	1100(PAL)	3.8	94.	-1.2	830.	20	1
17	6.8	24200.	-	19.	14.	-	53700.	67	-

TABLE 8 (Continued)

Event No.	$M_L$	$M_o$ (dyne-cm $\times 10^{21}$ )	$M_o$ (AR) (dyne-cm $\times 10^{21}$ )	$2r$ (km)	$\Delta\sigma$ (bars)	High Freq. Fall-off	$E_{GR}$ (dyne-cm $\times 10^{17}$ )	$\eta\bar{\sigma}$ (bars)	$\frac{E_{GR}}{E_{MIN}}$
OCTOBER-NOVEMBER 1954									
18	4.7	38.	-	2.5	8.3	-1.2	21.	20	150
19	5.4	820.	-	11.3	2.0	-0.9	290.	11	40
20	5.7	-	32000(PAL)	22.6	10.3	-3.2	830.	1	0.5
21	6.0	11700.	-	12.9	17.	-0.8	2500.	7	3
22	6.3	-	30000(PAL)	55.	1.1	-1.3	7900.	6	85
GULF OF CALIFORNIA									
23	4.3	260.	150	9.0	1.3	-1.3	4.6	1	3
24	4.4	250.	170	8.1	1.7	-1.7	6.3	1	3
25	4.7	810.	360	13.1	1.1	-1.8	21.	1	4
26	4.9	810.	490	20.6	0.3	-1.2	45.	2	35
27	5.1	1580.	-	11.4	3.7	-1.8	100.	2	4
28	5.7	-	13000(NUR)	25.4	3.3	-2.2	830.	2	5

apparent stresses have been computed.

All computed source parameters are listed in Table 8.

### Seismic Moments

The seismic moments obtained are listed in column 3 of Table 8 and plotted on a semi-log scale against local magnitude in figure 38. Shown on the same figure are the moment-magnitude curves of Wyss and Brune for Parkfield and for an average of all data in the western United States. Gulf of California data from Chapter III obtained from measurements of surface wave spectra are plotted on the same figure (open triangles). The plot merely re-emphasizes the remarkable differences in long wave excitation between Baja and Gulf sources which have been studied previously by Brune and his co-workers. This difference averages at least an order of magnitude and persists undiminished down to  $M_L = 4$ .

Values of AR at Palisades for six underground nuclear explosions taken from Brune et al. (1963) have been converted to equivalent "moments" and are shown plotted as diamonds in figure 38. Also plotted is their maximum line for explosions. Near magnitude 4.5 the long period excitation for the explosions and the Northern Baja earthquakes differ by a factor of two or less, underlining a further difficulty of discrimination at small magnitudes.

Northern Baja earthquakes which occurred during October-November 1954 are plotted with different symbols (open squares) to emphasize their behavior as a group. The largest magnitude events ( $M_L = 5.7, 6.0, 6.3$ ) all have relatively large moments, though for

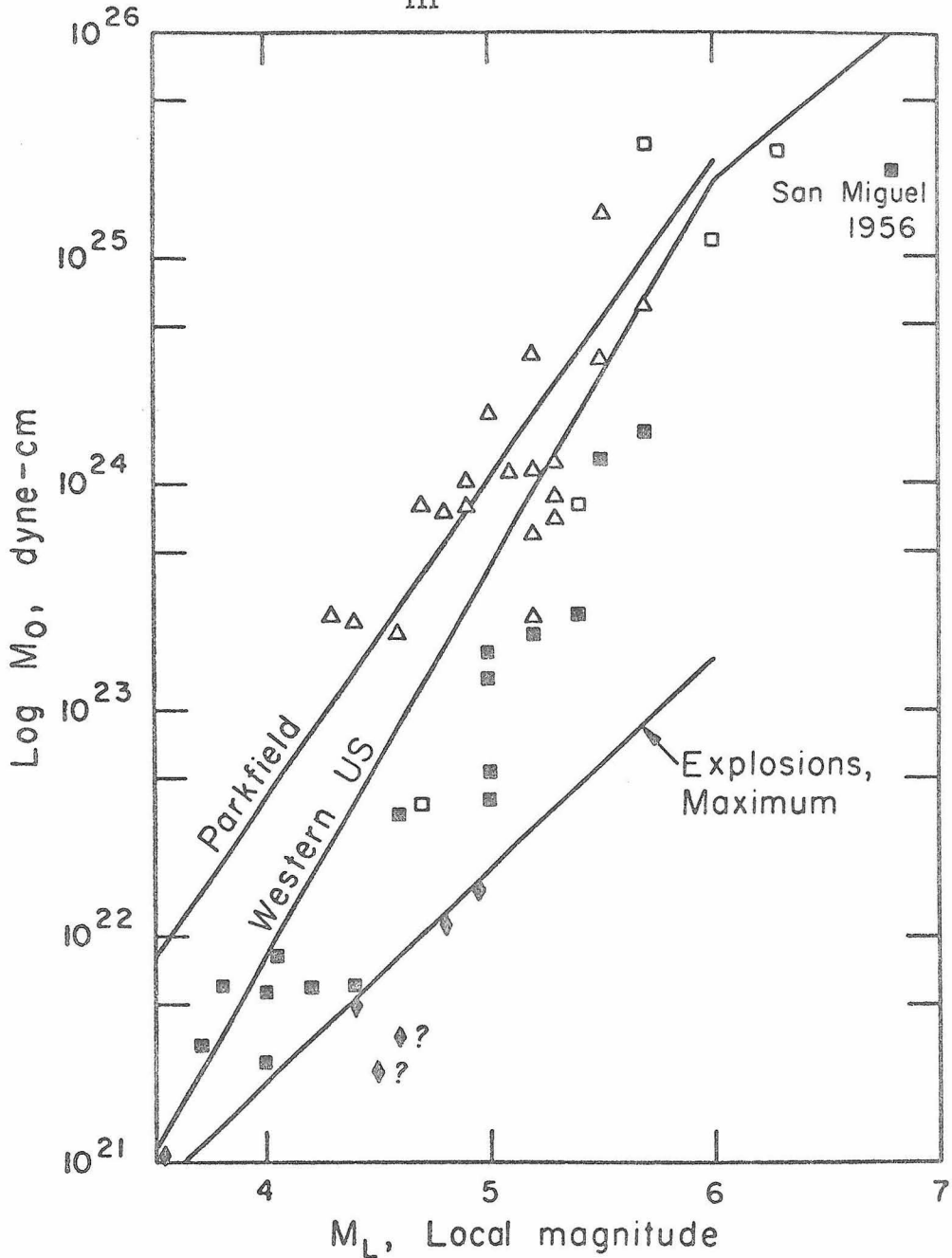


Figure 38. Logarithm of seismic moment plotted as a function of local magnitude compared with average lines for Parkfield and the western U.S. from Wyss and Brune (1968), and Gulf of California moments from Chapter III. Gulf data are denoted by open triangles, North Baja data solid squares, and the October-November 1954 Baja sequence open squares. Explosion data taken from Brune *et al.* (1963) are shown as solid diamonds, along with their maximum line.

smaller magnitude sources the long period excitation approaches that of the other Northern Baja shocks. As shall be seen, their source dimensions behave similarly. Examination of seismograms from other events of this sequence confirms the same general behavior as for the data which is shown here. No other sources from North Baja which were examined in this study showed these large moments and source dimensions. However there is no evidence to preclude their occurrence at other times or in different localities within Northern Baja California.

Also plotted is the moment of the 1956 San Miguel earthquake, estimated from observations of the surface faulting by Shor and Roberts (1958).

#### Source Dimensions

Rupture dimensions determined from the corner frequencies of spectra are listed in column 5 of Table 8 and plotted on a semi-log scale against local magnitude in figure 39. Also plotted for comparison are the magnitude-fault length curves proposed by Press (1967) and by Wyss and Brune. The data set as a whole appears to be roughly confined by the two lines, though the Gulf of California earthquakes have distinctly larger source dimensions than the bulk of the Northern Baja data. The exceptions comprise four of the larger events ( $M_L \geq 5.4$ ) from the October-November 1954 sequence, whose source dimensions are comparable with Gulf earthquakes in the same magnitude range. Between magnitudes 5 and 6 these four events and the Gulf group have source dimensions from 11 to 25 km (and lie near Wyss

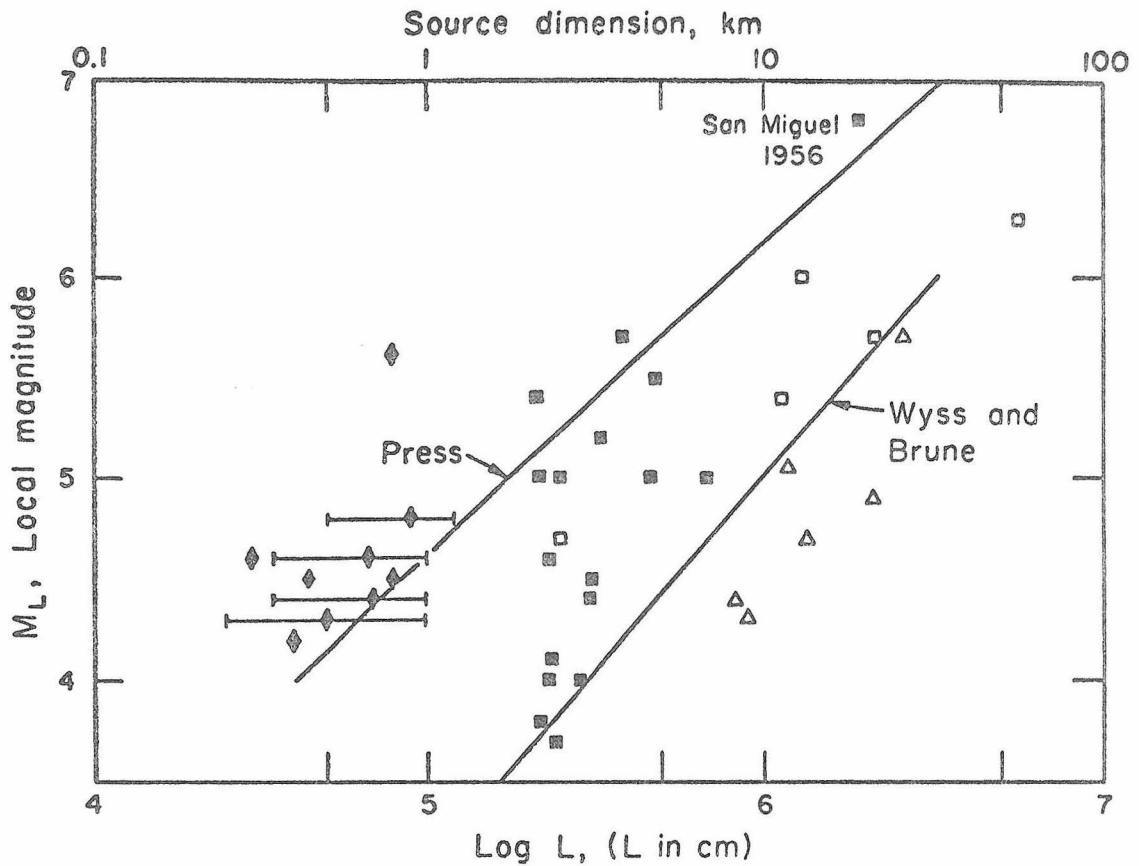


Figure 39. Local magnitude plotted versus the logarithm of the source dimension (here taken as the diameter of an equivalent circular rupture, i.e.  $L \equiv 2r$ ). Same symbols as figure 38. The magnitude fault length curves proposed by Press (1967) and Wyss and Brune (1968) are shown for comparison, along with some source dimensions for underground nuclear explosions (solid diamonds) from Wyss *et al.* (1970).

and Brune's line), while those for the rest of the Northern Baja group vary between 2 and 7 km. For  $M_L < 5$  all Baja source dimensions are relatively insensitive to magnitude and are near 3 km, while Gulf sources average near 12 km. Near magnitude 4 the difference in source size is still at least a factor of three.

Also plotted on figure 39 are some source dimensions of underground nuclear explosions taken from Wyss et al. (1970). The dimensions of the explosions are at least a factor of two smaller than North Baja earthquakes of the same magnitude.

Note that the "fault length" obtained here is, from Brune's theory, the diameter of an equivalent circular rupture, which may not correspond precisely to a length of observed surface rupture. In Brune's model the corner frequency and the flat long period level of the spectrum are a result of diffraction of long waves around the "ends" of the fault. Thus in the case of nearly rectangular faults it may be the width (smaller dimension) or an area-averaged length which the corner frequency really measures.

### Stress Drops

Stress drops are shown listed in column 6 of Table 8 and plotted logarithmically against local magnitude in figure 40. Since the stress drop is proportional to the ratio of seismic moment to cube of source dimension, it is subject to greater uncertainty than either of the parameters which determine it, and may sometimes be in error by as much as an order of magnitude.

Again the Gulf and October-November 1954 points are separated

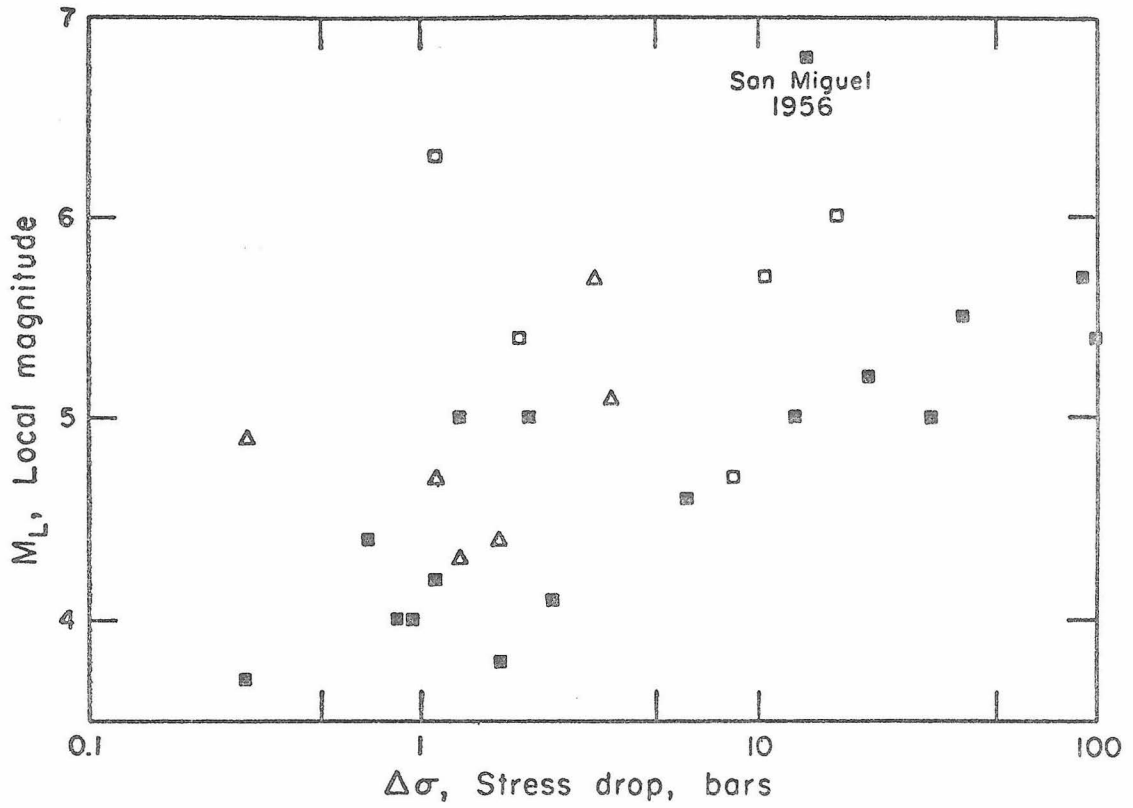


Figure 40. Local magnitude as a function of the logarithm of the stress drop in bars. Same symbols as figures 38 and 39.

from the other data for  $M_L > 5$ , having generally smaller stress drops at a given magnitude than the remainder of the Northern Baja data. Towards lower magnitudes the two groups of data converge.

Though the scatter in the observations is great, figure 40 also indicates that stress drop is an increasing function of magnitude for the North Baja data in the range  $M_L = 4 \rightarrow 6$ , averaging less than 1 bar at  $M_L = 4$  and about 100 bars near  $M_L = 6$ . In the same magnitude range Wyss and Brune's 1966 Parkfield data, which may be characteristic of the relatively unlocked segments of the San Andreas system, give an almost constant stress drop of 4 bars. Stress drops for Gulf earthquakes are similarly insensitive to magnitude and average near 2 bars.

#### High Frequency Spectral Amplitude Decay

The observed rate of spectral amplitude fall-off past the corner frequency has been measured for each event studied here. However, there are several reasons why the observed rate will not be an accurate measure of the high frequency fall-off of the spectrum at the source. The data are tabulated in column 7 of Table 8, but as can be seen show no strong consistency, though slopes may be slightly steeper for Gulf sources. The high frequency amplitudes for waves which have traversed paths longer than 100 km are certainly sensitive to changes in the chosen average  $Q$  value of 300. For example, if a corner frequency near 0.5 cps is observed at  $R \approx 350$  km a decay rate of  $\omega^{-1.0}$  assuming  $Q = 300$  would become  $\omega^{-1.6}$  if  $Q$  were 600. In addition, propagation of some phases can modify the source

spectrum significantly. Critically refracted waves decay approximately as  $1/R^2$  past the critical distance, and the source spectrum is multiplied by a  $1/\omega$  factor (see e.g. Grant and West, 1965). Hill (1971) has made an intensive theoretical and observational study of refracted crustal wave amplitudes and finds them to be very sensitive to vertical gradients as well as to lateral contrasts and anelastic attenuation. In addition, high frequencies may be unpredictably focused and defocused by scattering.

Complex rupture propagation such as Haskell (1964) has suggested could certainly affect high frequency amplitudes and this point will be discussed further below. However, quite aside from this possibility, even a smoothly propagating rupture will focus energy in preferred directions and produce maxima and minima in the observed spectrum.

Even if all of the preceding effects were of secondary importance, the available frequency band past the corner is not wide enough to unambiguously define an amplitude decay rate. It must then be concluded that fractional stress drop cannot be estimated from the spectra of individual earthquakes studied here. As a result, neither effective shear stress nor spectral estimates of seismically radiated energy are accurately determined, though a lower bound for the seismically radiated energy may be estimated.

#### Radiated Energy and Apparent Stresses

Seismically radiated energies and the apparent stresses which have been computed using them are listed in columns 8 and 9 of

Table 8. Radiated energies were calculated from the energy-magnitude relation given in Richter (1958):

$$\log E_{GR} = 9.9 + 1.9 M_L - 0.024 M_L^2 .$$

This is the appropriate relation between energy and local magnitude and differs somewhat from the energy-surface wave magnitude relation used by Wyss and Brune (1968) and Thatcher and Brune (1971) for computing apparent stresses (Tom Hanks, personal communication). The appropriate relation reduces energies by a factor of eight at  $M_L = 3$  and by a factor of two near  $M_L = 6.5$ . For consistency over a large magnitude range, the local magnitude relation will be used henceforth.

Apparent stresses thus computed for Northern Baja shocks are on the average about an order of magnitude larger than those obtained for Gulf of California events, with earthquakes from the October-November 1954 sequence intermediate between the two extremes. There is a suggestion that apparent stress is an increasing function of magnitude for the Northern Baja data.

#### RADIATED ENERGY ESTIMATES

The assumed relationship between local magnitude and seismic energy strongly affects the apparent stress computations made in the previous section, and for this and other reasons some inquiry into the derivation of this relation is in order. This energy estimate may be then assessed from the vantage point of current understanding of

seismic source spectra.

In deriving their empirical relationship between seismically radiated energy and local magnitude, Gutenberg and Richter (1956) (hereafter referred to as G-R) carried out an approximate time domain integration of the high frequency portion of the Wood-Anderson seismogram. On the basis of a large number of observations this was corrected back to the source, and energy was computed using

$$E_{GR} = 3\pi^3 \rho \beta h^2 \left( \frac{A_0}{T_0} \right)^2 t_0 \quad (11)$$

where

$E_{GR}$  = Gutenberg-Richter estimate of seismically radiated energy

$\rho$  = density

$\beta$  = shear wave velocity

$h$  = hypocentral depth of source

$A_0, T_0$  = amplitude and period corresponding to maximum trace deflection on seismogram which would be recorded at the surface directly above the source

$t_0$  = duration of the maximum wavetrain.

The derivation of equation 11 considers a point source radiating equally in all directions, corrects for the free surface effect on SH amplitudes, assumes simple  $1/R$  amplitude decrease due to geometrical spreading, and includes P-wave energy assuming it is one-half that for S. The factors  $(A_0/T_0)$  and  $t_0$  were obtained from measurements of these quantities on seismograms at a range of distances out

to about 300 km. The amplitudes and durations were normalized to account for differences in magnitude, and the indicated variation with epicentral distance of  $(A/T)$  and  $t$  allowed these quantities to be corrected back to the source. In the range from  $M_L = 3 \rightarrow 7$ ,  $T_o$  increased from 0.2 to 0.5 seconds and  $t_o$  increased from 1.0 to 10 seconds, and hence only a very narrow high frequency bandwidth and very short record duration were used in estimating energy.

As a standard of comparison with the G-R result, energy radiated by Brune's shear stress dislocation source can be computed by integrating the spectrum shown in figure 33. Assuming here a double couple radiation pattern and other assumptions as for equation 11, it may be shown that (Thatcher and Hanks, 1971)

$$E_{\text{SPECTRUM}} \cong 6\pi^3 \rho \beta R^2 \left\{ \Omega_o^2 f_o^3 \left( \frac{2}{\epsilon} - \frac{2}{3} \right) \right\} \quad (12)$$

where

$R$  = hypocentral distance

$\Omega_o$  = low frequency level of spectrum.

Gutenberg and Richter's result may be easily rewritten in a form which is more conveniently compared with radiated energies computed from equation 12. Amplitudes are related to amplitude spectral densities by assuming a group of sine waves with  $n$  peaks each. The relation is

$$\bar{u} \approx A \frac{nT}{2} \quad (13)$$

where  $n$  is the number of waves of period  $T$  and ground amplitude  $A$ .

Then to sufficient approximation equation 11 becomes

$$E_{GR} = 6\pi^3 \rho \beta R^2 \left\{ \bar{u}_o^2 F_o^3 \right\} \quad (14)$$

where  $\bar{u}_o$ ,  $F_o$  are amplitude spectral density and frequency corresponding to  $A_o$  and  $T_o$  of equation 11.

Equations 12 and 14 have a similar form, but the former result shows clearly the explicit dependence on physical parameters of the source. In particular, note the strong dependence of radiated energy on the fractional stress drop  $\epsilon$ .

The two estimates may be further compared if it is assumed that the high frequency amplitudes measured by Gutenberg and Richter are identical with those predicted by Brune's theory. The comparison will then provide some useful insights into the nature of the two energy estimates. Consider only the cases where  $F_o > f_o$ , which should be true for all  $M_L \geq 2$ . It may be expected that G-R's energy will be low with respect to a source spectrum estimate if the high frequency fall-off is  $\omega^{-2}$ . Furthermore, this divergence will increase as  $(F_o - f_o)$  increases. Similarly, for  $\omega^{-1}$  fall-off,  $E_{GR}$  will be higher or lower than  $E_{SPECTRUM}$  depending upon  $\epsilon$  and the difference between  $F_o$  and  $f_o$ .

Comparison of  $E_{GR}$  and  $E_{SPECTRUM}$  is, however, a rather different matter in considering real data, since  $\epsilon$  is not in general determined from the observations. This difference can be illustrated by examination of the spectral data collected in this study. In addition to the radiated energy computed from G-R's formula, a minimum

estimate of radiated energy ( $E_{MIN}$ ) was also made using observed long period spectral levels and corner frequencies and assuming complete effective stress drop (i. e. equation 12 with  $\epsilon = 1$ ). The ratio  $E_{GR}/E_{MIN}$  is listed in column 10 of Table 8. This ratio is nearly always quite large, especially at smaller magnitudes. The reason for this difference is made clear when equations 12 and 14 are considered in conjunction with the Baja and Gulf observations and the actual values of the high frequency amplitudes used by Gutenberg and Richter in their study, and the next figure demonstrates this. Figure 41 is a log-log plot of amplitude spectral density (corrected to a standard distance of 100 km) versus frequency. The  $(\Omega_o, f_o)$  values for each earthquake in Table 8 are plotted with the same symbols as in figures 37-39, with the assigned local magnitude written beside each symbol. The approximate seismic moment corresponding to these plotted points is shown by the left vertical axis of the figure. The  $(\bar{u}_o, F_o)$  values from G-R are plotted as large solid circles with the corresponding magnitude. The point at  $M_L = 7$  is a minimum estimate. The high frequency amplitude spectral densities  $\bar{u}_o$  were computed from G-R's basic data using equation 13. The slope of the line connecting  $(\Omega_o, f_o)$  to  $(\bar{u}_o, F_o)$  points of the same magnitude then determines the ratio  $E_{GR}/E_{MIN}$ , since  $\Omega_o^2 f_o^3$  is less than, equal to, or greater than  $\bar{u}_o^2 F_o^3$  as the slope is less than, equal to, or greater than  $\omega^{-1.5}$ . Again, the amount of discrepancy depends upon the difference  $(F_o - f_o)$ . The slopes of the lines in figure 41 vary between -1.4 and +0.3 and their variation agrees with that of  $E_{GR}/E_{MIN}$ . In the case of the Northern Baja data (solid squares), the slopes tend to flatten out with



decreasing magnitude, which in terms of Brune's theory is consistent with smaller fractional stress drops at smaller  $M_L$  and agrees with the stress drop versus magnitude curve in figure 40. However, Gutenberg and Richter's amplitudes are averaged over a large number of sources from different tectonic regions of California, and the apparent consistency may be fortuitous. For example, plotting Wyss and Brune's Parkfield moments, fault lengths and magnitudes on the same graph shows that slopes steepen with decreasing magnitude, being  $\omega^{-1.0}$  at  $M_L = 6$  and  $\omega^{-1.9}$  at  $M_L = 4.0$ .

It should be noted that diagrams such as figure 41 provide a basis for understanding other recent studies which have compared spectrum integration and Gutenberg and Richter estimates of radiated energy. For example, a study by Chandra (1970) of five intermediate and deep focus events found P + S energies from spectra comparable to or greater than those obtained using the energy-magnitude relation. A deep focus event in South America studied by him was also used by Wyss (1970c), and from these two papers the seismic moment (from Wyss) and the corner frequency (a maximum estimate from diagrams in Chandra) may be estimated and compared to G-R spectral amplitudes for the same magnitude. The result of the comparison shows that in the case of this particular event the two energy estimates should be about the same. This agrees with Chandra's result, in which the spectrum integration was based exclusively on the observations and used no source model to predict the shape of the spectrum. The earlier radiated energy estimates of Wu (1966) were carried out in a similar manner to Chandra's and his high estimates may be similarly

explained, though Wu shows no spectra from which a comparison can be made.

A plot of long period level versus corner frequency such as figure 41 provides a very versatile means of displaying several different seismic source parameters, as has been pointed out by Hanks (1971b). For example, a line of slope -3 is a line of constant stress drop. Such a line for a stress drop of 1 bar is shown for reference in figure 41. Points above and to the right of this line correspond to stress drops greater than 1 bar, while those below and to the left of it have stress drops less than 1 bar. All of the Gulf of California data lie close to this line, while the bulk of the Northern Baja earthquakes lie above it for  $M_0 > 10^{22}$  dyne-cm (i.e. stress drop increases with seismic moment or magnitude, as shown in figure 40). Thus in this two parameter description of the seismic source the Northern Baja California earthquakes are distinctly separated as a group from events within the Gulf of California.

Looked at in another way, figure 41 shows the variation of source dimension with seismic moment, since the corner frequency is inversely proportional to source size and the long period level is proportional to moment. Again the separation of Gulf and North Baja data sets is clear.

## SPECTRAL AMPLITUDES AT HIGH FREQUENCIES

Discussion of radiated energy estimates has demonstrated that the high frequency spectral amplitudes measured by Gutenberg and Richter are considerably larger than those which would be expected assuming  $\omega^{-2}$  fall off of the SH source spectrum at high frequencies. This difficulty, which cannot be entirely a source size effect for their data, may be explained by Brune's (1970) modification to his model for the case of small fractional stress drop, since in this case the source spectrum falls off as  $\omega^{-1}$  at intermediate frequencies (viz. see figure 33). This hypothesis is an attractive one in view of the small stress drops measured for many of the events studied here, and it shall shortly be considered further. However, first the high frequency excitation predicted by several other recently proposed source models is examined in an attempt to gain some understanding of the physical mechanisms which might enhance the high frequency portion of the seismic source spectrum.

Haskell (1964) showed that a shear fault with a displacement discontinuity across it is mathematically equivalent to an area distribution of double-couple point sources, and used this formulation to compute the P and S energies for a unilaterally propagating rupture. The source spectra predicted by his model are very similar to Brune's, having a long period level proportional to the moment of an equivalent double couple point source, a corner frequency inversely related to rupture dimension, and a high frequency amplitude fall-off of  $\omega^{-2}$ . Haskell's model considered a completely smoothly propagating

rupture, an assumption which he pointed out must fail on some time scale, and he recognized that this breakdown of coherency could have important implications on estimates of radiated energy (Haskell's observation was pointed out to the writer by Dr. James C. Savage). Haskell was led to the conclusion because the source spectrum predicted by his fault model fell off as  $\omega^{-2}$  at high frequencies and greatly underestimated the high frequency excitation of the great Kamchatka earthquake of 1952: De Noyer's (1959) integration of the Wood-Anderson seismogram from this event gave radiated energies at least an order of magnitude larger than Haskell's theory would have predicted using the complete seismic spectrum and reasonable durations of rupture. On this basis and in analogy to the expected stick-slip behavior of real seismic sources, he proposed that the displacement-time function on the fault surface must be significantly more irregular than the ramp function which he had originally assumed, and demonstrated such a modification to his model would significantly enhance the excitation of high frequency waves, in accord with De Noyer's observations.

In a subsequent paper, Haskell (1966) further investigated incoherently propagating faults, and appealing to the complicated character of strong motion accelerograph records at short epicentral distances, proposed a statistical source model which he suggested would account for these complications. Rather than assuming a simple ramp source-time function and a constant offset across the dislocation surface, he assumes a particular mathematical form for the space- and-time autocorrelation of dislocation acceleration over the fault

plane. The most physically tangible parameters which may be extracted from this formulation are the correlation length  $k_L^{-1}$ , analogous to fault length, and correlation time  $k_T^{-1}$ , analogous to rupture duration time. Haskell assumed that  $k_L^{-1}$  and  $k_T^{-1}$  were considerably smaller than rupture length and duration time respectively. Aki (1967) used Haskell's formulation taking a particular form for the autocorrelation function of dislocation velocity, and also provided some physical motivation for his and Haskell's assumed functional forms. He gives very useful explicit expressions for the displacement spectra for the two assumed autocorrelation functions. They both have the form

$$\frac{w \bar{u} L}{\left\{ 1 + \left( \frac{\cos \theta}{c} - \frac{1}{v} \right)^2 \left( \frac{\omega}{k_L} \right)^2 \right\}^{\frac{1}{2}} \left\{ 1 + \left( \frac{\omega}{k_T} \right)^2 \right\}^m} \quad (15)$$

where

$w, L$  = dislocation width and length

$c$  = wave velocity

$v$  = rupture velocity

$\theta$  = angle between propagation direction and observation point

and  $m = 1$  for Haskell's " $\omega^3$  model" and  $m = \frac{1}{2}$  for Aki's " $\omega^2$  model." Though the spectra fall off differently at very high frequencies, they may still decay as  $\omega^{-1}$  at intermediate frequencies. Thus far dislocation dimensions enter only as scaling factors and do not affect the shape of the spectrum, which is controlled entirely by

$k_L$ ,  $k_T$  and the directivity factor in (15), which accounts for the finite rupture propagation velocity. Aki has made a further assumption of similarity, taking  $(vk_L)^{-1}$  and  $k_T^{-1}$  proportional to fault length which implies stress drop is constant for sources of all sizes. Even within Northern Baja this is not a justified assumption, and hence similarity is not further considered here. Haskell's purpose in inserting some statistical space and time roughness into his source model was to put more radiated energy into high frequencies, and whichever form of equation 15 is chosen, this is what occurs if  $k_L$  and/or  $k_T$  are sufficiently small, regardless of the behavior of the spectrum at very high frequencies.

It should be noted that for Haskell's unilaterally propagating fault model (1964 paper) and for the statistical sources described by equation 15, part (i.e.  $\omega^{-1}$ ) of the fall-off of spectral amplitude at high frequency is due entirely to the effect of finite rupture propagation (directivity factor). Such perfect destructive interference at high frequencies requires exact phase coherency in the directivity function on a very small length scale, and seems incompatible with the expected behavior of realistic tectonic sources. Above some frequency it may then be expected that directivity will no longer influence high frequency amplitudes, and the spectrum will fall off at a rate which is determined by other parameters of the particular source model (Dr. James N. Brune, personal communication).

Archambeau (1964, 1968) has pointed out the rather arbitrary nature of dislocation sources in which the space and time behavior of displacement on the rupture surface are taken to be mathematically

separable, and their form being a basic assumption of the source theory. His more fundamental mathematical approach is to model tectonic sources in terms of an initial value problem which involves the elastic relaxation of a pre-stress field in response to the sudden introduction into the medium of a region of low strength (source region). This circumvents the arbitrariness of dislocation sources, but at the expense of increased analytic difficulty. Thus far Archambeau's theory has been applied to various forms of spherical propagating ruptures, and with this geometry the source spectrum has a distinct peak (which occurs at a frequency which depends inversely on rupture length), falls off approximately as  $\omega$  at low frequencies and as  $\omega^{-2}$  at high frequencies.

As stated earlier, fractional stress drop as modeled by Brune (1970) offers a convenient explanation for Gutenberg and Richter's observations of relatively high SH amplitudes at high frequencies for California earthquakes. Incomplete stress drop may include a variety of rupture mechanisms which are somewhat analogous to the statistical models of Haskell and Aki. For example, a multiple source in which slippage occurs independently or sequentially over a number of relatively small subregions of the total surface of rupture would have a spectrum rather similar to the lower curve in figure 33. A special case of this mechanism is a propagating rupture which seals itself after the rupture has passed. The portion of the spectrum falling off less steeply than  $\omega^{-2}$  would then be controlled by the dimensions of the subregions and the stress drops across them, modified appropriately by propagation effects. The transition from  $\omega^{-1}$  to  $\omega^{-2}$  need not be a sharp one. These mechanisms are mentioned by Brune and

may be viewed as simple extensions of his source model. Hence several plausible but distinctly different rupture mechanisms proposed by several different investigators can be shown to enhance the high frequency portion of the SH source spectrum in accord with the expectations based on Gutenberg and Richter's measurements and the observations made here.

#### DISCUSSION AND SPECULATIONS

It has been shown that pronounced regional variations exist between the Gulf of California and Northern Baja in seismic moments, source dimensions, stress drops and estimates of seismically radiated energy. Visual examination of seismograms from southern California earthquakes show similar regional variations in these source parameters within this area as well. These variations are similar to the regional differences in seismic moment with local magnitude (i. e. apparent stress) reported by Wyss and Brune (1968) and Wyss (1970a) and are supported by the recent observations of Thatcher and Hanks (1971). This preliminary examination suggests that low relative surface wave excitation correlates well with small source dimensions (e. g. "big bend" of San Andreas), and that high surface wave excitation indicates larger source size (Imperial Valley, Parkfield-Cholame). This in turn suggests that high apparent stress earthquakes may in general be characterized by small source dimensions. With all these observations in mind it is thus appropriate to speculate on possible causes of these significant differences.

A consistent interpretation of the high stress drops and apparent stresses of North Baja compared with the Gulf region is that higher effective shear stresses are acting across faults in Baja California.

Provided the G-R radiated energy estimate is a good one, this interpretation would agree with the increase of  $E_{GR}/E_{MIN}$  with decreasing stress drop observed for the Baja data. However, this latter consistency may not be significant, since there is considerable uncertainty concerning the accuracy of the energy-magnitude relation, especially in cases where spectral shapes vary significantly, as has been shown in this study. Furthermore, the unusual October-November 1954 sequence is unexplained by this interpretation unless some unusual stress inhomogeneities occur within Northern Baja. Hence, although regional differences in effective shear stress are suggested by the data examined here, they are by no means proven.

Differences in source size between Baja and the Gulf cannot be conveniently explained by differences in effective shear stresses, and an additional explanation of this difference may be required. A rupture will stop propagating when it encounters a region of increased strength or a segment of the fault across which shear stresses have been relieved by a preceding event (Dietrich, 1971). Increased strength would correspond to an increase in frictional stress, due to changes in rock type and/or normal stresses acting across the fault surface. In this regard Allen (1968) has suggested that differences in rock type along various segments of the San Andreas system can strongly affect the mode of strain release. For example, serpentine zones along major faults might favor creep and frequent moderate earthquakes while granitic rocks could lock fault zones more easily and allow strain release only by infrequent large shocks. Such inhomogeneity would have to be much more localized within Baja

California in order to explain the small source dimensions of earthquakes which occur there.

Small source dimensions might alternatively be understood if all corresponding focal mechanisms showed a significant component of thrust faulting, since in this case increasing source size might then be accomplished only by doing work against the force of gravity. Thrusting may be important on some of the faults in Northern Baja California, particularly those on the east face of the Sierra Juarez, but is probably not dominant on either the Agua Blanca or San Miguel faults.

A third possibility is that incoherent source models such as Haskell's (1966) are appropriate for interpreting the observed spectra. In this case the regional variations in spectra would be interpreted as reflecting differences in coherency lengths, rather than fault dimensions, and a precise mechanical explanation for this regional difference would still remain to be made.

### CONCLUSIONS

Remarkable regional differences in source dimensions and seismic moments exist between Northern Baja California and Gulf of California earthquakes. These differences are often clearly evident from visual examination of seismograms and require no subtle analysis to discern. Fourier analysis of the seismic records has allowed these differences to be quantitatively evaluated, and although the results have been interpreted in terms of Brune's (1970) theory,

similar differences in source parameters would be found if other source models were used. Results show that Northern Baja California earthquakes characteristically have source dimensions at least a factor of four smaller and seismic moments an order of magnitude less than sources with the same local magnitude within the Gulf of California. Though in principle it is possible that differential attenuation and/or propagation effects might explain these spectral differences, the similarity of paths traversed and the magnitude of the effect which would be required argue against these explanations. Furthermore, preliminary visual examination of seismograms from southern California sources suggest that similar regional variations in moments and source size occur there as well.

Stress drops for Northern Baja sources are typically one to two orders of magnitude larger than those for Gulf of California events, though the stress drops converge at smaller seismic moment (or smaller  $M_L$ ). This roughly agrees with the differences in apparent stresses computed using the Gutenberg-Richter energy-magnitude relation to estimate seismically radiated energies. The stress drops are, however, the better-determined quantities, and their regional variation is independent of both the local magnitude definition and the energy-magnitude relation.

A minimum estimate of the seismically radiated energy may be made from the observed spectrum provided complete effective stress drop is assumed (i.e.  $\omega^{-2}$  high frequency fall-off of spectrum). Under this assumption the Gulf and Baja data again separate, Gulf

source minimum radiated energies being roughly comparable to those determined by the energy-magnitude relation, while for Baja earthquakes the spectrum estimate averages nearly two orders of magnitude lower for  $M_L < 5$ . This is consistent with the lower stress drops of the smaller Baja events. However this consistency is significant only if the Gutenberg and Richter relation is a good estimate of the total radiated energy, which is quite unclear at this time.

Finally, in the magnitude range  $M_L = 4 \rightarrow 5$ , Northern Baja California earthquakes have long period excitation and source dimensions which average only about a factor of two larger than corresponding quantities for underground nuclear explosions with comparable magnitudes. This comparison points out a further difficulty in the problem of discrimination at small magnitudes.

## REFERENCES

- Aki, K., Crustal structure in Japan from the phase velocity of Rayleigh waves, Part I. Use of the network of seismological stations operated by the Japan Meteorological Agency, Bull. Earthquake Res. Inst., Tokyo Univ., 39, 255-283, 1961.
- Aki, K., Generation and propagation of G waves from the Niigata earthquake of June 16, 1964, Part 2. Estimation of earthquake moment, released energy, and stress-strain drop from G wave spectrum, Bull. Earthquake Res. Inst., Tokyo Univ., 44, 73-88, 1966.
- Aki, K., Scaling law of seismic spectrum, J. Geophys. Res., 72, 1217-1231, 1967.
- Aki, K., Seismological evidence for the existence of soft thin layers in the upper mantle under Japan, J. Geophys. Res., 73, 585-594, 1968.
- Aki, K., and K. Kaminuma, Phase velocity of Love waves in Japan, 1. Love wave from the Aleutian shock of March 9, 1957, Bull. Earthquake Res. Inst., Tokyo Univ., 41, 243-259, 1963.
- Allen, C. R., The tectonic environments of seismically active and inactive areas along the San Andreas fault system, Stanford Univ. Pub. Geol. Sci., 11, 70-82, 1968.
- Allen, C. R., L. T. Silver, and F. G. Stehli, Agua Blanca fault -- a major transverse structure of Northern Baja California, Mexico, Bull. Geol. Soc. Am., 71, 457-482, 1960.
- Allen, C. R., P. St. Amant, C. F. Richter, and J. M. Nordquist, Relationship between seismicity and geologic structure in the

- southern California region, Bull. Seismol. Soc. Am., 55, 753-797, 1965.
- Allison, E. C., Geology of areas bordering the Gulf of California, in Marine Geology of the Gulf of California, T. H. van Andel and G. G. Shor, Eds., Amer. Assoc. Petrol. Geol., Tulsa, Oklahoma, 1964.
- Anderson, D. L., and C. B. Archambeau, The anelasticity of the earth, J. Geophys. Res., 69, 2071-2084, 1964.
- Anderson, D. L., A. Ben Menahem, and C. B. Archambeau, Attenuation of seismic energy in the upper mantle, J. Geophys. Res., 70, 1441-1448, 1965.
- Anderson, D. L., and D. G. Harkrider, Universal dispersion tables, II. Variational parameters for amplitudes, phase velocity, and group velocity, for first four Love modes for an oceanic and a continental earth model, Bull. Seismol. Soc. Am., 58, 1407-1499, 1968.
- Anderson, D. L., M. N. Toksoz, Surface waves on a spherical earth, 1. Upper mantle structure from Love waves, J. Geophys. Res., 68, 3483-3489, 1963.
- Atwater, T., Implications of plate tectonics for the Cenozoic evolution of western North America, Bull. Geol. Soc. Am., 81, 3513-3536, 1970.
- Archambeau, C. B., Elastodynamic source theory, Ph.D. thesis, California Institute of Technology, Pasadena, 1964.

- Archanbeau, C. B., General theory of elastodynamic source fields, Revs. of Geophys., 6, 241-288, 1968.
- Banghar, A., and L. R. Sykes, Focal mechanism of earthquakes in the Indian Ocean and adjacent areas, J. Geophys. Res., 73, 632-649, 1969.
- Basham, P. W., Canadian magnitudes of earthquakes and nuclear explosions in the southwestern United States, Geophys. J. R. astr. Soc., 17, 1-13, 1969.
- Ben Menahem, A., and D. G. Harkrider, Radiation patterns of seismic surface waves, J. Geophys. Res., 69, 2605-2620, 1964.
- Biehler, S., R. L. Kovach, and C. R. Allen, Geophysical framework of the northern end of the Gulf of California structural province, in Marine Geology of the Gulf of California, T. H. van Andel and G. G. Shor, Eds., Amer. Assoc. Petrol. Geol., Tulsa, Oklahoma, 1964.
- Brune, J. N., A. Espinosa, and J. Oliver, Relative excitation of surface waves by earthquakes and underground explosions in the California-Nevada region, J. Geophys. Res., 68, 3501-3513, 1963.
- Brune, J. N., and C. R. Allen, A low-stress-drop, low-magnitude earthquake with surface faulting: The Imperial, California earthquake of March 4, 1966, Bull. Seismol. Soc. Am., 57, 501-514, 1967.
- Brune, J. N., and J. Dorman, Seismic waves and earth structure in the Canadian Shield, Bull. Seismol. Soc. Am., 53, 167-210, 1963.

- Brune, J. N., J. E. Nafe, and J. E. Oliver, A simplified method for the analysis and synthesis of dispersed wave trains, J. Geophys. Res., 65, 287-295, 1960.
- Brune, J. N., Seismic moment, seismicity and rate of slip along major fault zones, J. Geophys. Res., 73, 777-784, 1968.
- Brune, J. N., Tectonic stress and the spectra of seismic shear waves from earthquakes, J. Geophys. Res., 75, 4997-5009, 1970.
- Burridge, R., and L. Knopoff, Body force equivalents for seismic dislocations, Bull. Seismol. Soc. Am., 54, 1874-1888, 1964.
- Carder, D. S., D. W. Gordon, and J. N. Jordan, Analysis of surface foci travel times, Bull. Seismol. Soc. Am., 56, 815-840, 1966.
- Cleary, J., and A. Hales, An analysis of the travel times of P waves to North American stations, in the distance range 32° to 100°, Bull. Seismol. Soc. Am., 56, 467-489, 1966.
- Chandra, U., Analysis of body wave spectra for earthquake energy determination, Bull. Seismol. Soc. Am., 60, 539-564, 1970.
- DeNoyer, J., Determination of the energy in body and surface waves, Part II, Bull. Seismol. Soc. Am., 49, 1-10, 1958.
- Dietrich, J. M., Computer modeling of earthquake stimulation by fluid injection, EOS, 52, 343, 1971.
- Evernden, J. F., Study of regional seismicity and associated problems, Bull. Seismol. Soc. Am., 60, 393-446, 1970.
- Fisher, R. L., G. A. Rusnak, and F. P. Shepard, Submarine topography of the Gulf of California, chart accompanying Marine Geology of the Gulf of California, T. H. van Andel and G. G. Shor, Eds.,

- Amer. Assoc. Petrol. Geol., Tulsa, Oklahoma, 1964.
- Gibbs, J. F., and J. C. Roller, Crustal structure determined from seismic refraction measurements between the Nevada Test Site and Ludlow, California, U. S. Geol. Survey Prof. Paper 550-D, D125-D131, 1966.
- Grant, F. S., and G. F. West, Interpretation Theory in Applied Geophysics, McGraw-Hill, New York, 584 pp., 1966.
- Gutenberg, B., Reflected and minor phases in records of near-by earthquakes in southern California, Bull. Seismol. Soc. Am., 34, 137-160, 1944.
- Gutenberg, B., and C. F. Richter, Earthquake magnitude, intensity, energy and acceleration (second paper), Bull. Seismol. Soc. Am., 46, 105-145, 1956.
- Hales, A. S., and S. Bloch, Upper mantle structure: are the low velocity layers thin?, Nature, 221, 930-934, 1969.
- Hamilton, W., Origin of the Gulf of California, Bull. Geol. Soc. Am., 72, 1307-1318, 1961.
- Hanks, T. C., and M. Wyss, The use of body wave spectra in the determination of seismic source parameters, EOS, 52, 276, 1971.
- Hanks, T. C., The Kuril trench-Hokkaido rise system: large shallow earthquakes and simple models of deformation, Geophys. J. R. astr. Soc., in press, 1971a.
- Hanks, T. C.,  $\Omega_0$ - $f_0$  diagrams, Seismological Society of America meeting, Riverside, California, March, 1971b.
- Harkrider, D. G., and D. L. Anderson, Surface wave energy from point sources in plane layered earth models, J. Geophys. Res., 71,

2967-2979, 1966.

Haskell, N. A., Total energy and energy spectral density of elastic wave radiation from propagating faults, Bull. Seismol. Soc. Am., 54, 1811-1841, 1964.

Haskell, N. A., Total energy and energy spectral density of elastic wave radiation from propagating faults, Part II. A statistical source model, Bull. Seismol. Soc. Am., 56, 125-140, 1966.

Herrin, E. (Ed.), E. P. Arnold, B. A. Bolt, G. E. Clawson, E. R. Engdahl, D. W. Gordon, A. L. Hales, J. L. Lobdell, O. Nuttli, C. Romney, J. Taggart, and W. Tucker, 1968 Seismological tables for P phases, Bull. Seismol. Soc. Am., 58, 1193-1242, 1968.

Hill, D. P., High frequency wave propagation in the earth: theory and observations, Ph.D. thesis, California Institute of Technology, Pasadena, 1971.

James, D. E., Anomalous Love wave phase velocities, J. Geophys. Res., 76, 2077-2083, 1971.

Jobert, N., Excitation des oscillations propre de la terre, Ann. Geophys., 18, 372-383, 1962.

Jobert, N., Excitation of torsional oscillations of the earth: higher modes, J. Geophys. Res., 69, 5223-5234, 1964.

Jobert, N., Excitation des harmoniques d'ondes de Love, Ann. Geophys., 22, 1-8, 1966.

Johnson, L. R., Array measurements of P velocities in the lower mantle, Bull. Seismol. Soc. Am., 59, 973-1008, 1969.

- Julian, B. R., and D. L. Anderson, Travel times, amplitudes, and apparent velocities of body waves, Bull. Seismol. Soc. Am., 58, 1811-1841, 1968.
- Kaminuma, K., The crust and upper mantle structure in Japan, 1. Phase velocities of Love and Rayleigh waves, Bull. Earthquake Res. Inst., Tokyo Univ., 44, 481-494, 1966a.
- Kaminuma, K., The crust and upper mantle structure in Japan, 2. Crustal structure in Japan from the phase velocity of Rayleigh waves, Bull. Earthquake Res., Inst., Tokyo Univ., 44, 495-509, 1966b.
- Kaminuma, K., The crust and upper mantle structure in Japan, 3. An anisotropic model of the structure in Japan, Bull. Earthquake Res., Inst., Tokyo Univ., 44, 511-518, 1966c.
- Knopoff, L., S. Mueller, and W. L. Pilant, Structure of the crust and upper mantle in the Alps from the phase velocity of Rayleigh waves, Bull. Seismol. Soc. Am., 56, 1009-1044, 1966.
- Knopoff, L., and F. A. Schwab, Apparent initial phase of a source of Rayleigh waves, J. Geophys. Res., 73, 755-760, 1968.
- Kovach, R. L., and D. L. Anderson, Higher mode surface waves and their bearing on the structure of the earth's mantle, Bull. Seismol. Soc. Am., 54, 161-173, 1964.
- Kovach, R. L., C. R. Allen, and F. Press, Geophysical investigations in the Colorado delta region, J. Geophys. Res., 67, 2845-2871, 1962.
- Larson, R. L., H. W. Menard, and S. M. Smith, The Gulf of California:

- A result of ocean-floor spreading and transform faulting,  
Science, 161, 781-784, 1969.
- Le Pichon, X., Sea-floor spreading and continental drift, J. Geophys. Res., 73, 3661-3697, 1968.
- McEvelly, T. V., Central U. S. crust-upper mantle structure from Love and Rayleigh wave phase velocity inversion, Bull. Seismol. Soc. Am., 54, 1997-2015, 1964.
- McKenzie, D. F., and W. J. Morgan, The evolution of triple junctions, Nature, 224, 125-133, 1969.
- McKenzie, D. P., and R. L. Parker, The north Pacific: An example of tectonics on a sphere, Nature, 216, 1276-1280, 1967.
- Mogi, K., Some discussions on aftershocks, foreshocks, and earthquake swarms--the fracture of a semi-infinite body caused by an inner stress origin and its relation to earthquake phenomena, 3., Bull. Earthquake Res. Inst., Tokyo Univ., 41, 615-658, 1963.
- Molnar, P., and L. R. Sykes, Tectonics of the Caribbean and Middle America regions from focal mechanisms and seismicity, Bull. Geol. Soc. Am., 80, 1639-1684, 1969.
- Morgan, W. J., Rises, trenches, great faults, and crustal blocks, J. Geophys. Res., 73, 1959-1982, 1968.
- Phillips, R. P., Seismic refraction studies in Gulf of California, in Marine Geology of the Gulf of California, T. H. van Andel and G. G. Shor, Eds., Amer. Assoc. Petrol. Geol., Tulsa, Oklahoma, 1964.

- Pilant, W. L., and L. Knopoff, Observations of multiple seismic events, Bull. Seismol. Soc. Am., 54, 19-41, 1964.
- Press, F., Seismic wave attenuation in the crust, J. Geophys. Res., 69, 4417-4418, 1964.
- Press, F., Dimensions of the source region for small shallow earthquakes, Proc. of the VESIAC Conference on the Current Status and Future Progress for Understanding the Source Mechanism of Shallow Seismic Events in the 3 to 5 magnitude range, 1967.
- Richter, C. F., Elementary Seismology, W. H. Freeman, San Francisco, 768 pp., 1958.
- Rusnak, G. A., and R. L. Fisher, Structural history and evolution of the Gulf of California, in Marine Geology of the Gulf of California, T. H. van Andel and G. G. Shor, Eds., Amer. Assoc. Petrol. Geol., Tulsa, Oklahoma, 1964.
- Shepard, F. P., Submarine topography of the Gulf of California, pt. 3 of The 1940 E. W. Scripps cruise to the Gulf of California: Geol. Soc. Am. Mem. 43, 32 p.
- Shor, G. G., Jr., and E. Roberts, San Miguel, Baja California Norte, earthquakes of February 1956: A field report, Bull. Seismol. Soc. Am., 48, 101-116, 1958.
- Sykes, L. R., Mechanism of earthquakes and the nature of faulting on the mid-ocean ridges, J. Geophys. Res., 72, 2131-2153, 1967.
- Sykes, L. R., Seismological evidence for transform faults, seafloor spreading, and continental drift, in Proc. of NASA Symposium, History of the Earth's Crust, R. A. Phinney, Ed., Princeton

University Press, New Jersey, 1968.

Sykes, L. R., Earthquake swarms and sea-floor spreading, J. Geophys. Res., 75, 6598-6611, 1970.

Sykes, L. R., and J. Oliver, The propagation of short period seismic surface waves across oceanic areas, part II--Analysis of seismograms, Bull. Seismol. Soc. Am., 54, 1373-1415, 1964.

Takeuchi, H., Y. Hamano, and Y. Hasegawa, Rayleigh-and-Love-wave discrepancy and the existence of magma pockets in the upper mantle, J. Geophys. Res., 73, 3349-3351, 1968.

Talwani, M., X. LePichon, and M. Ewing, Crustal structure of the mid-ocean ridges, 2. Computed model from gravity and seismic refraction data, J. Geophys. Res., 70, 341-352, 1965.

Thatcher, W., and J. N. Brune, Higher mode interference and observed anomalous apparent Love wave phase velocities, J. Geophys. Res., 74, 6603-6611, 1969.

Thatcher, W., and J. N. Brune, Seismic study of an oceanic ridge earthquake swarm in the Gulf of California, Geophys. J. R. astr. Soc., in press, 1971.

Thatcher, W., and T. C. Hanks, Source dimensions, seismic moment, and stress drop from the shear wave spectra of local earthquakes in the southern California region, EOS, 52, 275, 1971.

Tobin, D., and L. R. Sykes, Seismicity and tectonics of the northeast Pacific Ocean, J. Geophys. Res., 73, 3821-3854, 1968.

Trygvasson, E., Crustal structure of the Iceland region from the dispersion of surface waves, Bull. Seismol. Soc. Am., 52, 359-374, 1962.

- Trygvasson, E., Arrival times of P waves and upper mantle structure, Bull. Seismol. Soc. Am., 54, 727-736, 1964.
- Tsai, Y. B., Determination of focal depths of earthquakes in the mid-oceanic ridges from the amplitude spectra of surface waves, Ph.D. thesis, Massachusetts Institute of Technology, Cambridge, 1969.
- Wickens, A. J., and K. Pec, A crust-mantle profile from Mould Bay, Canada to Tucson, Arizona, Bull. Seismol. Soc. Am., 58, 1821-1832, 1968.
- Wilson, J. T., A new class of faults and their bearing on continental drift, Nature, 207, 343-349, 1965.
- Wu, Francis T., Lower limit of the total energy of earthquakes and partitioning of energy among seismic waves, Ph. D. thesis, California Institute of Technology, 1966.
- Wyss, Max, and J. N. Brune, Seismic moment, stress, and source dimensions for earthquakes in the California-Nevada region, J. Geophys. Res., 73, 4681-4694, 1968.
- Wyss, Max, J. N. Brune, T. C. Hanks, and B. E. Tucker, Source dimensions of nuclear explosions and small shallow earthquakes, ARPA Woods Hole Conference on Seismic Discrimination, vol. 2, 1970.
- Wyss, Max, Observation and interpretation of tectonic strain release mechanisms, Ph.D. thesis, California Institute of Technology, Pasadena, 1970a.

Wyss, Max, Apparent stresses of earthquakes on ridges compared to apparent stresses of earthquakes in trenches, Geophys. J. R. astr. Soc., 19, 479-488, 1970b.

Wyss, Max, Stress estimate for South American shallow and deep earthquakes, J. Geophys. Res., 75, 1529-1544, 1970c.